CAPACITIVE DEIONIZATION TECHNOLOGY™: DEVELOPMENT AND EVALUATION OF AN INDUSTRIAL PROTOTYPE SYSTEM

THOMAS J. WELGEMOED

Submitted in partial fulfillment of the requirements for the degree of Master of Engineering in the Faculty of Engineering, the Built Environment and Information Technology, University of Pretoria, Pretoria

2005

CAPACITIVE DEIONIZATION TECHNOLOGY™: DEVELOPMENT AND EVALUATION OF AN INDUSTRIAL PROTOTYPE SYSTEM

By: Thomas J. Welgemoed

Supervisor : Prof. C.F. Schutte

Department: Chemical Engineering

Degree: M.Eng (Water Utilisation)

SYNOPSIS

The Lawrence Livermore National Laboratory (LLNL), in Berkley, California, developed a laboratory scale non-membrane electrosorption process known as Capacitive Deionization Technology™ (CDT™) for the continuous removal of ionic impurities in water. A saline solution flows through an unrestricted capacitor type module consisting of numerous pairs of high-surface area (carbon-aerogel) electrodes. The electrode material (carbon aerogel) contains a high specific surface area (400 – 1 100 m^2/g), and a very low electrical resistivety (< 40 mΩ.cm). Anions and cations in solution are electrosorbed by the electric field upon polarization of each electrode pair by a direct current (1,4 Volt DC) power source.

Testing conducted on a laboratory scale unit at LLNL has proved that CDT™ has the potential to be an alternative desalination technology (Farmer[5] *et al*., 1995). The primary objective of this research was to continue, where the laboratory scale research ended. Thus taking CDT™ from a laboratory scale technology to an industrial scale process, by developing and evaluating an industrial CDT™ prototype system.

First, a process was developed to manufacture a cost effective industrial sized CDT™ module. During this process various manufacturing techniques were evaluated to produce an optimum prototype. As part of the developmental process the prototype was tested and water treatment efficiency results were first compared to results obtained on the laboratory scale module and secondly to established desalination technologies like reverse osmosis, electrodialysis, and distillation.

Due to the wide variety of potential saline feed water sources, research for this dissertation focused on brackish water applications (which includes wastewater reuse applications). After establishing a cost effective small-scale model of a potential industrial manufacturing process, the prototype was tested with regard to water treatment efficiency. Test results on brackish type waters (1 000 mg/l), indicated that the industrial CDT™ prototype had an energy requirement of 0,594 kWh/1000 liters. Research results compared well to the laboratory scale energy consumptions of 0,1 kWh/1000 liters (Farmer[5] *et al*, 1995) and to the best available existing brackish water membrane based desalination systems with energy requirements of 1,3 to 2,03 kWh/1 000 liters (AWWA, 1999). The thermodynamic minimum energy required (due to osmotic pressure) to desalinate a 0,1% or 1 000 mg/l sodium chloride solution, is 0,0234 kWh/1 000 liters.

Development and evaluation results indicated that CDT™ industrial modules could be manufactured cost effectively on a large scale and that such units have the potential to be very competitive with existing technologies with regards to overall operational and maintenance costs. Therefore Capacitive Deionization Technology™ can be viewed as a potential alternative to membrane technologies in the future. Regardless of the benefits to the potable water industry, CDT™ have the potential to incur a dramatic step reduction in the operational costs of desalination plants, which will make desalination a more viable alternative technology for large-scale agricultural and industrial uses.

KEY WORDS: brackish water, carbon aerogel, desalination, electrochemical, Capacitive Deionization Technology™.

ACKNOWLEDGEMENTS

My sincere thanks to, and appreciation for, all persons and institutions whom made this study possible. A special word of appreciation to the following:

- My Heavenly Father that blessed me with the capability to complete this study.
- Prof. Frik Schutte for his patience and encouragement over the extended period needed to complete this research.
- To my family, my wife Anneline and my son, Ethan – you were my inspiration for contributing in a small way, to solving tomorrow's environmental challenges.
- To Mr. Chris Sheppard for his technical guidance, Mr. Dallas Talley and the personnel of CDT Systems, Inc; Texas A&M University and AirWater, Inc. (Japan) for your assistance with the experimental data collection.
- Miss Christina Oster for your assistance in proofreading this dissertation.

TABLE OF CONTENTS

CHAPTER 4: INDUSTRIAL PROTOTYPE DEVELOPMENT PROCESS

CHAPTER 5: TEST METHODOLOGY, RESULTS AND DISCUSSION

CHAPTER 6: COST: EVALUATION AND COMPARISON

CHAPTER 7: CONCLUSIONS AND RECOMMENDATIONS

LIST OF TABLES

LIST OF FIGURES

NOMENCLATURE / TERMINOLOGY AND UNITS

Standard Symbols

Unless stated otherwise the symbols used in this manuscript have the following meanings and if no dimension appears in brackets it means that the symbol is dimensionless.

A	Unit Area (m^2)
C	Capacitance (F)
d	Distance (m)
E	Energy (J)
E_o	Standard Redox Potential
F	Faraday's constant (= 96 487 C/mol)
gpd	gallon per day
I	Applied Electric Current (A)
i	Current density (mA/cm^2 or A/m^2)
lpd	liter per day
m	mass (kg)
mgd	million gallons per day
mg/l	milligrams per liter
n	Number of electrodes
P	Power (W)
Q	Electric Charge (C)
R	Electric resistance (Ω)
T	Temperature (°C)
V	Volume (*l*)
V	Applied electrical potential (V)

Standard Abbreviations

AA	Atomic Adsorption Spectroscopy
BET	Brunauer-Emmett-Teller
CDT™	Capacitive Deionization Technology™
CBMA	Coal Bed Methane
ED/EDR	Electrodialysis/Electrodialysis Reversal
LLNL	Lawrence Livermore National Laboratory
RO	Reverse Osmosis
TDS	Total Dissolved Solids

Unit Conversions

1 acre-foot = 43 560,17 ft^3 = 1 233,49 m^3 = 1 233 486,65 liters

1 US gal = 3,785 liters

Numeric Conventions

As this dissertation is submitted to a South African and metric orientated University the following numeric conversions were followed.

- Thousands are separated by a space and not by a comma as per US practice. Example 1 000 and not written as 1,000.
- A comma indicates fractions and not a point as per US practice. Example: 5,5 is equal to 5.5 (US numeric system)

CHAPTER 1

INTRODUCTION

"We have made some exceptional scientific advances in the last decade and some of them – they are not as spectacular as the man-in-space, but are important….. If we could ever competitively, at a cheap rate, get fresh water from seawater, that would be in the long–range interests of humanity and would dwarf any other scientific accomplishment".

John F. Kennedy: April 12, 1961

1.1 BACKGROUND

Capacitive Deionization Technology™ (CDT™) is a low-pressure non-membrane desalination process, with the potential to be a "power tool" in the desalination toolbox of the future (Farmer[5] *et al.*, 1995). However at the time when this research was started in 1998, the technology was only at the laboratory scale level. The research objective was to move from laboratory scale to industrial scale by developing and evaluating the first industrial CDT™ prototype.

The motivation for this research came from the continuous global need to improve on existing desalination technologies to facilitate a major step-change in the overall cost of desalinated water to make it viable not only for potable use, but also for industrial and agricultural uses as well (USA-Bureau of Reclamation, 2004). It is important to view the research conducted for this dissertation, against the existing world water crises, which is briefly summarized in the rest of this section.

The Problem, Solution and Tools

The existing global water crises is covered in detail by various authors (Simon, 1994/1998; Gleick, 1993/ 2000; Postel, 1992; Montaigne, 2002), where they discuss several aspects of the growing need for water over the next century.

Solutions require both national and international measures be taken, including resolution of water disputes and increased funding for desalination research and alternative technologies. One of the key tools to resolve future international water crises is the continued research into methods that will provide low-cost desalination. Thereby creating greater economic and political stability in many regions of the world, where scarcity of water could lead to warfare in the same way that oil has lead to wars in the past (Simon, 1998).

> "The consequences of the increasing global water scarcity will largely be felt in the arid and semi-arid areas, in rapidly growing coastal regions and in the megacities of the developing world. Water scientists predict that many of these cities already are, or will be, unable to provide safe, clean water and adequate sanitation facilities for their citizens — two fundamental requirements for human well being and dignity.'' (United Nations, 1999)

Already in 1992, more than 7 500 desalination plants operated worldwide, turning 4,8 billion cubic meters of salt water into fresh water annually. Nevertheless, this accounts for only one percent of the world's water use. The reason for desalination's small contribution to the water supply is its cost (Postel, 1992). Most existing technologies like reverse osmosis and distillation require a great deal of energy. Even nuclear power has proven too expensive for large-scale desalination.

Existing advances in membrane technology is gradually reducing the required cost to produce potable water for human consumption. However, membrane technologies are not yet economically viable for the mass desalination of industrial and agricultural markets. These markets utilize ± 85% of all water used by humanity (Simon, 1998). Existing energy consumption levels, as for membrane processes, would need to be dropped drastically before desalination becomes a source for industrial and agricultural water supply (USA-Bureau of Reclamation, 2004).

Most of the existing industrial scale desalination facilities get their energy from the combustion of fossil fuels, and thus in effect exchange potable water for CO_2, which causes global warming and eventually contributes to the demise of fresh water (Simon, 1998). As a result, Global warming increases the need even more for additional desalination. Therefore, it is imperative to find more energy efficient methods to desalinate water. Electrochemical desalination tools like Capacitive Deionization Technology™, as the first new desalination technology in over 50 years (Farmer[5] *et al.*, 1995), have the potential to be such an energy efficient desalination method.

1.2 OBJECTIVES OF RESEARCH

CDT™ has been identified as a potential mass desalination alternative in laboratory conditions by Lawrence Livermore National Laboratories (Berkeley, USA). The overall objective for this research was to convert a laboratory scale CDT™ system into an industrial system to be used in the "real world". Previous laboratory scale test work has been conducted successfully (Farmer [1,2,3,4,5,6,7] *et al.*), but in order for the technology to be evaluated a potential competitor for existing technologies, a more industrialized prototype test unit was needed.

The research objective was to develop and evaluate an "industrially re-producible" CDT™ module by using the initial laboratory scale test work as a starting point. "Industrially re-producible" in this contents meaning a small-scale model of a future industrial manufacturing process.

Once a successful industrial prototype is created, an evaluation phase would be used to determine if the industrial CDT™ prototype could compete as a unit alternative to desalination processes in the future. The following criteria were identified to serve in the comparison of a "real world" CDT™ prototype unit to other desalination processes:

i) Feed and product water quality requirements

ii) Energy consumption per volume water treated

iii) Pre-and-post treatment requirements

iv) Overall water recovery rate

v) Automatic Control or Operation/Maintenance Requirements

vi) Fouling and scaling tendencies

By comparing these six operational parameters to existing desalination technologies like reverse osmosis and electrodialysis, it is possible to establish the potential of CDT™ as a future alternative desalination method.

1.3 SCOPE OF RESEARCH

Due to the relatively young (less than 10 years) nature of this technology, most of the research had to be conducted in the USA, more specifically Tucson, Arizona and San Diego, California (both areas are considered water poor, with ample brackish water). It must further be noted that although various international patents currently exist for the electrochemical desalination of brackish and seawater, the research conducted for this dissertation focused on Capacitive Deionization Technology™ specifically.

It was further decided to limit the scope for the research, to brackish water applications. The main reasons for this scope selection was that 70% of the worlds available ground water is brackish (Simon, 1998) and the need for desalination of brackish water sources is increasing more rapidly than the need for seawater desalination (International Desalination Association, 1997).

Also, initial laboratory test work at LLNL has indicated a major energy benefit for specifically brackish water applications (Farmer[5] *et al*, 1995). It must be noted that CDT™ could also be a future cost effective desalination tool for seawater applications (Farmer[7] *et al*, 1995), however seawater applications did not form part of this dissertation's scope.

Capacitive Deionization Technology™ has an extremely wide potential application field, it was therefore decided to limit the scope of this research to brackish desalination applications, namely the removal of ions or dissolved solids from brackish water sources like ground waters, secondary municipal effluent, industrial effluent, river and dam waters.

Other potential future applications of CDT™ include:

i) Boiler feedwater treatment
ii) Ultrapure water production
iii) Hydrogen fuel cell water treatment
iv) Selective removal of resources dissolved in water streams like precious metal extraction and recovery. For example, dissolved gold recovery from water-based streams.
v) Seawater desalination.

The research scope for this dissertation can be summarized as follow:
Develop (Design & Manufacture) an industrial scale CDT™ prototype, based upon LLNL laboratory scale test work and evaluate it as a viable industrialized desalination technology by focusing on brackish water applications.

1.4 METHODOLOGY

The following research methodology was used:

i) **Background and Literature Review**: Conduct a thorough literature review of CDT™ research already conducted. The literature review included an intensive review of existing desalination technologies to determine realistic evaluation criteria for the CDT™ industrial prototype.

ii) **Development Phase:** Design and manufacture an industrial prototype unit. This phase served as the main research objective.

iii) **Evaluation Phase**:

- Establish experimental operating procedures - Collect and manage data.
- Compare desalination efficiency and energy requirements of the "real world" CDT™ prototype unit to previously conducted laboratory scale CDT™ experiments. Compare desalination efficiency and energy consumption and overall cost (capital and operations/maintenance) to existing technologies.
- Economics Evaluation.: Estimate CDT™ treatment costs and compare to existing technologies to determine if the technology has the potential to be competitive in the future.

iv) **Conclusion and Recommendations**: If results from a "real world" CDT™ unit compares well to existing technologies, then it would have the potential to be an alternative desalination technology, once manufacturing and industrialization of the full-scale units are complete.

The above-mentioned methodology, which was followed to prepare this dissertation, can be illustrated graphically as per **Figure 1.1.**

1.5 FLOW DIAGRAM OF DISSERTATION PREPARATION.

Figure 1-1 illustrates the dissertation planning and preparation process.

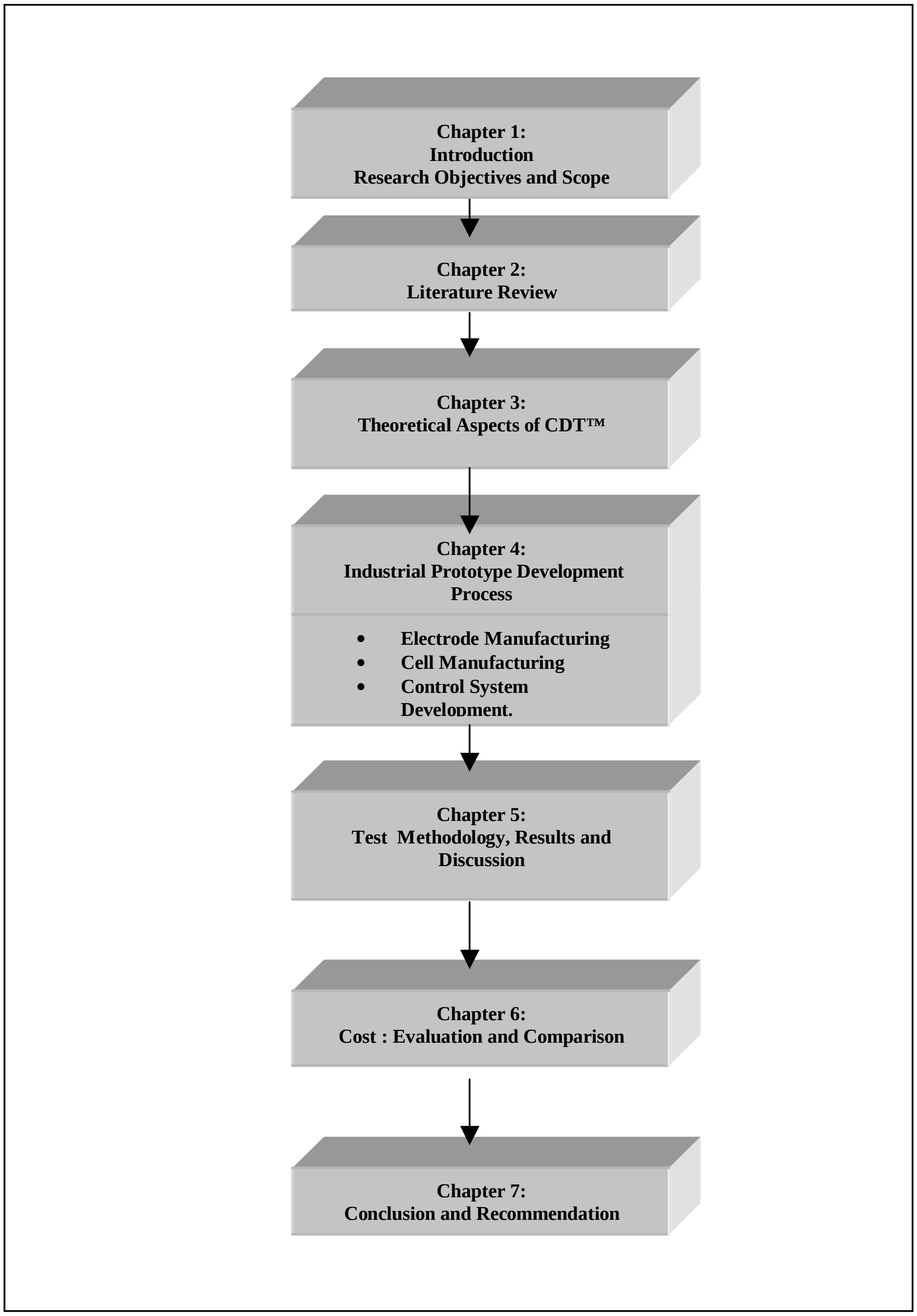

FIGURE 1-1: Flow Diagram of Dissertation Preparation

CHAPTER 2

LITERATURE REVIEW

Existing information, with regard to the various desalination technologies, and more specifically CDT™, was reviewed to assist with the design/manufacturing of an industrial prototype test unit, and with planning the required evaluation (test work) methods. To effectively evaluate CDT™ as an alternative desalination technology, a thorough understanding of the latest benefits and disadvantages of existing technologies was required.

2.1 EXISTING TECHNOLOGIES

There are several existing desalination technologies in use, with each source water presenting its own unique design and operational challenges. Desalination technologies are primarily used to reduce the total dissolved solids content of a source water. Typical applications are potable water, boiler feed water, and ultra pure water production. Existing competing desalination technologies in use on a global scale can be categorized into thermal and membrane processes.

Other processes such as freezing, gel filtration, and two-film gas membranes process are in research and did not form part of this dissertation's literature survey.

Table 2.1 summarizes the main technologies in each category with a description of the basic operating principle. Ion exchange technologies are also listed as they form part of the overview of existing technologies used to remove ions. However, a typical ion exchange technology does exactly what its name implies, it exchanges one undesirable ion for a more acceptable ion on the solid surface of a resin. Therefore, depending on the type of resin used, the overall TDS content of the source water is not really reduced. However, residential water softeners (regenerated with sodium chloride) are in wide use today, and CDT™ is a potential alternative to traditional ion exchange softeners.

Table 2.1: Existing Desalination Technologies and Operating Principles

Technology	Typical Application	Operating Principle
Thermal Processes		
Multistage Flash Evaporation (MFE)	Sea water desalination	Thermal evaporation. Less scale formation problems as compared to submerged tube distillation.
Multiple effect Distillation with Mechanical Vapor Recompression (MED-MVR)	Sea water desalination	Thermal evaporation with mechanical vapor recompression to improve energy efficiency.
Multiple Effect Distillation with Thermal Vapor Recompression (MED-TVR)	Sea water desalination	Thermal evaporation with thermal vapor recompression. More energy efficient than typical direct distillation, but less energy efficient than MVR.
Membrane Processes		
Reverse Osmosis	Sea water and brackish water desalination.	Pressure driven and diffusion controlled membrane process. Removes particles down to 0,0001 µm.
Nanofiltration	Industrial process/waste water and potable water treatment	Pressure driven and diffusion controlled membrane process. Removes particles down to 0,001 µm to 0,01 µm.
Ultrafiltration	Industrial process/waste water and potable water treatment	Pressure driven membrane process, but does not remove ions. Removal of dissolved substances are based on a sieving mechanism, down to 0,01µm. to 0,1 µm.
Microfiltration	Industrial process/waste water and potable water treatment	Pressure driven membrane process, but does not remove ions. Removal of substances are based on a sieving mechanism. 0,1 µm. to 1,0 µm.
Electrodialysis/Electrodialysis Reversal	Primarily brackish water desalination	Charge driven membrane process that removes ions, but not turbidity or micro-organisms.
Ion Exchange Processes		
Anion/Cation Exchange	Boiler feed water and water softening.	Anion and Cation ions in a source water is exchanged for more desirable, less troublesome ions.
Electro deionization (EDI)	Ultra pure water production.	Charge driven ion exchange process.

Data Source: Framer[5] *et al*, 1995

One of the main operating cost components for the desalination of sea-and-brackish water is the amount of energy required to produce a fixed volume of product water. This is also the reason why energy consumption formed primary criteria for evaluating CDT™ as a potential alternative desalination technology. **Table 2.2** lists the average energy requirement for some of the main desalination technologies. As the two main source waters are sea water and brackish water, the associated energy requirements are listed as such.

Table 2.2 : Energy Requirement Per Desalination Technology

Desalination Technology	**Energy Requirement**
Mechanical Vapor Compression (MVR)	6,6 kWh/m^3 (~ 25 Wh/gal) – Sea Water
Multiple Effect Distillation with Mechanical Vapor Compression (MED-MVR)	7,9 – 10,8 kWh/m^3 (30-41 Wh/gal) – Sea Water
Multiple Effect Distillation with Thermal Vapor Compression (MED-TVR)	56,8 – 83,2 kWh/m^3 (215-315 Wh/gal) Sea Water
Multi Stage Flash Evaporation (MFE)	~ 84,5 kWh/m^3 (~320 Wh/gal) – Sea Water
Reverse Osmosis (RO) (Depending on energy recovery)	6,6 – 9,3 kWh/m^3 (25-35 Wh/gal)– Sea Water 2,3 kWh/m^3 (8,5 Wh/gal)- Brackish Water
Electrodialysis	2,03 kWh/m^3 (7,7 Wh/gal) – Brackish Water
CDT (Includes Energy Recovery)	~ 4.2 – 8.5 kWh/m^3 (16-32 Wh/gal) – Sea Water 0,05-0,1 kWh/m^3 (0,2 – 0,4 Wh/gal) – Brackish Water

Brackish Water TDS : 800 – 3 200 mg/l

Sea Water TDS : 35 000 mg/l

Data Source: **CDT - Lawrence Livermore National Laboratory, USA**
Other Desalination Technologies - AWWA

Initial laboratory test work (Farmer[5] *et al*, 1995) indicated that the potential energy advantages of CDT™ to that of thermal processes are dramatic and very competitive with regards to membrane process.

The energy requirements stated in **Table 2.2,** are typical and more accurate energy consumptions are available per technology for specific TDS removal requirements (Farmer[6] *et al*, 1997). In 1993 typical desalination costs could be summarized as follows: reverse osmosis costing US $97 to US $322 per acre foot, while distillation costs ranged from US $530 to US $880, freezing US $299 to US $513, and electrodialysis US $224 to US $435 per acre foot (Gleick, 1993). More detailed RO costs are presented in section 2.2.

Figure 2.1 illustrates the installed desalination capacity in 1998 on a global basis, as listed by the International Desalination Association.

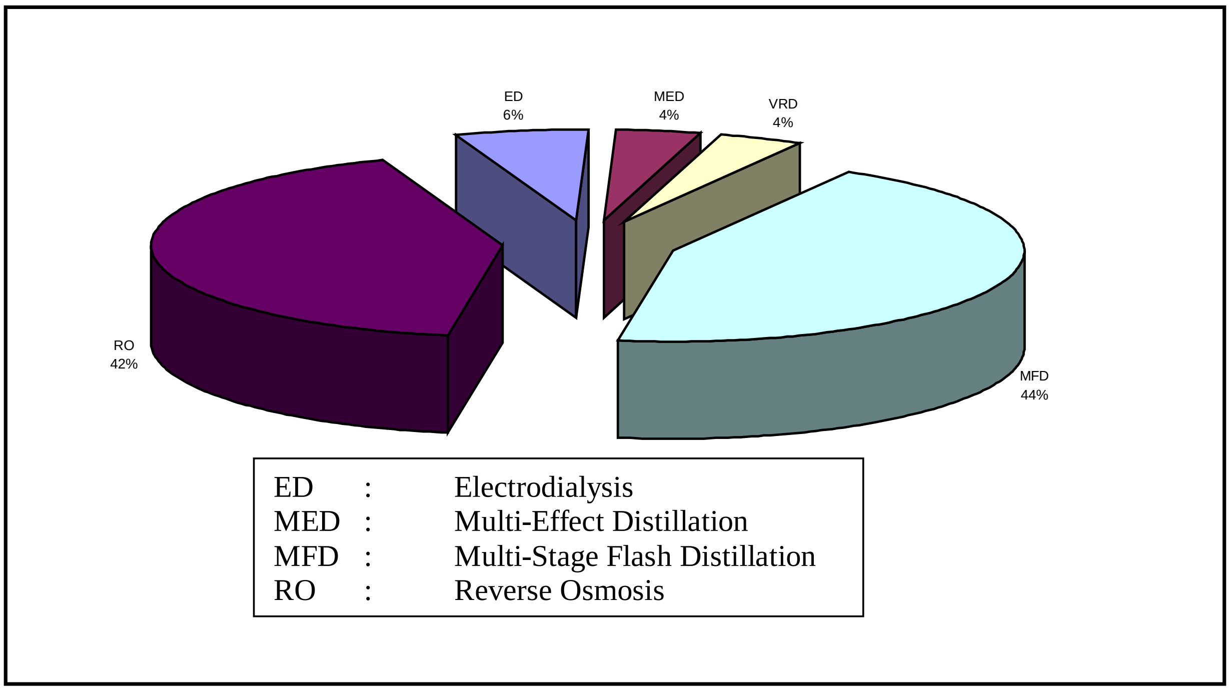

FIGURE 2.1: Installed Global Desalination System (1998)

Source: International Desalination Association

2.2 MEMBRANE PROCESSES

2.2.1 OVERVIEW

As illustrated above, with regards to energy requirements, membrane processes will ultimately be the main competitor to alternative desalination technologies, for example CDT™. It was therefore important to review and understand the existing status of membrane processes, specifically reverse osmosis. A literature study followed to ensure that the most recent data is used in the comparing/evaluation of CDT™ as an alternative technology to membrane process.

Reverse osmosis, nanofiltration, and electrodialysis/electrodialysis reversal are the membrane processes with comparable applications to CDT™. For the desalination of sea water via membranes, RO is the existing technology of choice. High pressures (5 515 to 8 273 kPa or 800 to 1 200 psi) are typically required for sea water desalination. Brackish water desalination via RO requires less pressure, typically 1 723 – 2 758 kPa (250 – 400 psi) (AWWA M46, 1999).

Membrane processes are capable of desalting, softening, removing THM precursors, pathogens, suspended particulate material, and specific organic compounds. A potential alternative technology must also be able to deliver at least the same level of treatment, either directly or by secondary integrated technologies.

Most source waters used to feed membrane processes must undergo some form of pretreatment. Acid and/or antiscalant addition are required to prevent precipitation of salts during membrane filtration, followed by 5 to 15 µm cartridge filtration. Additional pretreatment might be required if the source water contains excessive fouling materials. After membrane filtration, typical potable water post treatment includes processes like aeration-degasification, disinfection, and corrosion control. Specific care must be taken in feed waters containing high Ferrous (Fe^{2+}) concentrations, as not to introduce oxygen and thus precipitate the iron as Ferric (Fe^{3+}) compounds.

A thorough understanding of source water characteristics is vital to the successful design and operation of a membrane plant. Brine concentrate produced during the operation of a membrane plant, depending on the plants location, might require significant treatment before disposal. In the USA, the concentrate is regulated as a industrial waste, and a permit from the USEPA (United States Environmental Protection Agency) is required for disposal. Existing membrane brackish water desalination facilities in the USA vary in size from 50,5 liters/second (800 gpm) to 613,3 liters/second(14 mgd). With the average size at 22 liters/second (0,5 mgd).

Membrane processes are typically used in the following applications:

- Desalting (TDS removal)
- Disinfection By-Product Precursor Removal
- Hardness, Color and Turbidity Removal
- Inorganic Chemical Removal
- Nitrate Removal
- Fluoride Removal
- Synthetic Organic Chemical Removal
- Pathogen Removal

2.2.2 COST

Capital Costs

For reasons mentioned in Chapter 1, the scope of this dissertation was limited to brackish water applications. In Chapter 6, CDT™ is evaluated by comparing construction and operations and maintenance costs to that of reverse osmosis. For specifically brackish type feed water construction costs can vary considerably depending on site-specific factors. Site-specific factors that have an influence on a membrane plant construction costs include:

- Plant size and capacity
- Blending of source water with permeate.

- Source water quality (TDS and other constituents removal required)
- Concentrate disposal
- Intake type for source water.
- Pre-and post treatment requirements
- Indirect costs

Typical construction costs for a brackish water (Feed TDS 2 000 mg/l) membrane treatment plant, with a capacity of 3,785 Ml/d (1 mgd) is estimated at US $0,82/lpd (US $3,14/gpd) (AWWA M46, 1999: 94). For the following estimate, the source water is from a natural gas well field and concentrate disposal is to a surface body of water. Site specific factors are very important and can have a huge influence on the final construction costs. For the above mentioned example (1 mgd brackish water treatment plant) the construction cost can be as low as US $2 million, or as high as US $7 depending on site specific requirements. The construction cost can further be broken down as follows:

- Membranes and Skid: 26%
- Storage and Pump: 25%
- Feed: 14%
- Building: 10%
- Cleaning: 2%
- Instrumentation and Control: 5%
- High-Pressure Pumping: 7%
- Electrics: 4%
- Pretreatment and Post treatment: 8%

The unit costs for process equipment decreases as the overall plant capacity increases due to economy of scale factors. The unit process equipment capital costs for a 20 mgd plant is roughly two thirds that of a 1 mgd plant (US $1,49/gpd for a 1 mgd plant vs. US $1,00/gpd for a 20 mgd plant) (AWWA M46, 1999).

Operations and Maintenance Costs

From a survey conducted in the USA for 22 brackish water treatment plants (AWWA M46, 1999: 5), the average operations and maintenance cost was US $0,33 per 1000 liters (US $1,28 per 1000 gallons) of permeate produced.
The operations and maintenance costs can be broken down as follows:

- Management: 22 % (3.2 persons per 1 mgd capacity)
- Power: 33 %
- Chemicals: 16 %
- Maintenance: 7 %
- Other: 22 % (including membrane replacement)

For a brackish water source (< 2 000 mg/l TDS), ED/EDR and low-pressure reverse osmosis have very competing power consumption rates at around 1,3 kWh/1000 liters (4,9 kWh/1000 gallons).

2.3 CAPACITIVE DEIONIZATION TECHNOLOGY™

Non-membrane electrochemical technologies like Capacitive Deionization Technology™ (CDT™) have the potential to desalinate, remediate nuclear waste streams, and recover resources all via the same basic principal. The principle and mechanism used in CDT™ is not a recent discovery, however researchers were challenged by identifying an optimum material for electrode manufacturing (Farmer[6], *et al*, 1997). Recent advances in material sciences lead to the development of materials like carbon aerogels and carbon nanotubes. CDT™ has been developed as a non-polluting, energy-efficient and cost-effective alternative to ion exchange, reverse osmosis, electrodialysis, and evaporation.

Extensive laboratory scale research regarding CDT™ has been completed at LLNL prior to establishing the research objectives for this dissertation, which were to design, manufacture, and test an industrial prototype module based upon the laboratory test work already completed (Farmer[1], 2000; Farmer[2], *et al*, 1995; Farmer[3], *et al*, 1996; Farmer[4], *et al,* 1995; Farmer[6], *et al*, 1997; Farmer[7], *et al*, 1995; Farmer[8], *et al*, 1996). Chapter 3 will describe CDT™ in more detail, and summarizes some of the earlier research work conducted at LLNL. CDT™ has a number of potential advantages over current membrane and distillation processes:

i) Less energy is needed for the desalination process because high-pressure pumps are not required, particularly for the desalination of brackish water where the actual work is only performed on the unwanted species and not on the total volume of water, as is the case with membrane and distillation processes.
ii) Due to the low amounts of energy required (potentially 30% to 60% less than existing technologies), it is possible to make use of existing solar/wind power technology to power remote desalination units. It can also be used as a sustainable development water treatment tool in communities where no electrical power is accessible and the water quality available is of a non-potable nature.
iii) The carbon aerogel electrodes can withstand much higher temperatures than membranes, and thus can be more efficient for applications such as boiler condensate polishing, and fuel cell water deionizing systems.
iv) The fact that the liquid flows in a non-restricted path ensures that no aggressive secondary effluents are generated due the extensive cleaning operations as required by today's reverse osmosis type processes.
v) Volumes of brine that need to be disposed of are less than that for membrane processes due to the re-use of brine in the regeneration phase. As brine disposal is a problem, especially at inland applications, a smaller brine volume to manage is a big advantage.
vi) High-pressure equipment is not required, and the use of durable electrodes further decreases the operations and maintenance cost of CDT applications.

vii) As the modules act as capacitors, the actual energy recovery possible could be far more efficient than the methods used in current membrane processes.

However, it is important to realize that CDT™ currently also has some disadvantages :

- As the technology is relatively new compared to membrane processes, no long-term operational data is available for industrial size systems.
- As long term operational data is not available yet, it is difficult to predict the electrode lifetime and/or the effect of electrode fouling due to biological and/or chemical means.

CHAPTER 3

THEORECTICAL ASPECTS OF CDT™

3.1 BASIC ELECTROCHEMICAL CELL

In order to fully explain capacitive deionization, it is necessary to review some basic electrochemical principles. The basic electrochemical cell consists of a pair of electrodes, connected externally and immersed in an electrically conducting liquid or paste. The liquid is usually referred to as the electrolyte. **Figure 3.1** illustrates the basic electrochemical cell.

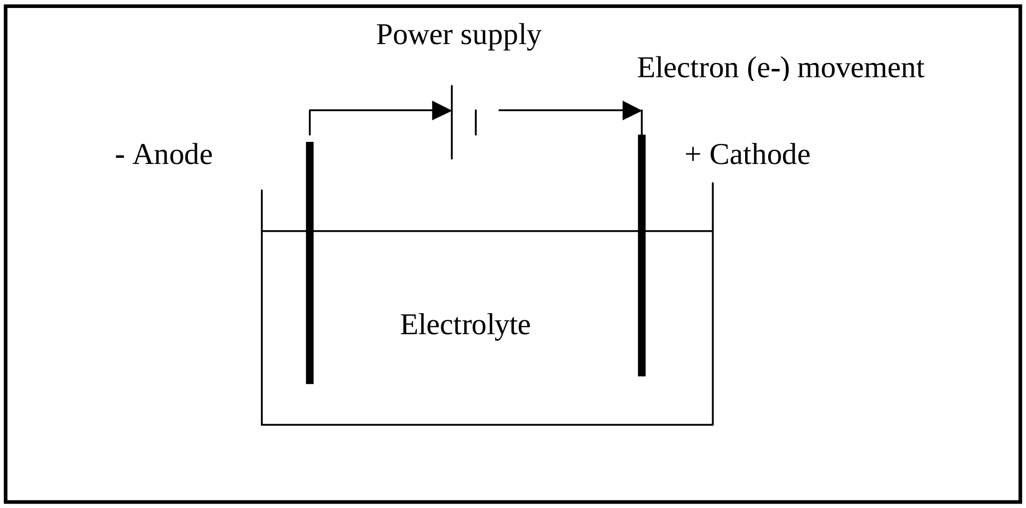

FIGURE 3.1: Basic Electrochemical Cell

The anode and cathode can be made out of any material, not necessarily only metals. In the case of capacitive deionization, the material is an inert carbon based solid (aerogel or other nanostructure). When two dissimilar metals with different electrochemical potentials are used as the anode and cathode, a current will flow in the external connection, without the need for a power supply (battery or voltaic cell). In a case where the anode is made from mild steel a typical anode reaction will be as follows:

$$Fe \rightarrow Fe^{+2} + 2e^{-} \quad \ldots\ldots(1)$$

The above-mentioned reaction is a typical corrosion reaction, taking place on the surface of steel in contact with an electrolyte. To balance the overall reaction, a cathodic half reaction is needed in both the cases of an electrochemical or voltaic cell. Typical reactions that take place at the cathode are as follows:

- Hydrogen Liberation: $2H^+ + 2e \rightarrow H_2$ …………………………………. (2)
- Acid Solutions - Oxygen Reduction: $O_2 + 4H^+ + 4e \rightarrow 2H_2O$………… (3)
- Basic/Neutral Solution Oxygen Reduction: $O_2 + 4H_2O + 4e \rightarrow 4OH^-$...(4)
- Metal Ion Reduction: $Metal^{+3} + e \rightarrow Metal^{+2}$ ……………………………(5)
- Metal Plating: $Metal^+ + e \rightarrow Metal$……………………………………….. (6)

The first three reactions are the most common, and the last two reactions only occur in certain conditions, typically when high concentrations of chromium, copper and/or zinc are present in the solution. Usually only wastewater from plating plants contains such high concentrations.

The above mentioned basic electrochemical principles are applicable to all electrochemical type water treatment technologies, including CDT™. Water treatment technologies either use the electrode in the solid state (e.g. Electrodialysis, electrodeionization and CDT™), or in the colloidal state (e.g. coagulation and flocculation) to achieve a specific water treatment goal. The goal is usually to remove an unwanted ion and/or particle from solution, thus purifying the electrolyte (water).

Electrode Surface Chemistry

When an object is electrically charged in an electrolyte (voltaic or electrolytic cell), an environment is created around the object, which has unique physical features. Such an object can be a solid-state electrode or a colloidal particle. There are interactions between the dissolved ions and the charged surface, the ions and the bulk liquid, and between the bulk liquid and the solid surface.

Water is a polar molecule, and is thus also electrochemically involved. The electrodes in capacitive deionization and other electrodes generally follow the electric double layer theory. This theory states that if an electrode is negatively charged and immersed in an electrolyte, then positively charged ions and solvent molecules (water in the case of this research) are adsorbed onto the surface, thus forming a layer of positive charge on the surface.

A second negative layer is formed by negative ions attracted to the positive charge, thus the double layer. The second layer contains less charge (negative) as compared to the total charge (positive) of the first layer. This is due to the effect of distance and shielding by solvent (water) molecules. Water molecules also undergo Brownian movement between the layers (Heald & Smith, 1974). **Figure 3.2** illustrates a simplified version of the Stern Double-Layer Theory.

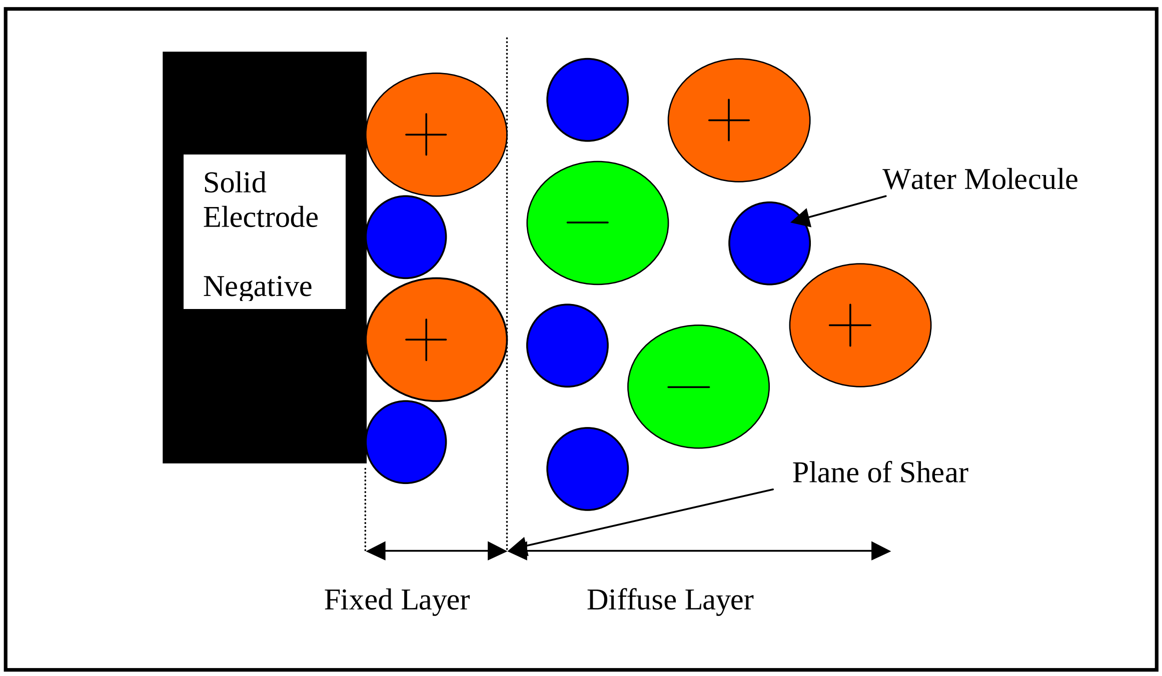

FIGURE 3.2: Stern Electric Double Layer Theory

Capacitance

Two parallel plates immersed in an electrolyte form a parallel plate capacitor. Electrical energy is stored in the capacitor when charged by an applied potential. The capacitance can be calculated by (Halliday & Resnick, 1988: 627):

$$C = Q/V \tag{3.1}$$

$$C = \frac{\kappa.\varepsilon_0.A}{d} \tag{3.2}$$

κ = Dielectric constant for a specific medium
= 80.4 for water at 20 °C and 78.5 for water at 25 °C

ε_0 = 8.85 x 10^{-12} $C^2/N.m^2$

A = Area of electrode plates

d = Distance between the plates

Capacitors can be connected in parallel or series, and the equivalent capacitance can then be calculated by:

$$\frac{1}{Ceq} = \sum_n Cn \qquad \text{Capacitors in Parallel} \tag{3.3}$$

$$\frac{1}{Ceq} = \sum_n \frac{1}{Cn} \qquad \text{Capacitors in Series} \tag{3.4}$$

3.2 CAPACITIVE DEIONIZATION

CDT™ utilizes all of the above-mentioned basic electrochemical principles to remove dissolved ions from an electrolyte (water) stream. **Figure 3.3** illustrates the basic operating principle applicable to CDT™.

An electrolyte stream flows between two electrodes. The electrodes typically have a potential difference of 1,2 – 1,5 volts (Direct Current). The various cations (positive charge) and anions (negative charge) in solution are attracted to opposite charged electrodes. The ions are adsorbed on the electrode surface and held in electric double layers (Stern Double Layer Theory). The normal operational cycle continues until the electrode surfaces are saturated with adsorbed ions.

During the regeneration cycle, the two electrodes are shorted, or to recover stored energy the capacitor can be discharged under controlled conditions. The ions are released into a rinse stream, which can have a much higher TDS level, as compared to the feed stream. CDT™ does not require high-pressure pumps, which contributes to the overall low energy requirements.

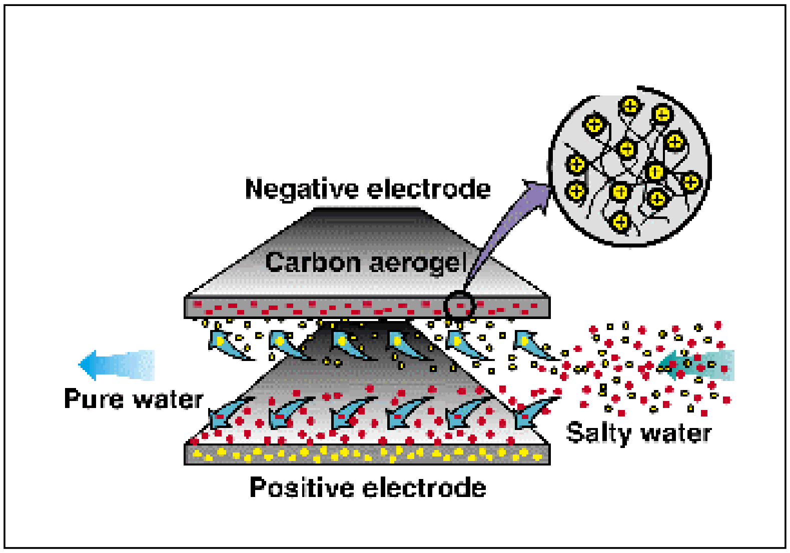

FIGURE 3.3: Illustration of Capacitive Deionization Process

Energy Requirement

The minimum theoretical work required by an isothermal process to separate seawater (35 000 mg/l) and brackish water (1 000 mg/l) into saturated brine and a 10 mg/l potable water stream can be calculated. The estimated minimum work required for desalination of seawater (35 000 mg/l TDS) and brackish water (1 000 mg/l TDS) are ~ 1,06 Wh/liter (4 Wh/gal) and 0,005 Wh/liter (0,02 Wh/gal) respectively (King, J.D, 1980 : 662).

The energy required by CDT™ is approximately $\left(\frac{Q.V}{2}\right).\left(1-e^{(-t/\tau)}\right)$, where Q is the stored electrical charge, V is the voltage between adjacent electrodes, t is the charging time, and τ is the time constant of the CDT™ module.

The time constant is determined by the internal resistance and capacitance of the CDT™ cell (Farmer[5],1995). Earlier laboratory work by Dr. Farmer and his team at LLNL determined that CDT™ could effectively desalinate brackish water (1 000 mg/l) by using only 0,095 kWh/m^3 (0,36 Wh/gal). This laboratory CDT™ unit energy requirement served as a benchmark for the industrial prototype unit.

3.3 CARBON AEROGEL ELECTRODES

Carbon Aerogel is an ideal electrode material because of its low electrical resistivity (< 40 mΩ cm), high specific surface area (400 – 1 100 m^2/g), and controllable pore size distribution (<50 nm). Aerogels are unique materials. They are known for their extremely low density, but because both their pores and particles are smaller than the wavelength of light, they have other important properties. Aerogels can be transparent, giving rise to the nickname "frozen smoke”.

Discovered in the 1930s, they were initially thought to have no practical use. However, new and improved processing techniques, and newly developed varieties are beginning to prove their commercial potential.

Aerogels can be made using several different compounds including silica, other metal oxides, resorcinol-formaldehyde (RF) and melamine-formaldehyde (MF). The RF and MF aerogels are pyrolized to form carbon aerogels. Each of these various aerogels was created for specific properties:

- Silica Aerogels - nonflammable, nontoxic, lightweight, transparent, and thermally stable to about 650°C, almost 30 times lighter than earlier aerogels, and possessing unique thermal and dielectric properties.
- Organic Aerogels (Carbon Aerogels) - created for their thermal capabilities, stiffer and stronger than silica aerogels. Carbon allows aerogels to become electrically conductive.
- Other Metal Oxide Aerogels

LLNL has been active in the development of carbon, silica and metal oxide aerogels. LLNL has developed patented methods for tailoring aerogel properties. These materials:

- Contain exceptionally large internal surface areas - 400 to 1 000 m^2/g - about the size of one to two basketball courts
- Provide exceptional mechanical integrity, supporting over 1 500 times their own weight
- Provide exceptional optical clarity
- Are exceptionally poor conductors of heat and sound
- Can be manufactured with a low density so that it is nearly as light as air

Carbon aerogel can be produced as monoliths, composites, thin films, powders and microspheres. **Figure 3.4** illustrates a spherical carbon aerogel structure, magnified 300 times.

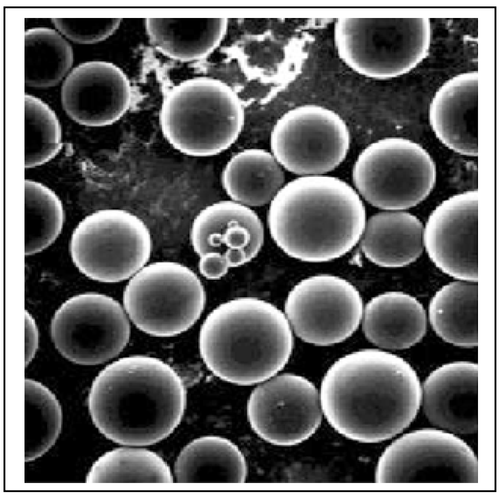

Scanning electron micrograph of carbon microspheres (300x). Although the aerogel structure within the microspheres cannot be delineated, it is clear that the particles are spherical with smooth surfaces.

FIGURE 3.4: Micrograph of Aerogel Microspheres

Monolithic aerogels are ideal for applications such as transparent window insulation, but the expensive processing equipment needed to produce these large aerogels has limited their commercial appeal.

Aerogel microspheres offer an attractive alternative to monolothic aerogels because they can be produced in a semi-continuous process. Silica microspheres have been produced commercially, and their thermal performance is known. Air-filled, thermal conductivities for monolithic aerogels are 12 m.W/m·K; for silica microspheres, they are 20 m.W/m·K.

Currently CDT™ utilizes a resorcinol-formaldehyde (RF) aerogel. Resorcinol-formaldehyde (RF) and melamine-formaldehyde (MF) microspheres should have even better thermal properties because their solid conductivity is lower than that of silica. RF microspheres can also be pyrolyzed in an inert atmosphere to produce carbon aerogel micro-spheres with properties different from those of conventional carbon blacks. Gas adsorption measurements reveal the microspheres to have cell-pore sizes greater than 100 nm and surface areas from 400 to 1 100 m^2/g - similar to those of their monolithic counterparts. The solid matrix within the aerogel microspheres is composed of interconnected colloidal like particles or fibers with characteristic diameters of 10 nm. **Figure 3.5** shows a magnified version of the carbon fibers.

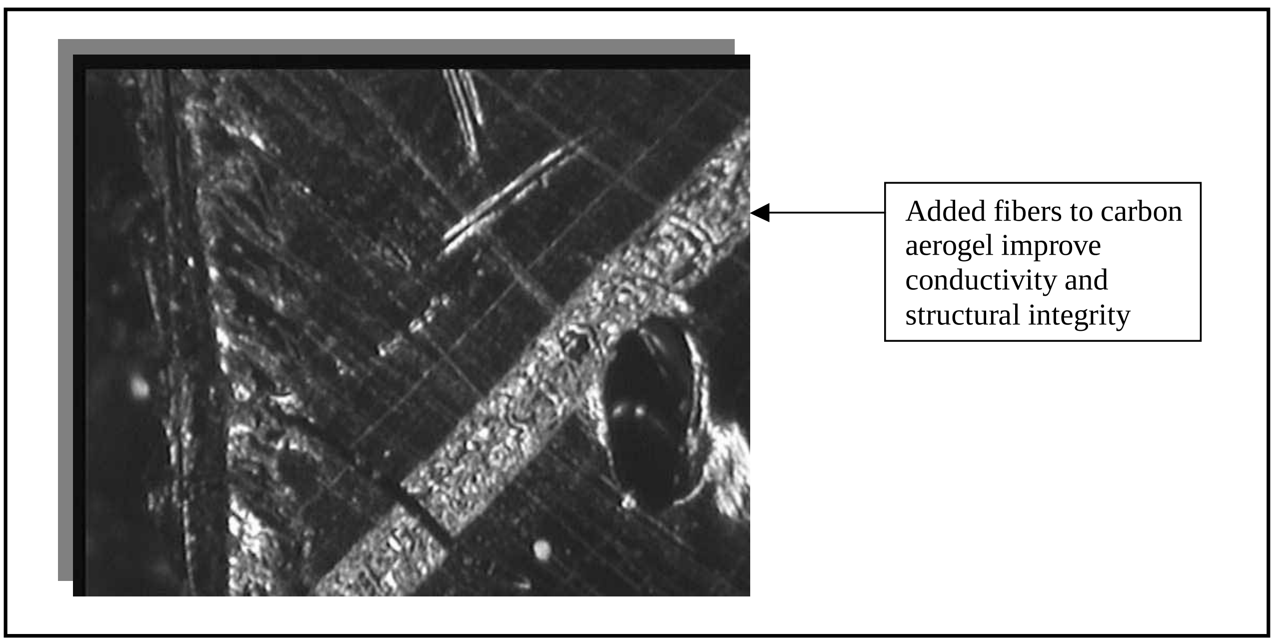

FIGURE 3.5: Magnified Aerogel Fibers

3.3.1 ELECTRICAL PROPERTIES

Dielectric Properties

Highly porous materials with unique nanostructures, aerogels exhibit unusual dielectric properties that are more like those of a gas than of a solid.

Their low dielectric constants, low loss tangents, and controllable thermal expansion properties will soon make aerogels the material of choice for thin films in high-speed, integrated digital and microwave circuitry.

- Dielectric constants of 1,008 to 1,990 (3–40 GHz)
- Loss tangents of 10^{-4} to 10^{-2} (3–40 GHz)
- Volume resistivities of 10^{13} to 10^{15} Ohm·cm
- Dielectric strengths of 120 to 140 kV/cm.

3.3.2 PHYSICAL PROPERTIES

Aerogels are the best thermal insulators available today. Two organic aerogels developed at LLNL have equivalent R-values of 12 when air-filled (equivalent to the insulating capacity of 152 mm (6 in.) of fiberglass batting) and greater than 38 when evacuated (equivalent to 483 mm (19 in.) of fiberglass). **Figure 3.6** shows the thermal conductivity of various types of aerogels and their associated relative densities.

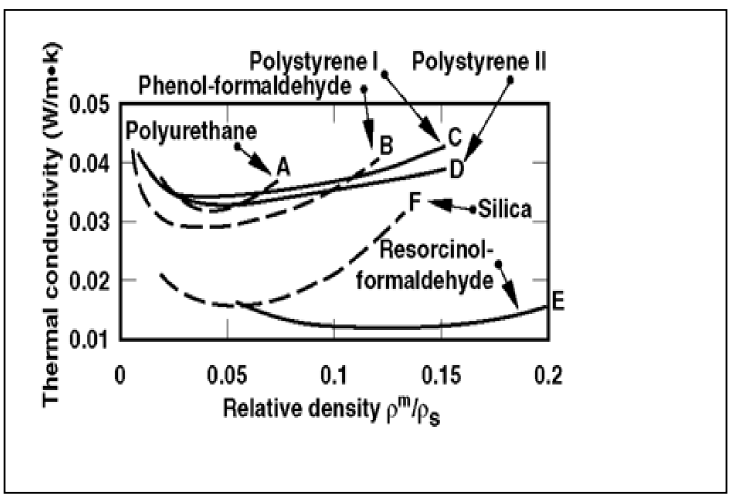

Aerogels are highly efficient, lightweight, and transparent insulating materials. Lightweight aerogels are much better insulators than common foams.

FIGURE 3.6: Thermal Conductivity of Aerogels

Measurable, low thermal conductivities:

- Silica aerogels at 300 °K and 1 atm have measured conductivities as low as 0,020 W/m·K (an R per inch value of about 7).
- Organic aerogels, like the existing RF aerogels in CDT™ have thermal conductivities of 0,012 W/m·K (an R per inch value of 12).
- Carbon particle-loaded (opacified) silica aerogels have thermal conductivities of 0,013 W/m·K (an R per inch value of 11).

Organic aerogel materials have lower intrinsic thermal conductivity than silica, and up to a factor of four higher infrared extinction coefficients than unmodified silica aerogel. Adding carbon particles to the silica aerogel decreases the dependence of the thermal conductivity on temperature. The dependence of thermal conductivity on density shows that conductivity is minimum at an optimal density, typically about 0,15 g/cm^3.

The unique microstructure of aerogels - nanometer-sized cells, pores, and particles - means low thermal conduction and superior insulation. Thermal conduction through the solid portion of the aerogel is limited by the small connections between the particles making up the conduction path. Gaseous conduction is limited because the cells/pores are only the size of the mean-free path for molecular collisions - molecules collide with the solid network as frequently as they collide with each other. Radiative conduction is low because aerogels have small mass fractions and large surface areas, although conductivity increases with temperature. This feature makes CDT™ an ideal candidate for water treatment at high temperatures, like fuel cells or condensate treatment.

CHAPTER 4

INDUSTRIAL PROTOTYPE DEVELOPMENT PROCESS

4.1 BASIS OF DESIGN

As stated in Chapter 1, the main objective of this research was to take CDT™ from laboratory scale to a "real world" industrially reproducible prototype scenario. The research conducted for this dissertation regarding the design, manufacturing, and testing of an industrial prototype, would serve as a foundation to future commercialization efforts and industrial pilot scale testing projects. In order not to re-invent the wheel, the main components of the technology as identified by the original laboratory research conducted at Lawrence Livermore National Laboratories were used as a starting point in the development an industrial prototype.

Physical size and weight constraints limited the maximum practical size of a full-scale industrial CDT™ cell. To assist with future design/construction of industrial plants, and to ensure that a single treatment module is of a practical size, the design team decided that the basis for the design of an industrial unit is to be 1 000 ft^2 (92,9 m^2) of aerogel/electrode surface area. Earlier laboratory test work indicated that on average, such an electrode surface area should be able to reduce the TDS of a feed stream by 1 000 mg/l at a flow rate of 1 000 gallons per day (3 785,4 liters per day). This basis of design would also make future scale-up formulations, more linear.

The above mentioned electrode surface area of 1 000 ft^2 (92,9 m^2), should be viewed as a maximum and it is possible, that as the technology is developed further, the water production capacity per module would increase, due to material and module design improvements. For the development process, it was decided to make the industrial prototypes as a fraction of the above-mentioned maximum. Such a step would allow the development team to design, manufacture and evaluate various alternatives to optimize the prototype to be evaluated. The prototype was around $1/40^{th}$ (per total aerogel surface area) the planned size of a full-scale industrial unit, with a total electrode surface area of ± 24,7 ft^2 (2,29 m^2).

LLNL laboratory experiments were conducted by utilizing extremely thin carbon aerogel films in expensive titanium housings. **Figure 4.1** illustrates the first laboratory scale capacitive deionization module developed by Lawrence Livermore National Laboratory.

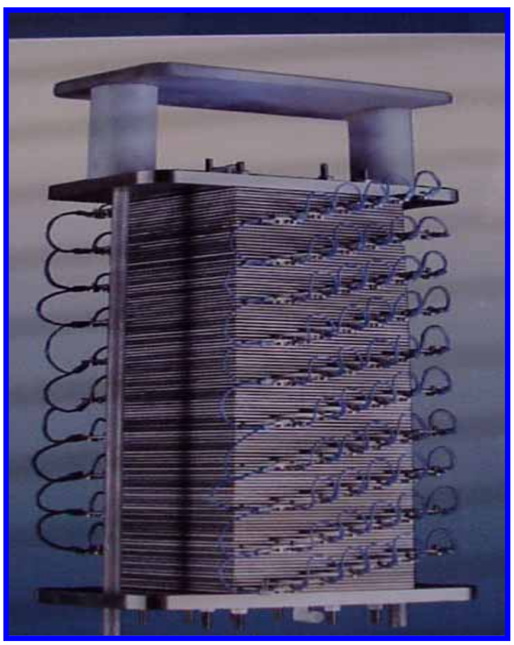

FIGURE 4.1: Laboratory Scale Capacitive Deionization Module : LLNL

Although these initial experiments were very successful ((Farmer[1], 2000; Farmer[2], *et al*, 1995; Farmer[3], *et al*, 1996; Farmer[4], *et al*, 1995; Farmer[6], *et al*, 1997; Farmer[7], *et al*, 1995; Farmer[8], *et al*, 1996), the technology still needed to be taken to the next level to prove cost effective industrial scale manufacturing and operation in a "real world" environment.

4.2 THE DEVELOPMENT PROCESS

The development (designing, engineering and manufacturing) process can be broken-down into three phases. The three phases are discussed in paragraphs 4.2.1, 4.2.2 and 4.2.3, and can be summarized as follow:

Phase 1: Electrode Manufacturing Process Development

During this phase, the aerogel electrode pilot manufacturing process was established. The researcher functioned as a resident chemical engineer during this phase, to assist with the design and construction of the resorcinol/formaldehyde aerogel manufacturing process. Due to the hazardous nature of the manufacturing process, the researcher was also the lead environmental engineer, responsible for air quality monitoring and treatment to comply with the United States Environmental Protection Agency (USEPA) requirements.

Phase 2: Cell/Module Manufacturing Process Development

During this phase the aerogel electrodes manufactured in phase 1, needed to be stacked and housed in a single module. A module thus needed to consist of a series of electrode pairs, with each pair making-up the anode and cathode of a capacitor.

During this phase, the researcher worked with an electro-mechanical engineer in producing the housing module design specifications and drawings. Specifications and drawings were submitted to a machining contractor for final manufacturing. Once manufactured, the researcher assisted in final assembly and quality control operations.

Phase 3: Control System Development

Once an industrial prototype alternative is successfully manufactured, it was needed to "plug" it into a control system to evaluate it's water treatment efficiency. A control system was developed to switch between the two main cycles, which is operation and regeneration. During this phase the researcher collected and interpreted water treatment efficiency data for an instrumentation and control specialist, who was responsible for the electronic circuit design of the control system. Water samples were taken during operational and regeneration cycles, analysis was conducted and the data was used to optimize instrumentation and control specifications.

The end result of completing the above mentioned three phases, for various alternatives, was an operating industrial prototype system, ready for more intensive water treatment testing and the basis of design for future full size industrial units. The three development phases are discussed in more detail during the following three paragraphs, 4.2.1, 4.2.3 and 4.2.4. It should be noted that the following description of the manufacturing process is a summary, a lot more information was developed during this research period, but could not be published due to the propriety nature of the technology.

4.2.1 ELECTRODE MANUFACTURING PROCESS – PHASE 1

The aerogel originally used in laboratory experiments were paper thin and within titanium frames (See **Figure 4.1**). The laboratory scale method of construction was not cost effective for an industrial type unit. Therefore an electrode pilot manufacturing process was developed that represented a typical full scale manufacturing process. The raw materials for the manufacturing of carbon aerogel electrodes used in this research project are formaldehyde, resorcinol, and carbon fiber veil. A pilot electrode manufacturing process was constructed in Tucson, Arizona and can be described as per the following three stages:

Stage 1: Polymerization

During this stage, carbon fiber veil is trimmed in sections and set in a polypropylene mold. Next a formaldehyde/resorcinol resin was prepared via a batch mixing operation in 5-gallon (18.93 liter) batches. The carbon veil was placed in a polypropylene molds. The veil was soaked with the resin and the molds containing the resin/carbon veil sheets were staked in a drying oven.

The polymerization process was completed in a temperature controlled (85ºC) oven over a period of 48 hours. The cured sheets were removed from the molds and solvent washed to eliminate any impurities and retained water. The solvent extracted sheets were then air-dried in ambient temperature.

Stage 2: Pyrolization

The air-dried polymerized sheets where then stacked in a furnace and connected to nitrogen gas to ensure a non-oxidizing environment.

The furnace temperature was controlled at 1 000°C for 72 hours. After pyrolization, the sheets were retort cooled in ambient temperature.

Stage 3: Cell Assembly

The carbon aerogel sheets were now ready to be stacked and included as electrodes in a specially machined polypropylene housing. A series of stacked electrodes in the polypropylene housing are known as a cell.

Electrode Production Quality Control

As in any manufacturing process, a quality control system had to be developed. After the manufacturing of the aerogel electrodes, a quality control test was conducted to ensure that the electrodes to be used in the prototype unit conformed to certain minimum standards.

Due to the fact that each pair of electrodes acts as a capacitor, the total energy stored and discharged from a electrode pair is measurable. The total potential capacitance of a series of electrodes or a cell can be calculated using equations 3.1 or 3.2 in Section 3. The energy storage capacity of an electrode is directly proportional to its ion storage capacity. A small quality control test unit was constructed whereby each batch of carbon aerogel produced could be quality controlled. One random sheet per batch were chosen and two 25 mm x 25 mm pieces were cut from the sheet. The two pieces of electrode where submerged in a 10 000 mg/l NaCl solution, at a fixed distance from each other. Energy to (capacitor charge cycle) and from (capacitor discharge cycle) the test capacitor could be determined by measuring the current (I) to the capacitor and potential difference (V) across the capacitor at fixed time intervals.

For the regeneration cycle, the capacitor was discharged through a resistor, and the associated energy calculated by means of the resistor size as well as the measured discharged current. The equations used to determine the energy for the charge and discharge cycles were as follows:

$$\mathbf{E = \mathit{V} \times I = I^2 \times R} \qquad \textbf{(4.1)}$$

Equation 4.1 was then used to generate quality control graphs, as illustrated in **Figure 4.2** for each batch of electrodes. **Figure 4.3** illustrates the laboratory set-up used to generate quality assurance data during electrode production.

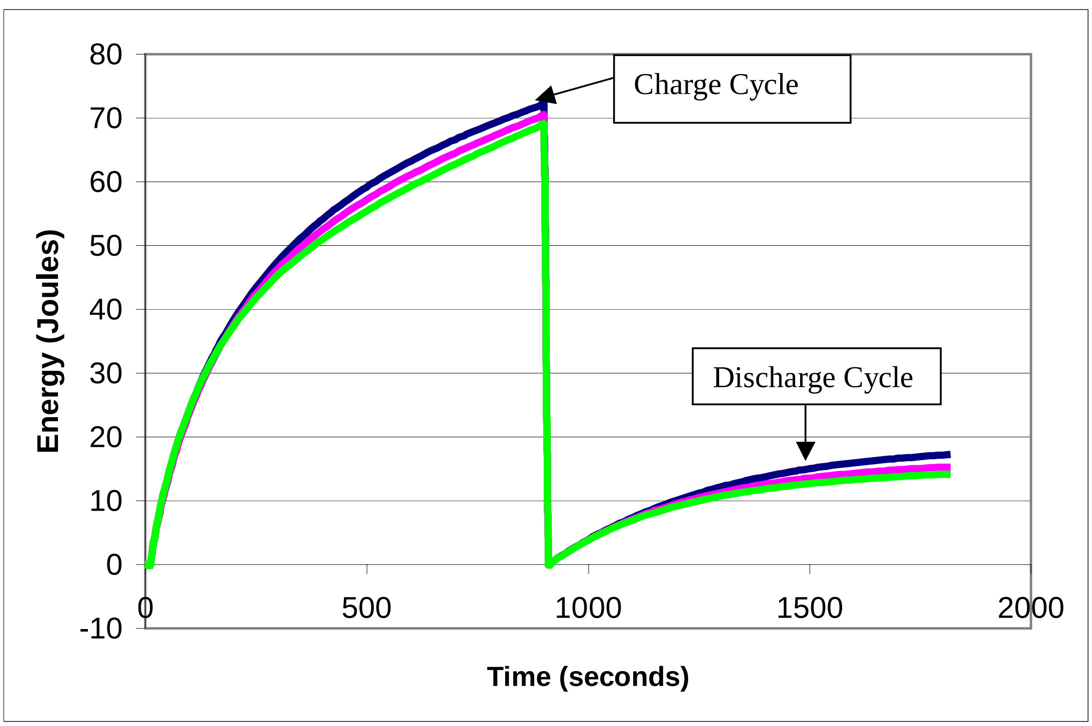

FIGURE 4.2: Electrode Quality Assurance Test: Charge & Discharge Cycles

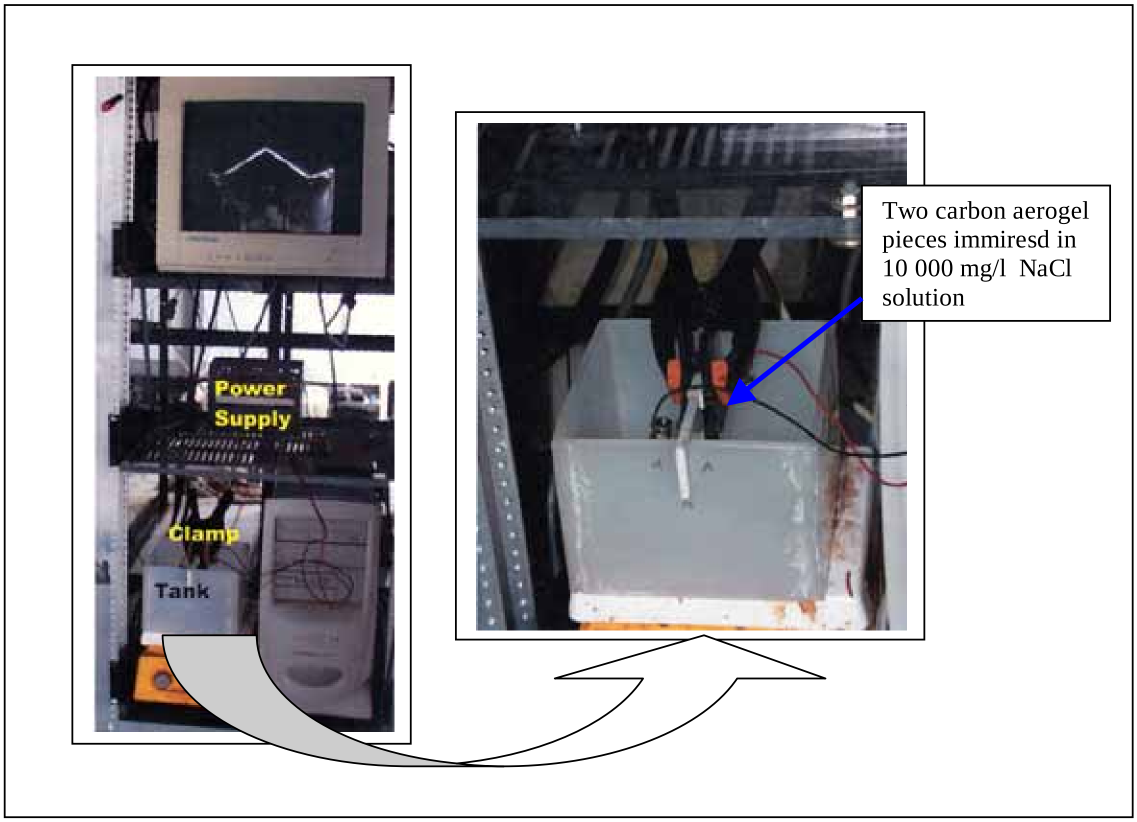

FIGURE 4.3: Electrode Quality Assurance Test Set-Up.

Appendix A contains typical quality control log sheets and data sets collected. The aerogel density was also checked as a quality assurance procedure. The average density was 0,78 g/cm^3. The aerogel sheets were then cut/trimmed into the following dimensions:

Length: 301,24 mm (11,86 inches)

Width: 158,75 mm (6,25 inches)

Thickness: 0,8128 mm (0,032 inches)

Various numbers of electrodes were tested and the optimum prototype unit, named MK-8A contained 24 sheets of electrodes (12 Cathodes + 12 Anodes).

This means that the total electrode area inside the unit, accessible to ions, was 2,29 m^2 (24,7 ft^2) or nearly 2.5 % (1/40th) of a future full scale industrial unit (92,9 m^2 or 1 000 ft^2). The aerogel produced during this research had the following typical physical and electrical characteristics:

Avg. BET Surface Area	: 600 m^2/g
Bulk Resistivity	: 20 m ohm cm
Specific Capacitance	: > 2 Farad/cm^2

4.2.2 CELL MANUFACTURING PROCESS – PHASE 2

The basic building block the industrial module/cell is a single electron pair. A pair of aerogel electrodes forms a basic capacitor. An industrial module will need to consist of multiple electrode pairs/capacitors inside a durable housing.
As no high pressures are required, the module design pressure could be low. It was decided to use 41,3 kPa (6 psi) as the module design pressure.

It is necessary to control the potential difference over each cell at relatively the same voltage. Therefore, a monopolar electrode arrangement, connected in parallel, was chosen for the electrode pair wiring arrangement inside the module. **Figure 4.4** illustrates a typical monopolar cell-wiring diagram, as used for the CDT™ prototype.

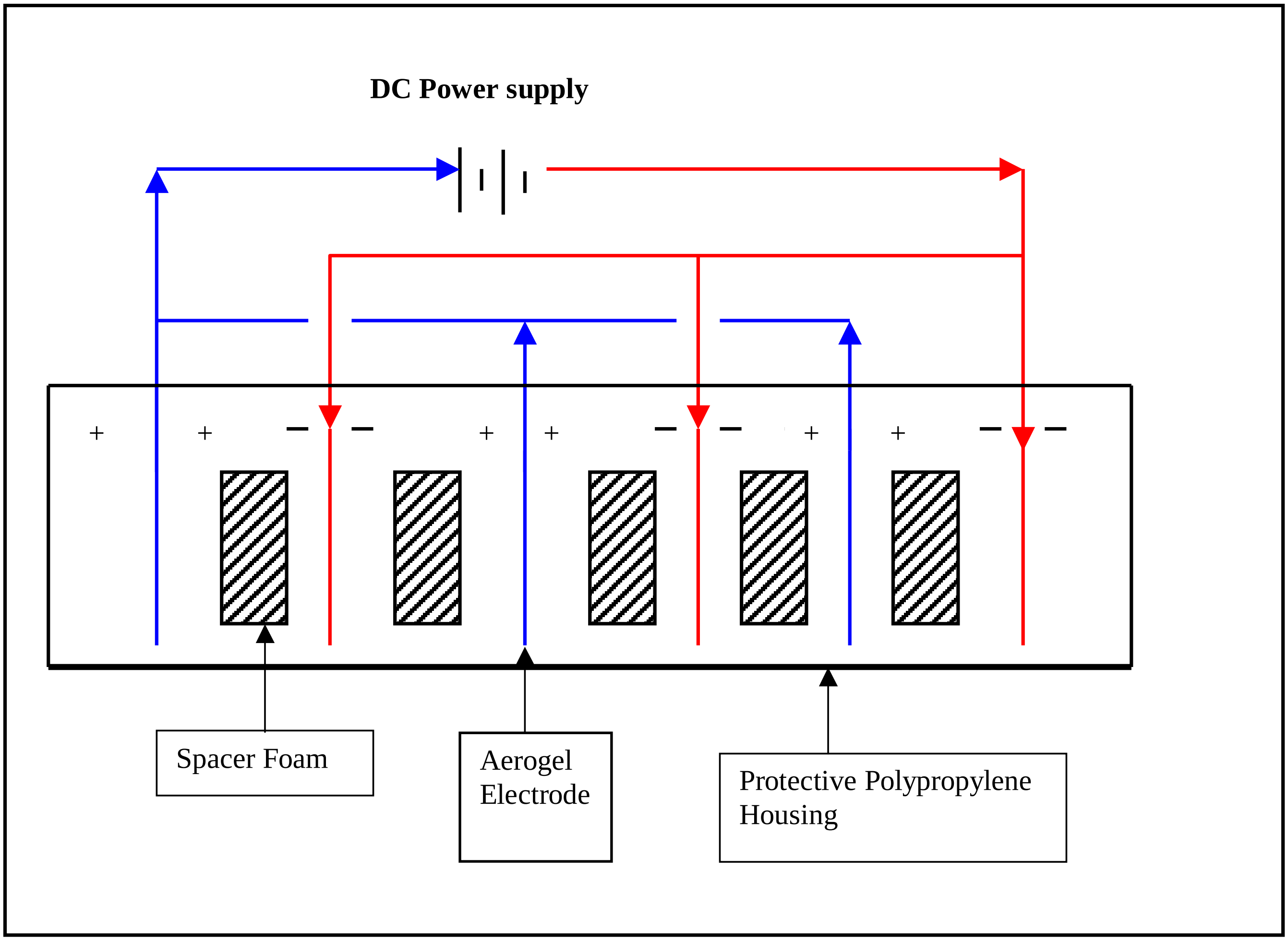

FIGURE 4.4: Typical Monopolar Cell Wiring Arrangement

The distance between each electrode is ± 0,8 mm (0,032 inches). Using non-conductive spacer foam between each electrode pair prevented short circuiting effects. The path that the water stream follows is between each electrode pair, through the spacer foam matrix (out of the page).

The cell arrangement as shown in **Figure 4.4** has several advantages:

- The potential difference over the entire module and between adjacent electrodes can easily be controlled at the required low values of 1,2 to 1,5 Volts. This low voltage arrangement makes it safer for operational personnel.
- Uniform conditions exist between all electrode pairs, thus ensuring a more uniform ion adsorption environment.
- Should fouling occur between one electrode pair, it won't influence the operation of the other pairs.
- All electrodes (except two at the end) are flanked by electrodes of the opposite charge, thus reducing losses due to electrical stray currents.

Monoplar electrodes in parallel do have some disadvantages as well.

- In industrial applications, large currents will be needed. This means very thick conductors from the power source to the cells.
- Generation of large electrical currents at low voltages is not ideal.
- A short between one electron pair is detrimental to the efficiency of the entire module.

Various other cell arrangements exist, but did not form part of this dissertations scope. In summary stacking 24 carbon aerogel electrodes and their associated electrical bus connections inside a polypropylene housing was the method used to manufacture the prototype unit. Maintaining to a simple manufacturing process was an objective. **Figure 4.5** illustrates the assembly of the preferred prototype (MK-8A).

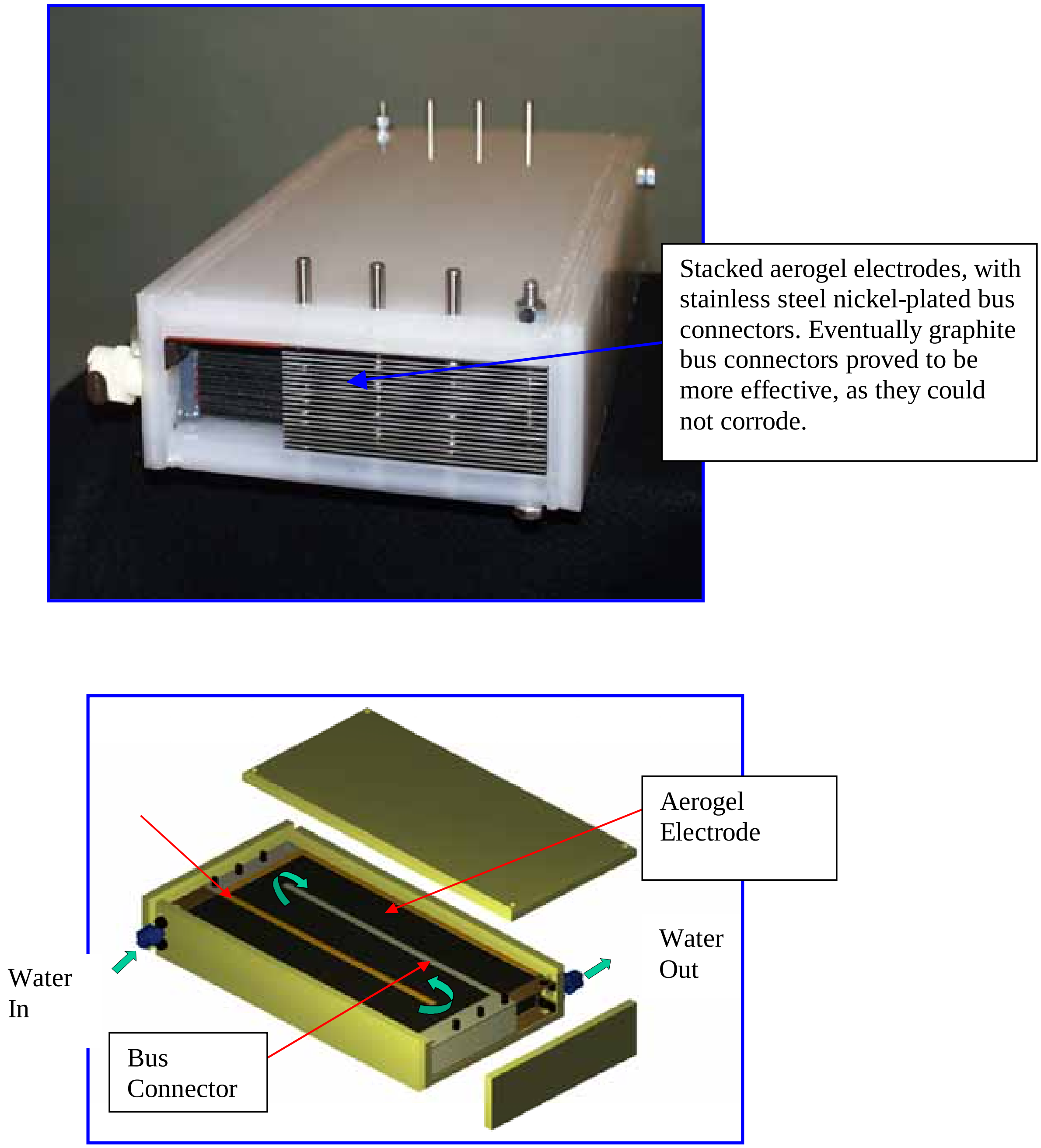

FIGURE 4.5: Industrial Prototype (MK-8A): Module Assembly

The first prototypes had stainless steel bus connections. Bus connections are the electrical connections to the electrode, dictating to the electrode to function as a cathode or anode. The high electrical currents and high salinity of the electrolytes created a very corrosive environment, even for stainless steel. **Figure 4.6** illustrates the stainless steel corrosion problems encountered. The final prototype module bus connections were machined from graphite and proved to be more effective than their stainless steel predecessors. Chapter 5 illustrates in more detail the benefits that were seen by using graphite instead of stainless steel as bus connector manufacturing material.

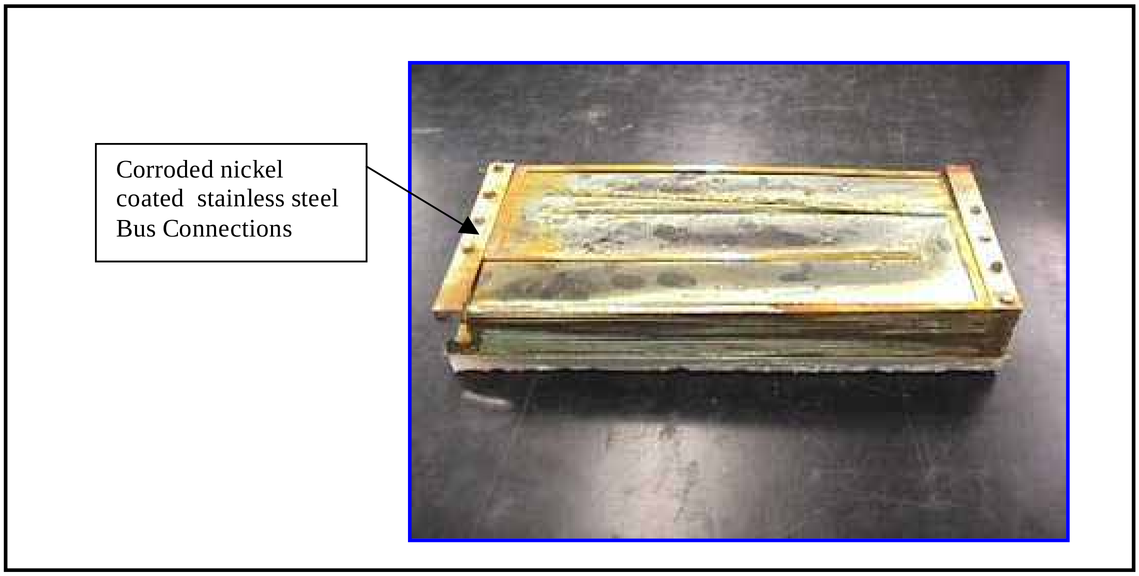

FIGURE 4.6: Stainless Steel Bus Connections : Corrosion Problem

Appendix B contains more detailed technical bulletins regarding the cell developmental process, with the final material of choice being graphite bus connectors in the MK-8A prototype module.

4.2.3 CONTROL SYSTEM DEVELOPMENT – PHASE 3

After the successful manufacturing of a prototype unit, it was necessary to develop a control system to operate the prototype during the evaluation phase. The control system had to have basically two flow paths, a once through scenario and a recycle scenario. **Figure 4.7** illustrates the overall control system set-up used for the prototype water treatment evaluation test runs.

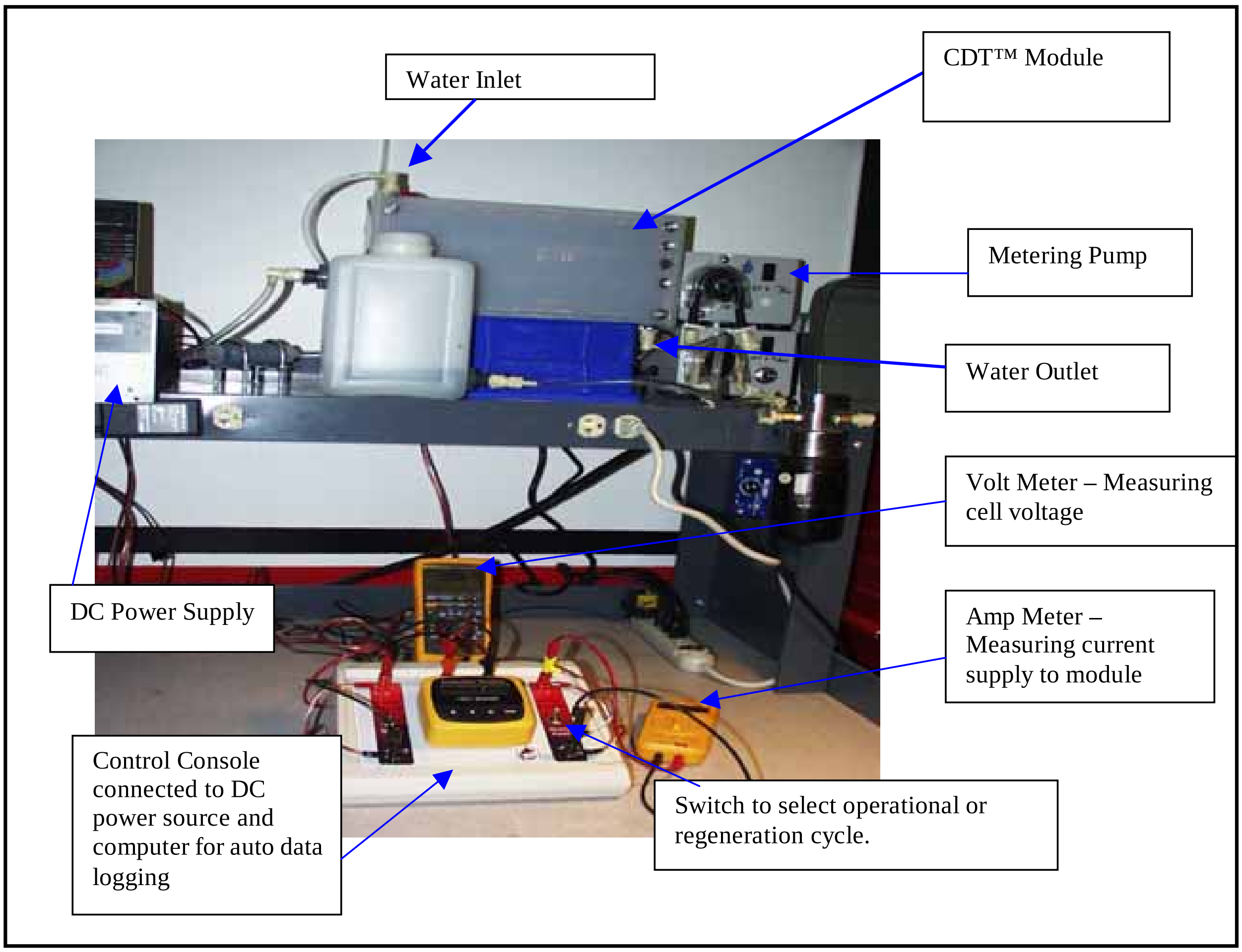

FIGURE 4.7: Prototype Control System Set-Up

A DC power supply was connected to the control console, and from the control console the DC power supply was connected to the cathode and anode connections of the prototype. The basis of all test runs was to monitor conductivity change of a metered feed stream, and the associated voltage and current requirements as a function of time.

Voltage and current as a function of time were automatically recorded on a computer. **Appendix A** contains an example of typical voltage and current data as a function of time. Once data has been recorded, a mass and energy balance was performed to determine the following main evaluation criteria:

- The quantity of ions adsorbed and at what rate (water production rate)?
- The quantity of energy required to adsorb the ions?

The control console, shown in **Figure 4.7** made it easy to switch from an operational cycle to a rinse cycle. Cutting the DC power to the brick and shorting the cathode and anode terminals, while a rinse stream was pumped through the cell, stopped an operational cycle and started a rinse cycle. Conductivity probes at the cell inlet and outlet ports were used to measure and record conductivity data. **Figure 4.8** illustrates a typical control system for a future industrial scale CDT™ operation. A typical industrial size plant would consist of pre-treatment, CDT™ modules, post-treatment and an overall control system.

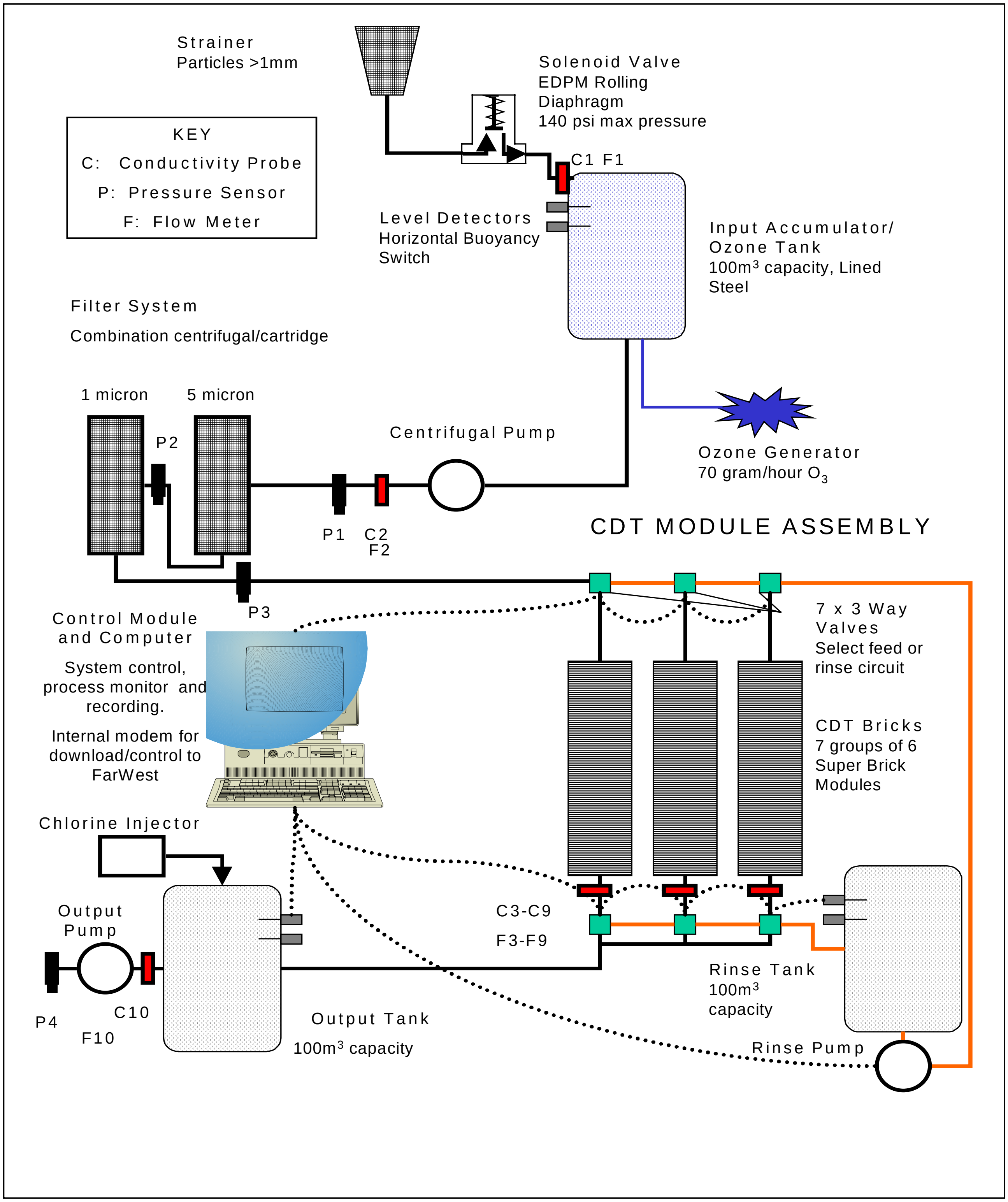

FIGURE 4.8: Typical Process Flow/Control Diagram of a Future Industrial Scale CDT™ Plant

CHAPTER 5

TEST METHODOLOGY, RESULTS AND DISCUSSION

5.1 LABORATORY FACILITIES

The laboratory test work conducted for this dissertation was performed in two locations. The main laboratory was in Tucson, Arizona (USA) and a second laboratory in Carlsbad, California (USA). During this phase, AirWater, Inc. in Otsuka, Japan conducted some supporting test work, under the guidance of the CDT Systems, Inc. research and development team. Results obtained from test work conducted in Japan, are referenced accordingly.

Laboratory test results can be divided into two main categories. Results obtained from developing the industrial prototype bench scale unit, and results from evaluating the prototype as a potential alternative desalination technology. Test work during the developmental stages mostly focused on electrode quality control and optimization of electrical connections and energy efficiency. After the development of an optimum prototype unit, the test work focused on evaluating capacitive deionization as a potential industrial scale desalination technology.

5.2 METHODOLOGY

Figure 4.6 in Chapter 4 illustrates the typical set-up for test work during the module development and technology evaluation phases. Conductivity probes in the inlet and outlet lines were used to measure solution conductivity. A volt and an amp meter were used to measure the electrical data required to determine energy consumption. A control console allowed for rapid change from a production/charge cycle to a regeneration/discharge cycle. Electronic wiring of the control console also allowed for automatic data logging of time, conductivity, bus voltage and current supplied during each test run. Graphical interpretations of typical capacitive deionization test data always have two main cycles.

Outlet water stream conductivity is decreased to below the inlet conductivity during the operational cycle, which is a result of ions being adsorbed into the electric-double layer on the electrode surface. The outlet water conductivity increases to above the inlet conductivity during the regeneration cycle, as the adsorbed ions are removed (washed-off) from the electrode surface. Rate of ion adsorption, associated energy consumption, overall water recovery and general operations & maintenance requirements, were used as the fundamental comparative factors in comparing capacitive deionization to other existing desalination technology's.

The following two sections in this chapter present and discuss the typical test results obtained during the prototype development and evaluation phases. During the development phase various tests had to be conducted to come-up with an optimum prototype design. Once the development phase results researched set criteria of performance, the optimum prototype was further tested and evaluated in more detail to determine the technologies potential as an industrial desalination technology.

Electrical conductivity probes were used to determine salt content. However for the purpose of comparison the following conversion factor can be used to convert conductivity to TDS in mg/l. Salt content as a conductivity reading in µS/cm (micro-siemans per centimeter) can be converted to TDS in mg/l by multiplying by 0,7. It must be noted that this factor will differ between source water's, but for most source water's tested during this research project it proved accurate enough.

5.3 RESULTS – PROTOTYPE DEVELOPMENT PHASE

The main objective of this phase was to develop a prototype, which could be manufactured and operated cost effectively on an industrial scale. Tests on the manufactured aerogel for quality control purposes were already discussed in Chapter 4. Results discussed here focus more on the quality control of the overall module development. **Appendix's A and B** contains detailed data and calculation methods used to produce graphical results discussed in this section, as well as applicable additional data.

One of the main challenges during the development phase was to ensure optimum electrical connection between the aerogel electrodes and their associated bus connectors. Various materials where tested for use in the manufacturing of the bus connectors. **Figure 5.1** illustrates the effect of changing the bus connection material from nickel-plated stainless steel (metallic) to graphite.

Similar **Figure 5.2** illustrates the ion adsorption improvement of the prototype by changing from a metallic to a graphite bus connector. A once-through system set-up conducted test runs for both **Figure 5.1 and 5.2**, with conductivity of the output water measured.

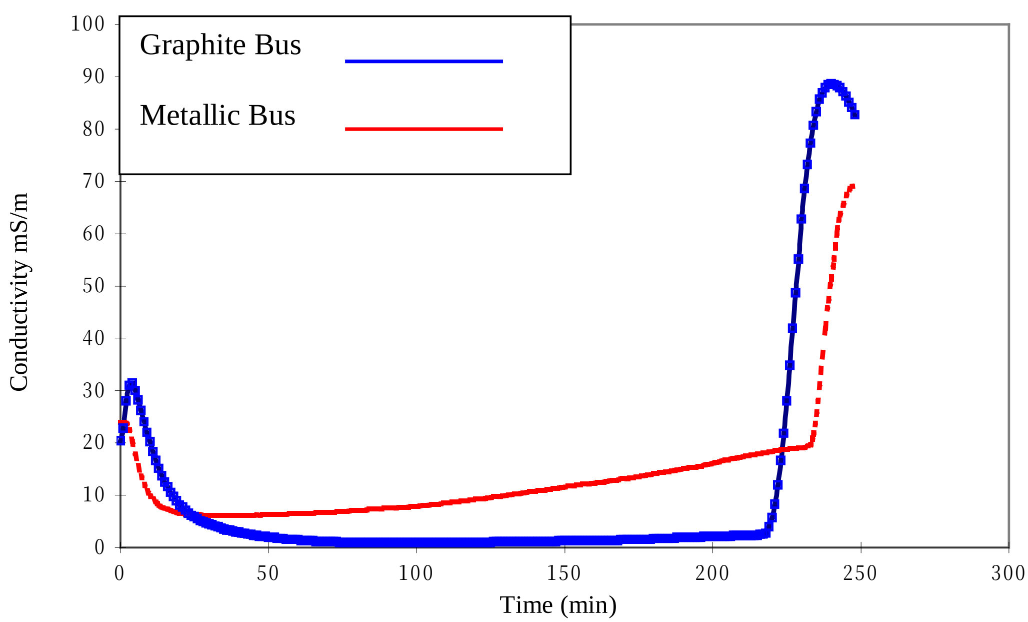

FIGURE 5.1: Nickel Plated/Stainless Steel vs. Graphite Bus Connections - A

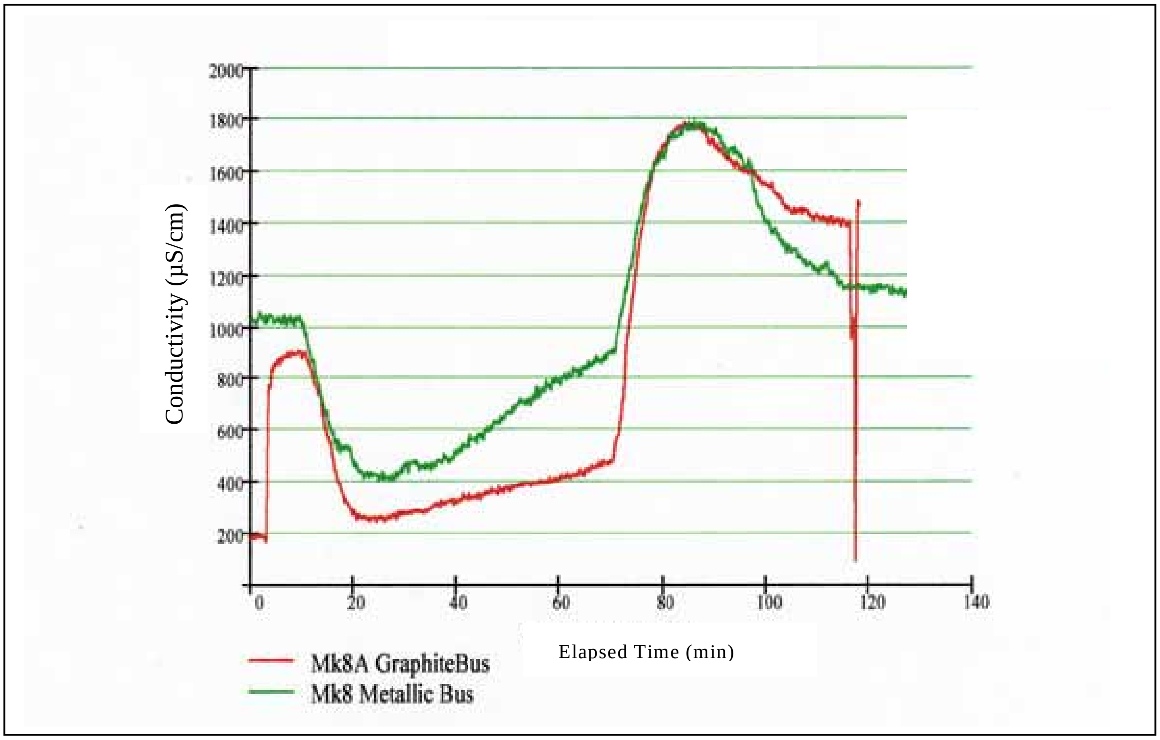

FIGURE 5.2: Nickel Plated/Stainless Steel vs. Graphite Bus Connections - B

Data presented in **Figure's 5.1** and **5.2** were generated by using a MK-8A prototype at a constant flow rate of 50 ml/min. The usage of graphite instead of stainless steel/nickel-plated bus connectors had an improved ion adsorption effect. It is noted that by the time the regeneration cycle was started (around 72,5 minutes), that the MK-8A prototype was not fully saturated as was the case for the metallic bus connector prototype (MK-8).

The next step of comparing bus connector efficiencies was to conduct continuous cyclic tests. **Figure 5.3** illustrates the results obtained from repetitive long term testing of two prototype modules, one containing stainless steel nickel plated bus connectors and the other the more efficient graphite connectors. The feed water conductivity was 22 mS/m (220 µS/cm).

Cyclic tests were conducted by measuring the prototype output conductivity and by switching between charge and discharge cycles. Adsorbed ions are washed off the electrode surface during the discharge cycle, therefore the increase in conductivity to above the feed conductivity.

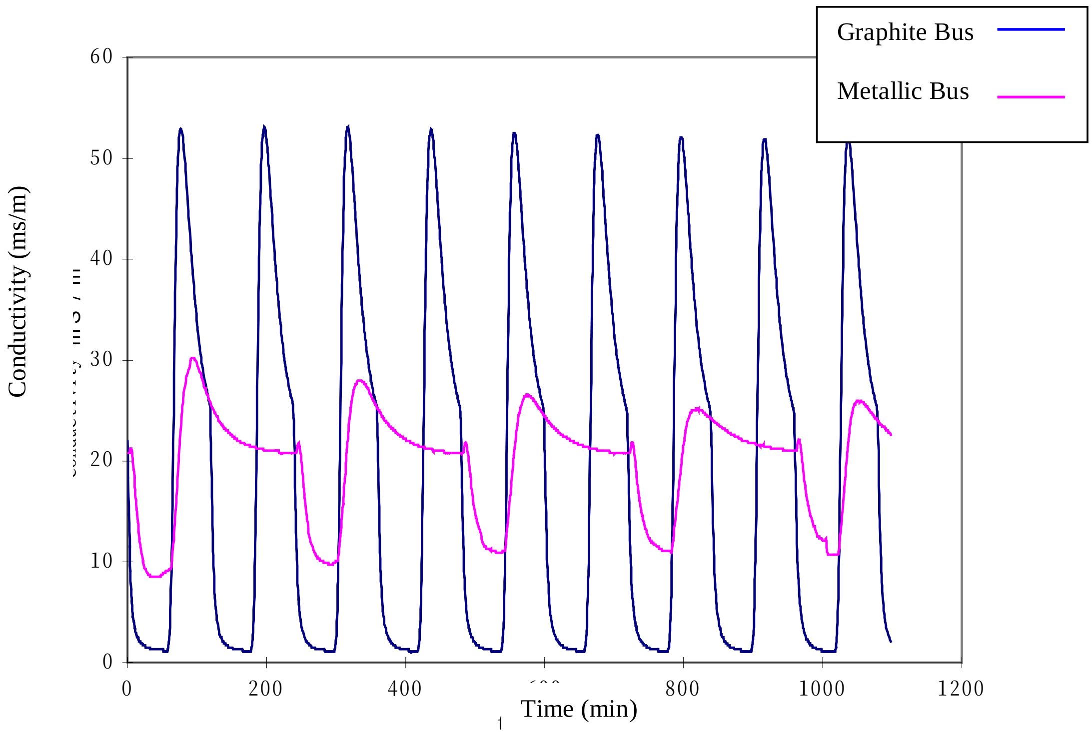

FIGURE 5.3: Repetitive Cycle Testing: Bus Connector Optimization

The higher peaks and deeper valleys of the graphite bus connector prototype, indicate more efficient ion adsorption and regeneration per unit time. **Figure 5.4** illustrates the typical charge and discharge cycles used in CDT™. The flow rate used to generate the data for **Figure 5.4** was 50 ml/min through the MK-8A prototype.

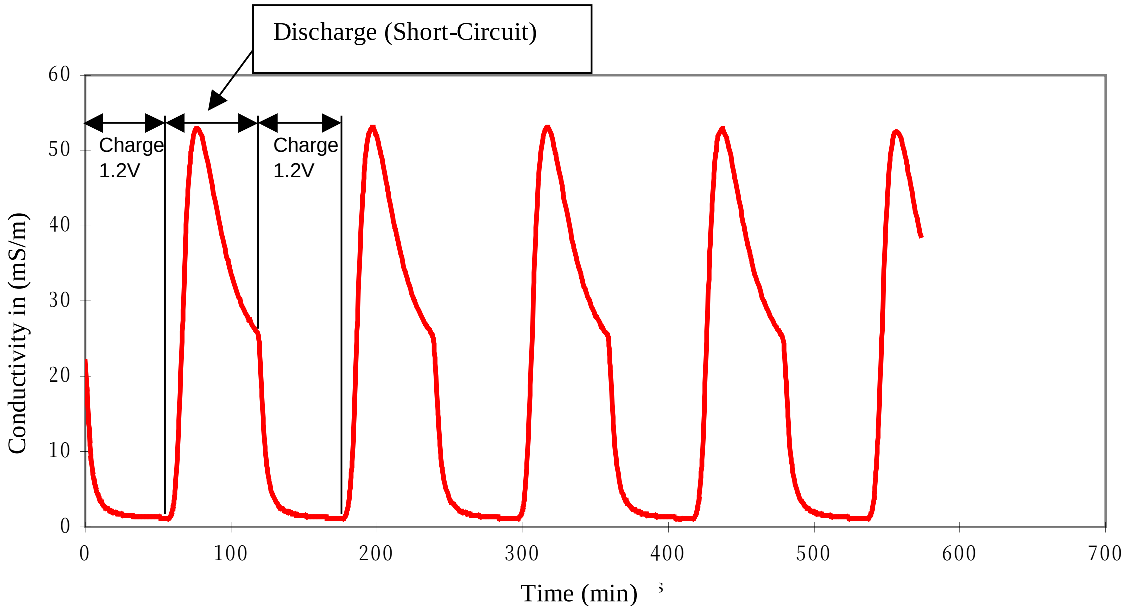

FIGURE 5.4: Production/Charge and Regeneration/Discharge Cycles

After the bus connector design had been optimized, the next step was to determine the prototypes optimum flow rate and hydraulic design for the desalination evaluation tests, to follow. **Figure 5.5** illustrates two test runs conducted on the same MK-8A prototype. For the test in **Figure 5.5** the feed water quality was the same; however the once-through test runs were conducted at two different flow rates, one at 52 ml/min and the other at 157 ml/min.

As expected, the higher flow velocity produced more rapid ion removal during the rinse phase. At around 100 minutes, the 157 ml/min flow conductivity started to fall as a second cycle was initiated. The sharp spikes on the graphs have been due to instrumentation and have no relevance on the overall experiment. Due to the low-pressure requirement for CDT™, optimization of head loss through the prototype was not of primary concern. However the manufacturer plans future hydraulic optimization to ensure lowest head loss possible.

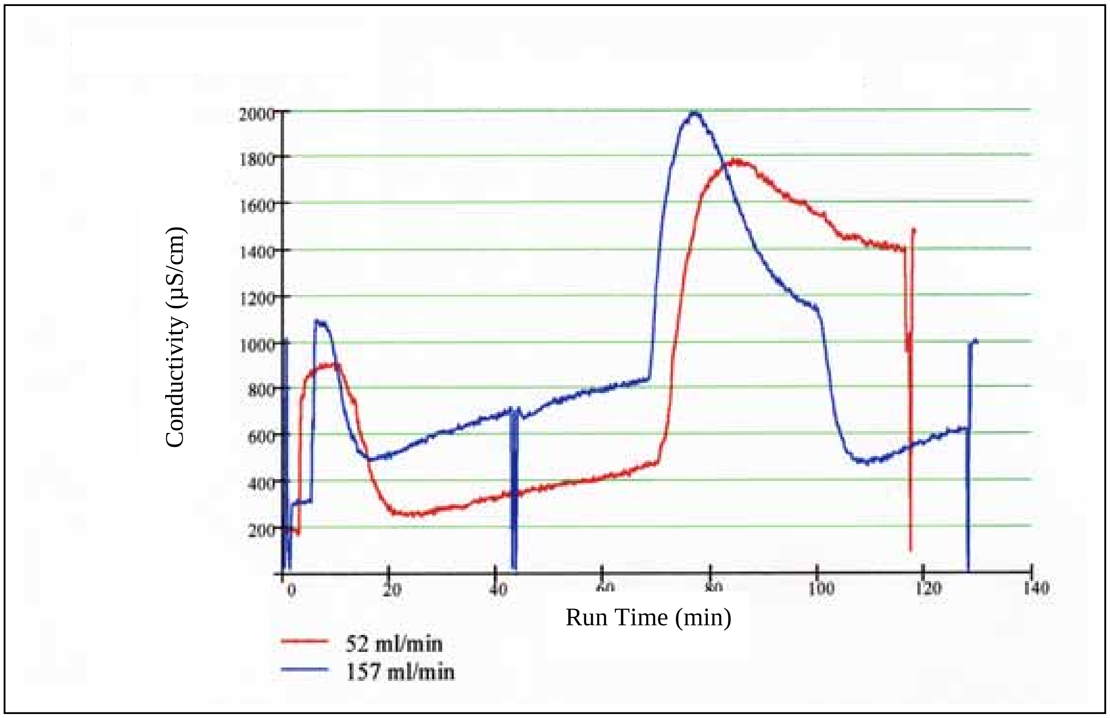

FIGURE 5.5: Effect of Flow Rate on Prototype Performance

Ion Adsorption

The final decision on which prototype design to use in further desalination efficiency testing was made after an ion adsorption test run was conducted on the two main prototype alternatives. **Figure 5.6** illustrates the ion adsorption capacity per prototype as a function of time.

Figure 5.6 represents the cumulative ion adsorption for a single charge/discharge cycle on each prototype alternative. The feed water was a 1 032 µS/cm NaCl solution at a flow rate of 52,6 ml/min. A potential difference of 1,3V was used on both alternatives. The MK-8A (graphite bus connectors) prototype adsorbed around 1,6 times more ions at the same energy consumption, as compared to the metallic bus connector prototype.

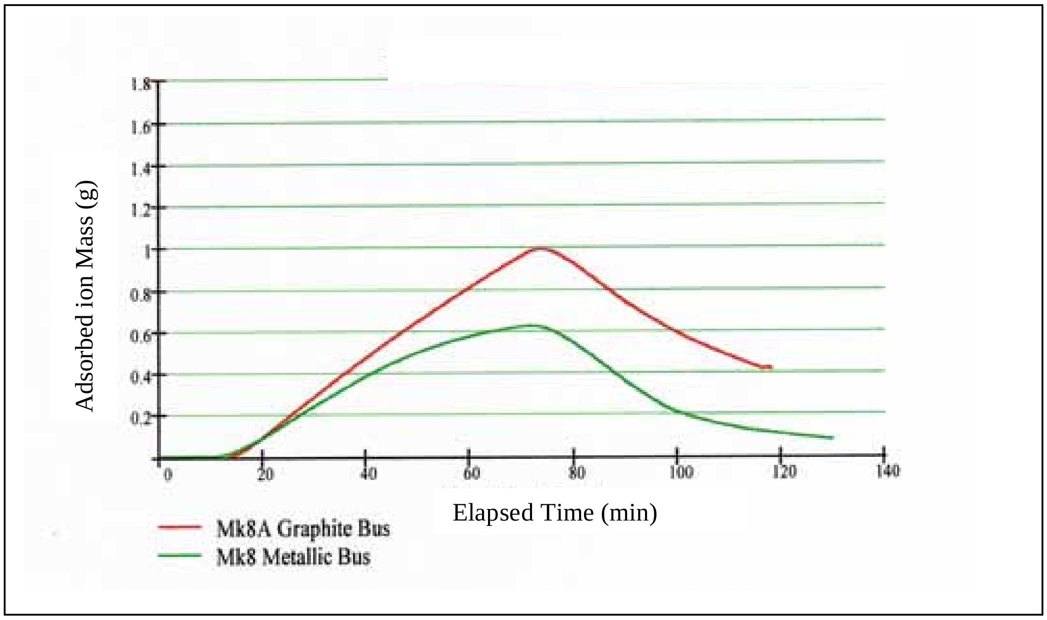

FIGURE 5.6: Ion Adsorption: Metallic vs. Graphite Bus Connectors

Energy Requirement

Figure 5.7 illustrates a comparative power use/energy requirement test run. The energy/power was calculated by multiplying voltage and current data. Flow was constant at 52,6 ml/min and the feed conductivity was 1 032 µS/cm. In this test run the MK-8 (metallic bus connector) prototype developed an increased current draw at approximately 12 minutes, this was not due to a direct short as the module voltage was maintained at 1,3 Volts by the power supply. The energy requirement graph of the MK-8A prototype (red line) would be typical of a CDT™ industrial module, due to the capacitive behavior of a module. As the capacitors charge up, less and less current is allowed to flow through the capacitors, resulting in the typical exponential decrease of the required energy. Saturation of the electrode surfaces are directly proportional to the over-all "charged state" of the various capacitors making-up a CDT™ module. Therefore a fully charged CDT™ module indicates a saturated electrode condition and visa versa.

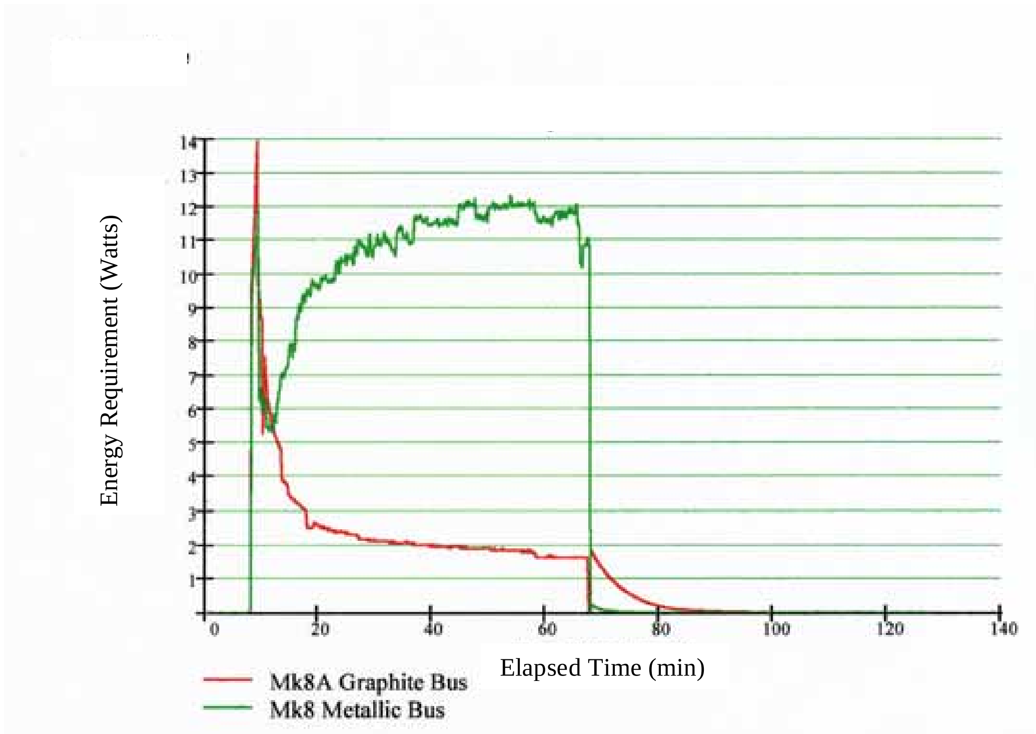

FIGURE 5.7: Energy Requirements : Metallic vs. Graphite Bus Connectors

The prototype developmental phase was concluded for research conducted in this dissertation, once the carbon aerogel electrode manufacturing process, design of electrical bus connectors and the module hydraulic design had been successfully integrated into a single industrially reproducible module. The MK-8A prototype was chosen as the optimum alternative, to be used in the following evaluation phase. During the next evaluation phase, CDT™'s overall potential, to compete on an industrial scale with existing desalination technologies was evaluated.

5.4 RESULTS – PROTOTYPE DESALINATION TESTING PHASE

This section discusses the results obtained from the following two final overall testing phases:

- General Prototype Performance Testing, and
- Brackish Water: Application Specific Testing

5.4.1 GENERAL PROTOTYPE PERFORMANCE TESTING

In order to realistically evaluate capacitive deionization as a potential alternative to existing industrial scale desalination technologies, two main parameters need to be investigated (1) ion adsorption per electrode surface area (percentage water recovery), and (2) energy required to facilitate adsorption. With regard to electrical energy, the typical operational mode of a CDT™ plant would be to switch between charging the cells (ion adsorption) and discharging the cells (ion removal). **Figure 5.8** illustrates a typical continuous/cyclic once through test run used during this phase of testing, which would also be the typical continuous scenario for a module as part of an industrial size application.

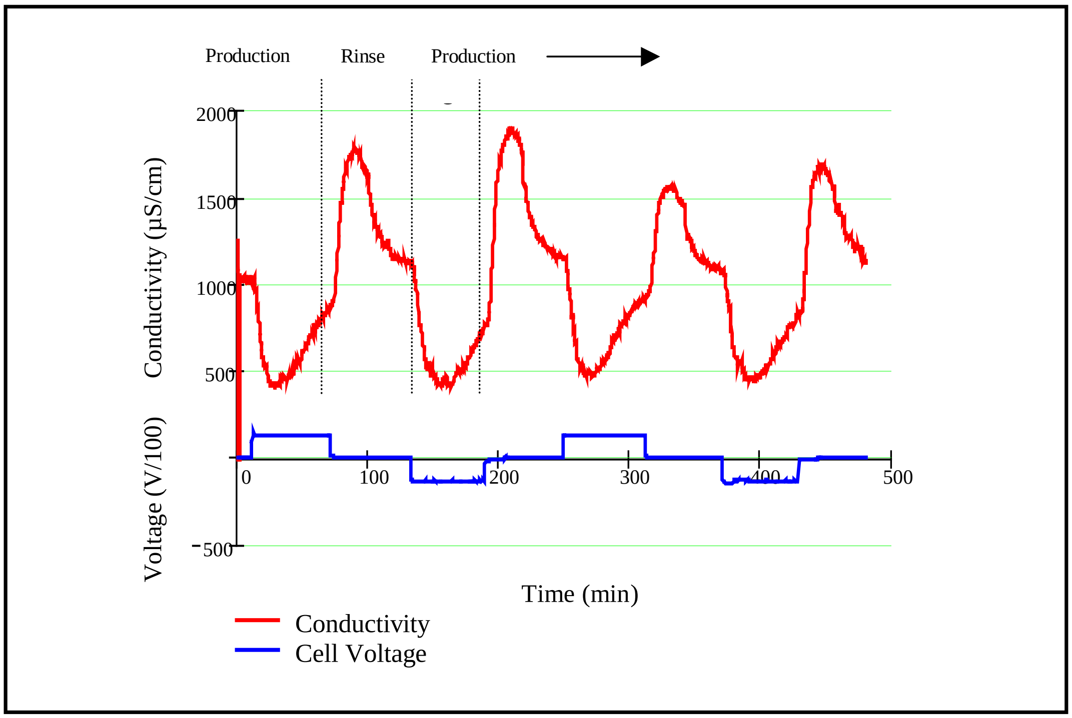

FIGURE 5.8: Typical Continuous CDT™ Desalination Evaluation Test Run

Figure 5.8 further illustrates the typical graphical interpretation of time, outlet conductivity and bus voltage/supply current data collected at each test run in this phase.

The feed NaCl solution conductivity for this specific test run was 1 088 µS/cm through a MK-8A prototype module. The blue trace shows the applied voltage as it was switched from +1,3v to 0 v to –1,3 v. Switching the polarity after each cycle, assists with the regeneration phase. During the production cycle, with a direct current voltage applied to the module, ions are removed from the water passing through the system; conductivity is reduced below the input level. Conductivity drops for about the first ¼ of the production cycle, then increase to again to close to the starting value.

During the regeneration cycle, with the module electrical connections grounded (energy can be recovered here in full scale systems), ions are released into the water and the output conductivity is increased above input level of 1 088 µS/cm. By integrating the TDS removal for the production cycle, the overall mass of ions removed, can be determined. Voltage and current data automatically collected during a test run is used to determine how much energy is required per volume of water. **Figure 5.9** illustrates the data from repetitive test runs done on the MK-8A prototype module.

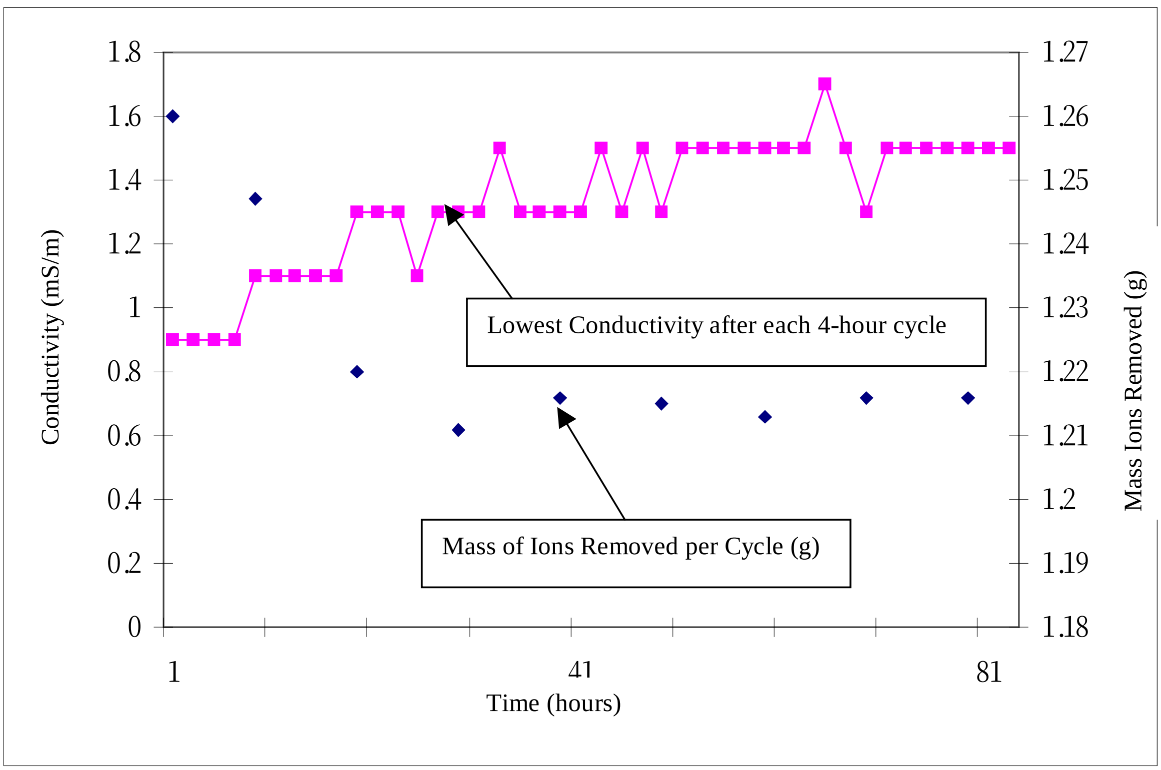

FIGURE 5.9: Ion Adsorption Repetitive Tests on MK-8A Prototype Module

A 20 mS/m (200 µs/cm) NaCl solution was continuously treated for 100 cycles (4 hour charge vs. 2 hour discharge) at 50 ml/min at the Air Water, Inc laboratory. Results indicated a 66% recovery rate, as the flow rate stayed constant. In **Figure 5.9** each cycle consisted of a 4-hour charge (operational) period, and a 2-hour discharge (regeneration) period. The graph shows the lowest conductivity recorded for each charge cycle, as well as the calculated mass of NaCl removed.

The ion adsorption capacity for the prototype stabilized at about 1,215 g per charge cycle. The overall ion removal decreased and then stabilized. This phenomenon could be due the physical adsorption that took place at the start of a test series. Ions that are physically adsorbed are not so easily removed as compared to ions electrically adsorbed. Next ion adsorption capacity, as a function of flow rate was evaluated for the MK-8A prototype. **Figure 5.10** illustrates the difference in cumulative ion adsorption capacity of the same prototype, but two different flow rates.

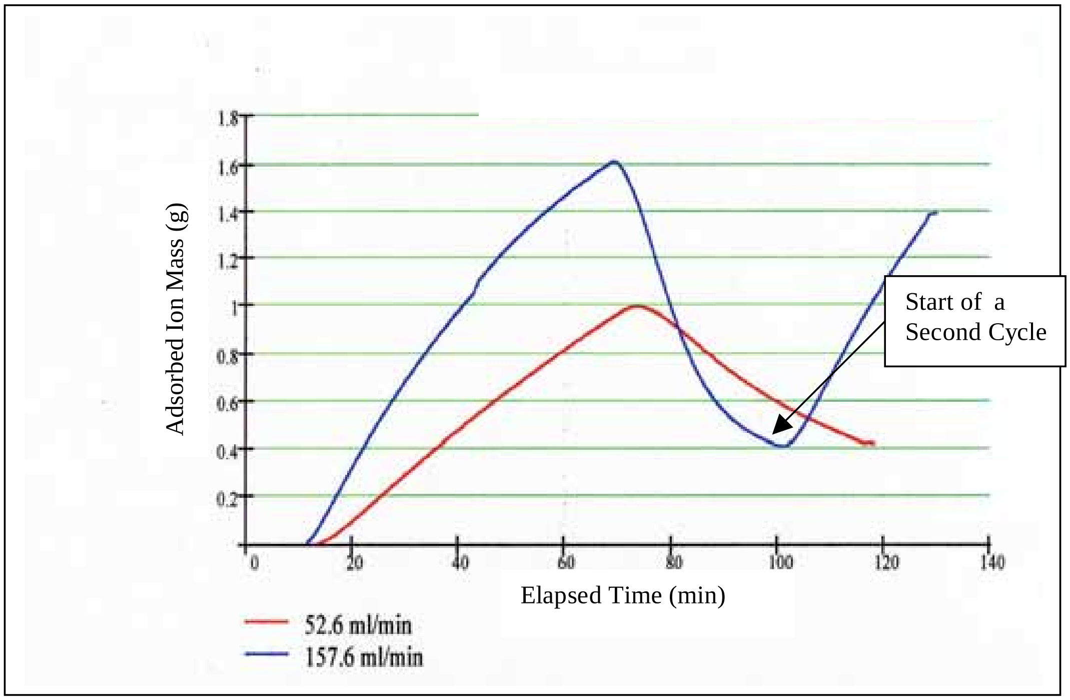

FIGURE 5.10: Effect of Flow Rate on Ion Adsorption Capacity for the MK-8A Prototype

Data in **Figure 5.10** indicate that an increase in flow rate improves ion adsorption and reduces regeneration time. This phenomenon was earmarked for further investigated in future research.

5.4.2 BRACKISH WATER: APPLICATION SPECIFIC TESTING

Table 5.1 summarizes the pre- and post treatment results on diluted artificial seawater (sea water intrusion scenario). A MK-8A capacitive deionization prototype module was used to generate data for **Table 5.1**. A feed stream of diluted artificially generated seawater at 1 000 µS/cm was treated to produce a product stream of 23.4 µS/cm at 50 ml/min.

TABLE 5.1: Pre-and Post Treatment Results on Diluted Artificial Seawater

		Feed Water	Product Water	Reduction %
Cation	Sodium as mg/l Na^+	180	39	78,33%
	Magnesium as mg/l Mg^{2+}	20	3.9	80,50%
	Calcium as mg/l Ca^{2+}	4.7	1.1	76,60%
	Potassium as mg/l K^+	16	2.6	83,75%
	Zinc as mg/l Zn^+	0.17	0.14	17,65%
	Boron as mg/l B^+	0.09	0.06	33,33%
Anion	Chlorine as mg/l Cl^-	260	58	77,69%
	Sulfate as mg/l SO_4^{2-}	40	9	77,50%
	Bromine as mg/l Br^-	0.36	0.05	86,11%
	Carbonic Acid HCO_3^-	120	72	40,00%

High ionic specie reduction as shown in **Table 5.1** on artificially prepared brackish water was a good start, however in order to evaluate capacitive deionization in a “real world” scenario, testing on naturally occurring brackish water was needed. Testing on naturally occurring brackish water follows next.

In the natural gas industry, a lot of brackish water is generated during well drilling. The brackish type water generated by drilling is called "produced water".

The first naturally occurring brackish water tested on a CDT™ industrial prototype was samples from the natural gas industry in Wyoming, USA. In these brackish water bicarbonates (< 1 900 mg/l) are the main contaminant. The same test methodology was used as for the laboratory-generated solutions. During the production cycle a 1,3 Volt potential difference was generated via direct current. During the regeneration cycle the electrodes were grounded. **Figure 5.11** illustrates the desalination of coal bed methane (CBME) produced water.

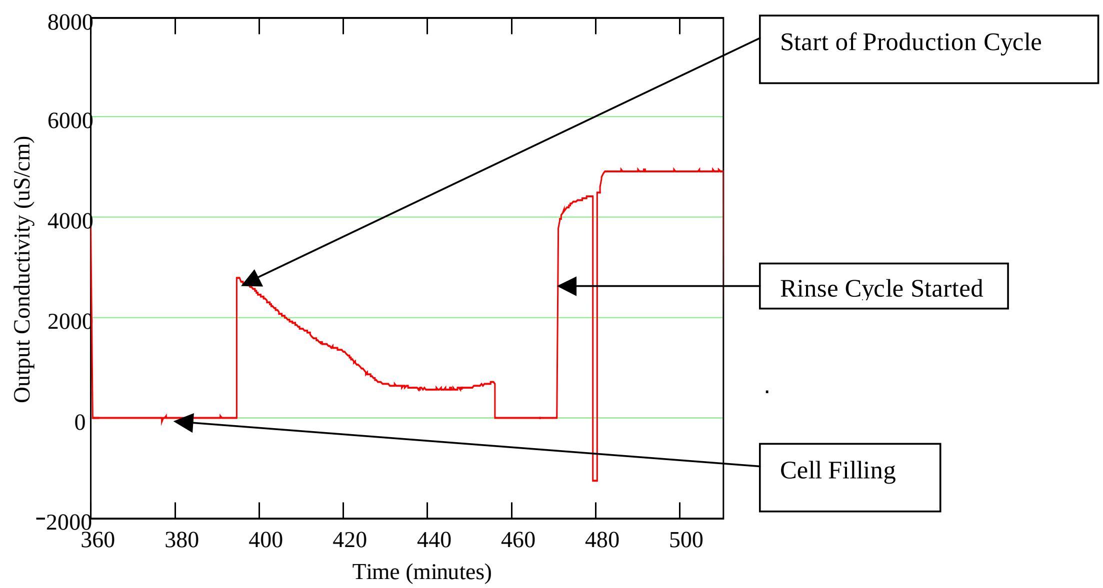

FIGURE 5.11: Desalination of CBME Produced Water

During the period from 360 to roughly 390 minutes, the module was filling, so there was no output from the conductivity probe located on the water output line. The input water conductivity was 2 095 µS/cm at 20,5˚C.

The output conductivity at the start of the cycle was above the input value due to residual rinse water being pushed out the system. The rinse began at roughly 470 minutes, the zero conductivity occurs during the fill time and is 1/3 the time of the production fill since the rinse flow rate was 3 times the production flow rate. Rinse conductivity saturated at 5 000 µS/cm since this was the maximum range set on the meter. It was increased for subsequent runs. For this test run the water recovery rate was around 70% and rinse water could be re-used for at least another rinse cycle, before discarding as brine. Reducing the volume of the brine has a major cost benefit in this industry, as it needs to be trucked and pumped underground at specific brine aquifer injection points.

Voltage and current data (see **Appendix A**) was used to determine that it would take an estimated 2,25 kWh to treat 1 000 gallons (3 785 liters) of the produced brackish water to below reinsertion/reuse limits (< 1 000 mg/l). This result is significantly higher than the 0,36 kWh per 1 000 gallons (3 785 liters) predicted by earlier research work from LLNL, however by including energy recovery and improved electrical connection, future industrial modules could approach the laboratory benchmark.

Carlsbad Pilot Plant

Next in the evaluation process was the design, construction and operation of a CDT™ pilot plant. A CDT™ pilot system was constructed and operated at the Encina Water Pollution Control Facility in Carlsbad, California (2000 to 2001). This specific wastewater treatment facility produced two streams of brackish source waters. The first is a brackish ground water stream, generated by the daily pumping down of the water table, under the secondary settlers. The second brackish water stream is the secondary effluent from the plant (Avg. TDS > 1 100 mg/l).

A small percentage of the secondary effluent is further treated and recycled as irrigation water. However the majority is disposed of via a dedicated sea outfall. **Figure 5.12** illustrates the control panel of the demonstration unit at the Encina Water Pollution Control Facility.

Behind the control panel source water was directed via a series of pumps to ¼ scale (250 ft^2) CDT™ cells. These cells were constructed as per the manufacturing process developed for the smaller MK-8A prototype.

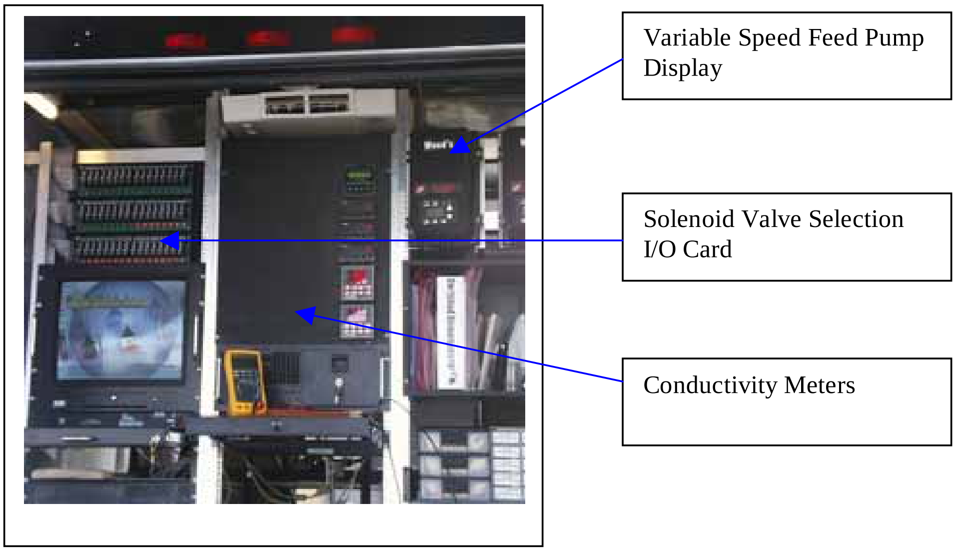

FIGURE 5.12: CDT™ Pilot Plant Control Panel at the Encina Water Pollution Control Facility

A test run was conducted at the pilot plant to determine the ion storage capacity of a larger industrial prototype type unit. A recirculation test was conducted on the brackish ground water. The purpose of the test work was to provide insight into the operating scenario's best suited to an industrial type unit. **Table 5.2** lists an analysis of the Encina brackish groundwater chemical specie composition, which constituted the feed water to the CDT™ pilot plant for this specific test run.

TABLE 5.2 : Encina Ground Water Chemical Analysis

Analysis	Results	US Analysis Method #
Alkalinity, as mg/l $CaCO_3$	283 mg/l	SM2320 B
Ammonia N	0,44 mg/l	SM 4500 NH C
Boron	0,6 mg/l	SM 4500 B-B
COD	86,2 mg/l	HACH 8000
Chloride	1 722 mg/l	SM 4500 Cl B
Total Hardness, as mg/l $CaCO_3$	1 440 mg/l	SM2340 C
Nitrate N	7,38 mg/l	USEPA 352.1
Nitrite N	< 0,1 mg/l	SM 4500 NO-B
Grease & Oil	0,2 mg/l	SM 5520 B
pH	7,20	
o-Phosphate	0,063 mg/l	SM 4500 E
t-Phosphate	0,067 mg/l	HACH 8190
TDS	4 598 mg/l	SM2540 C
TSS	1,9 mg/l	SM2540 C
VSS	1,3 mg/l	SM2540 E
Specific Conductance	6 370 µs/cm	SM2510 B
Sulfate	630 mg/l	USEPA375.4
Temprature	25,2 °C	SM2550
Turbidity	O,194 NTU	SM2130 B
Aluminum	0,18 mg/l	USEPA 6010 B
Antimony	0,002 mg/l	SM3113B
Arsenic	0,003 mg/l	SM3113B
Barium	0,073 mg/l	SM2130B
Beryllium	< 0,0005 mg/l	SM3113 B
Cadmuim	0,006 mg/l	SM3111B
Calcium	70,8 mg/l	SM3111B
t-Chromium	<0,1 mg/l	SM3111B
Copper	<0,05 mg/l	SM3111B
Iron	0,093 mg/l	SM3111B
Lead	0,1 mg/l	SM3111B
Magnesium	177,8 mg/l	SM3111B
Manganese	0,109 mg/l	SM 3111B
Mercury	0,0004 mg/l	SM3112B
Molybdenum	<0,01 mg/l	SM3113B
Nickel	0,056 mg/l	SM3111B
Potassium	15,4 mg/l	SM3500D
Selenium	<0,015 mg/l	SM3113B
Silver	<0,025 mg/l	SM3111B
Sodium	977 mg/l	SM3500 D
Thallium	< 0,005 mg/l	USEPA 279.2
Zinc	0,046 mg/l	SM3111B

Heterotrophic Plate Count	**7 700 cfu/ml**	**SM9215D**
Total Coliform m-F	**8 800 cfu/100 ml**	**SM9222B**
Fecal Coliform m-F	**<10 cfu/100 ml**	**SM9222D**
Enterococcus m-F	**140 cfu/100 ml**	**SM9230C**
Color	**2,0 color units**	**SM 2120B**
Odor	**2,9 TON**	**SM2150B**

Source : Encina Wastewater Authority Laboratory (Certification No. 1441) – Sample 5 September, 2000 @ 10:10 am – East Well.

By using a direct conversion from conductivity to mg/l for TDS, the estimated mass of contaminants adsorbed and released can be predicted.

Feed water Conductivity : 6 370 µS/cm

Feed Water TDS : 4 598 mg/l

The volume of water treated for the test run was 50 liters. **Figure 5.13** illustrates the main variables, output conductivity, bus voltage and current as measured during this test run of the pilot plant.

Pilot Plant Test Run Notes:

- Maximum Bus Voltage: 1,2 V
- Maximum Current Required: 110 A
- Bus connections shorted after 40 min to simulate regeneration cycle.
- Voltage not recorded during minutes 41 to 46, therefore dip in graph.
- Capacitor discharge current not measured.
- Total Electrode Surface Area: 23,23 m^2 (250 ft^2)

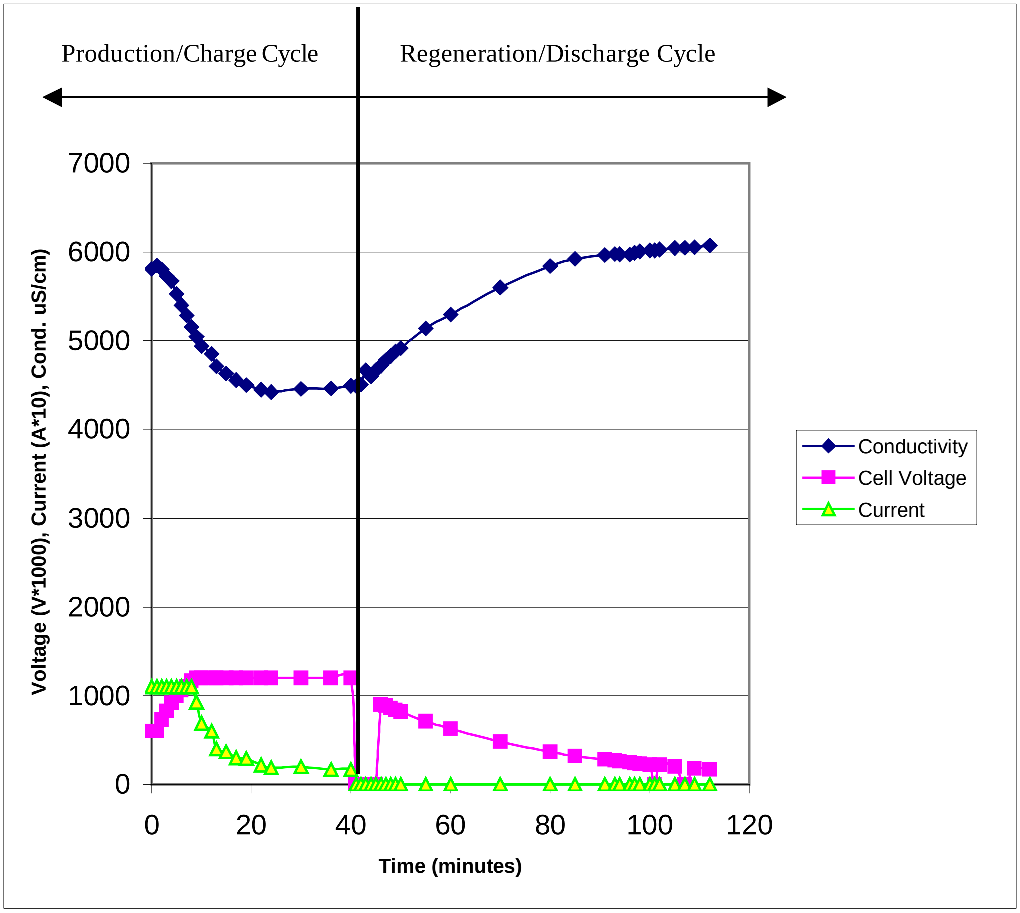

FIGURE 5.13: Pilot Plant : 250 ft² Industrial Cell : Ion Storage Test Run

The approximate mass of ions adsorbed can be calculated by looking at the change in conductivity of the output stream.

Conductivity Reduction = 6 075 µS/cm – 4 421 µS/cm = 1 654 µS/cm

By using a conductivity to TDS conversion factor of 0,722 {4598.10^{-6} / 6370.10^{-6} } it is estimated that 59,695 grams of ions had been removed by the operational cycle of the cell. Therefore the carbon aerogel electrode ion adsorption capacity for specifically brackish groundwater as per **Table 5.2** is 2,5697 g/m^2 (0,2388 g/ft^2).

Due to practical size and weight considerations the original bench mark for a full size industrial cell was set at 92.90 m^2 (1000 ft^2). Laboratory test work at LLNL indicated that this surface area should be able to remove 1 000 mg of TDS per 24 hours. The full cycle (charge and discharge) for the pilot plant test run took 110 minutes and 50 liters of brackish water was treated during this period. A scaled daily production for the pilot plant could be estimated by using the equation 5.1.

$$\text{Scaled\_Daily\_Production} = (24\ \text{hrs/Cycle Time}).(\text{M\_ions})/(10^{-3}.\rho\text{water}).(1/\text{Cell Scale}) \quad (5.1)$$

- Scaled_Daily_Production = Volume of brackish water treated by a singly CDT™ cell (1 000 ft^2 electrode surface) per day
- Cycle Time = 110 minutes = 1,833 hours
- M_Ions = Mass of TDS Removed = 59,695 g = 59 695 mg
- ρwater = 1 kg/liter
- Cell Scale (as compared to full size unit) = 0,25

By using the scaled production equation 5.1, it can be calculated that in a 24 hour period the cell would reduce the TDS of 825,76 gallons (3 125 liters) of brackish water by 1 000 mg/l. Additional experimental results obtained during pilot scale testing are contained in **Appendix B**. The testing phase for this research was thus successfully concluded, with test results on actual industrial type CDT™ prototypes coming close to laboratory scale test results. Test results achieved in this research will serve as a benchmark for an ongoing research and development program on Capacitive Deionization Technology™.

CHAPTER 6

COST: EVALUATION AND COMPARISON

6.1 BASIS OF COST EVALUATION

At the time of this research, technology license agreements limited manufacturing to the USA and as the majority of research for this dissertation was conducted in the USA, the currency used in this chapter is the US Dollar. In order to compare "apples-with-apples" a reference design will be used to compare the costs (capital and operational) of a 3,78 Ml/d (1 mgd) low-pressure brackish groundwater RO desalination facility to a 3,78 Ml/d (1 mgd) CDT™ brackish water facility treating a brackish feed water (TDS: 2 000 mg/l) to potable standards. **Table 6.1** summarizes the reference design conditions.

TABLE 6.1: Reference Design Parameters

Parameter	**Value**
Water Supply Source	Groundwater
Source Water TDS, mg/l	2 000
Required Produced Water TDS, mg/l	500
Finished Water Quantity, Ml/d (mgd)	3,78 (1)
Brine Concentrate Disposal	Surface Water Body
Intake Type	Well Feed pump

Data Source : AWWA M46: p 93

Section 6.2 discusses more specifically cost projections applicable to CDT™ capital, operations and maintenance requirements. A cost comparison, between the RO and CDT reference designs, follows in **Section 6.3.**

6.2 CDT™: COST PROJECTIONS

Capital and O&M cost projections for CDT™ are discussed in the following two sections.

6.2.1 CAPITAL COST PROJECTIONS FOR CDT™

During the CDT™ prototype developmental phase, the manufacturing cost of industrial size modules was estimated by using the pilot manufacturing process as a model. Acquisition of land, factory space, and machinery costs were taken into account. Like most new technologies, evolving from a laboratory to an industrial level, the initial manufacturing costs per module would be higher than manufacturing costs a few years down the full scale industrial manufacturing road. It is estimated by CDT Systems, Inc. that the initial purchase price per industrial size module, producing 3 785 liters/day (1 000 gpd) and removing 1 000 mg/l, would be in the range of US $1 000 to US $1 500. However based upon volume manufacturing and continuous electrode material improvements (Dietz, 2004), CDT Systems, Inc. estimates that they can reduce the purchase price to between US $600 and US $800 within the first three years of volume production. These estimates are based on manufacturing costs in the USA.

Table 6.2 illustrates the improvements made during the development process in reducing the cost to manufacture an industrial CDT™ module, as compared to initial laboratory scale test work and estimates.

TABLE 6.2: Reduction of CDT™ Module Manufacturing Costs

Development Stage	US$ Cost/ft^2 Aerogel	Module Sales Price in US Dollar
Technology Licensed from LLNL at Jan. 1997	75	75 000
Projected Cost by LLNL for 2004	30	30 000
CDT Systems, Inc at 1998	5	5 000
CDT Systems, Inc at 2000	3	3 000
CDT Systems, Inc at 2002	2.5	2 000
CDT Systems, Inc 2004	1.6	1 000
CDT Systems, Inc 2007 (projected)	1	600

Source: CDT Systems, Inc Dallas, Texas - 2004

It must be noted that **Table 6.2** includes the following changes to the manufacturing of a full size industrial CDT™ module.

- 1997 to 2000: 1 000 ft^2 per industrial size module
- 2000 to 2004: 500 ft^2 per industrial size module

Current advances in material sciences indicate that future electrode efficiencies would reduce the required electrode surface area, without sacrificing the overall treatment capacity. Depending on the volume and level of treatment required, modules will be stacked in either parallel or in series. **Figure 6.1** illustrates the typical layout of an future industrial type capacitive deionization plant (See **Figure 6.3** for a process flow diagram of a typical CDT™ system).

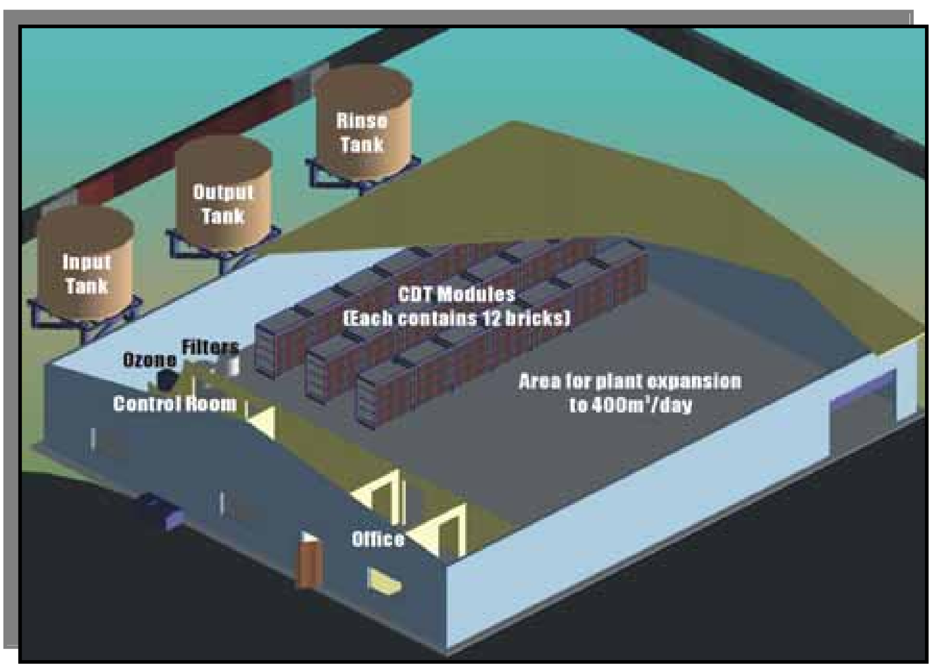

FIGURE 6.1: Typical Industrial Scale Capacitive Deionization Treatment Plant

To determine how many modules in series or parallel will be needed, a simple linear method can be used.

Number of Modules = [Flowrate (gpd) x Required TDS reduction (ppm)]/1 000 000

For example an industrial size treatment plant has the following basic design criteria. Produce 1 000 000 gallons per day (3,8 x 10^6 liters per day) of potable water at 500 mg/l TDS from a brackish source water at 2 000 mg/l TDS.

Number of Modules = (1 000 000 x 1 500)/1 000 000 = 1 500 modules
Total estimated capital cost could then be calculated by including site-specific civil, electrical, instrumentation and mechanical costs. For brackish type water treatment, a good starting point for the calculation of power required is 100 watts per module. Thus for the above-mentioned scenario, around 150 kW would be the maximum power needed to operate the plant at full capacity.

6.2.2 OPERATIONAL COST PROJECTIONS FOR CDT™

Test work conducted by using CDT™ on "real world" brackish water (Chapter 5) and laboratory samples indicated that the energy requirement to treat a brackish type water (2 500 to 3 000 mg/l TDS) to potable standards below 500 mg/l TDS, would be 2,25 kWh per 1 000 gallons or 0,594 kWh/m^3. These energy consumption rates do not include further potential energy savings by energy recovery due to the capacitor type operation.

CDT Systems, Inc. believes that with energy recovery, these energy consumption rates can be 20% to 50% lower. An industrial size treatment plant will not require a large operational staff contingent, as a centralized control room would be able to monitor/control of the entire plant. Module replacement (if necessary) would be like changing the batteries in a flashlight. Carbon aerogel is extremely durable and the minimum lifetime of a module is estimated to be approximately 10 years. **Table 6.3** summarize the estimated costs to produce potable quality water from various source waters at a flow rate of 3 785 411 liters per day or 1 000 000 gallons per day.

TABLE 6.3: Estimated CDT™ Costs for Reference Design

ITEM	VALUE
Feed Salinity Content, TDS in mg/l	2 000
Flow Rate in mgd (Ml/d)	1 (3,785)
Number of CDT Modules	1 500
Capital Cost (Modules + 30% for Other Direct and Indirect Costs)	**$1 560 000**
Annual Energy + O&M	$52 500
15-Year Capital Amortization	$93 600
Total Annual Costs	**$146 100**
Cost per 1000 gallons	**$0,40**
Cost per 1000 liters	**$0,11**

Data Source : CDT Systems, Inc 2004

Assumptions used in **Table 6.3**:

1. CDT Module/Cell Performance:
   - One module reduces TDS by 1000 mg/l per 1000 gpd.
   - Aerogel Material in one module 500 ft^2
   - Average sales price per module: US $800
2. Annual Energy consumption per module is $0.066/kWh + add 10% for general operations and maintenance costs.
3. Energy Recovery: 50%
4. 15 year Amortization with 10% residual.
5. Cost per 1 000 gallons (1 000 liters) is based on 1 000 000 gpd (3 785 411 lpd) x 365 days of operation per year divided into annual costs.

6.3 COMPARATIVE COSTS

Membrane technologies (low pressure RO and ED/EDR) are leading the existing desalination race for brackish water applications and it was therefore decided to compare capacitive deionization against low pressure RO with regards to capital and operations/maintenance costs.

Table 6.1 illustrates the reference design parameters. **Figure 6.2** illustrates a process flow schematic of a typical low-pressure RO system used for cost comparative purposes**.**

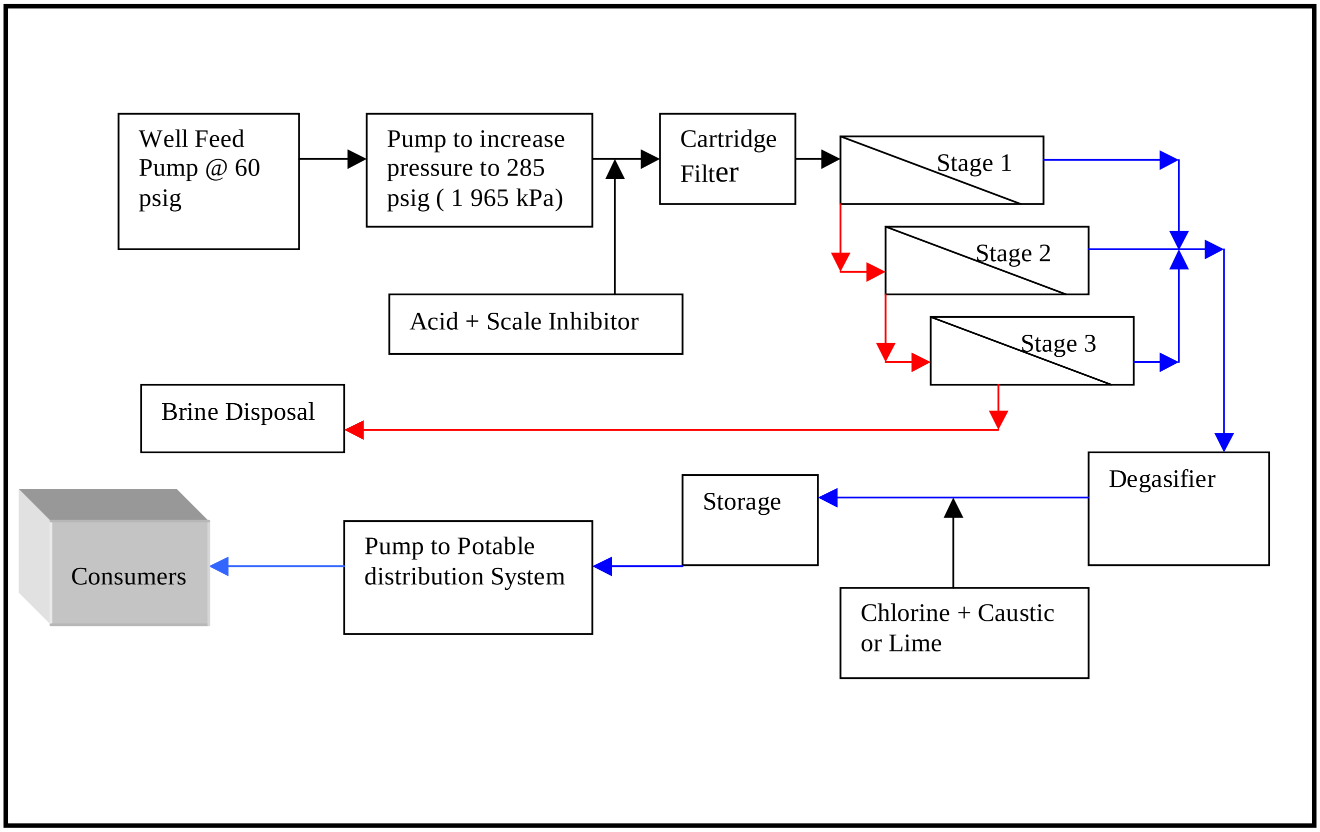

FIGURE 6.2: Typical Low Pressure RO Brackish Water Process Flow Schematic

Figure 6.2 illustrates a typical three stage low-pressure RO system used to achieve a recovery of 80%. **Figure 6.3** illustrates a typical CDT™ process flow schematic for treating the applicable brackish feed water to potable standards. A cost breakdown (capital and O&M) for this scenario is presented in **Table 6.3**.

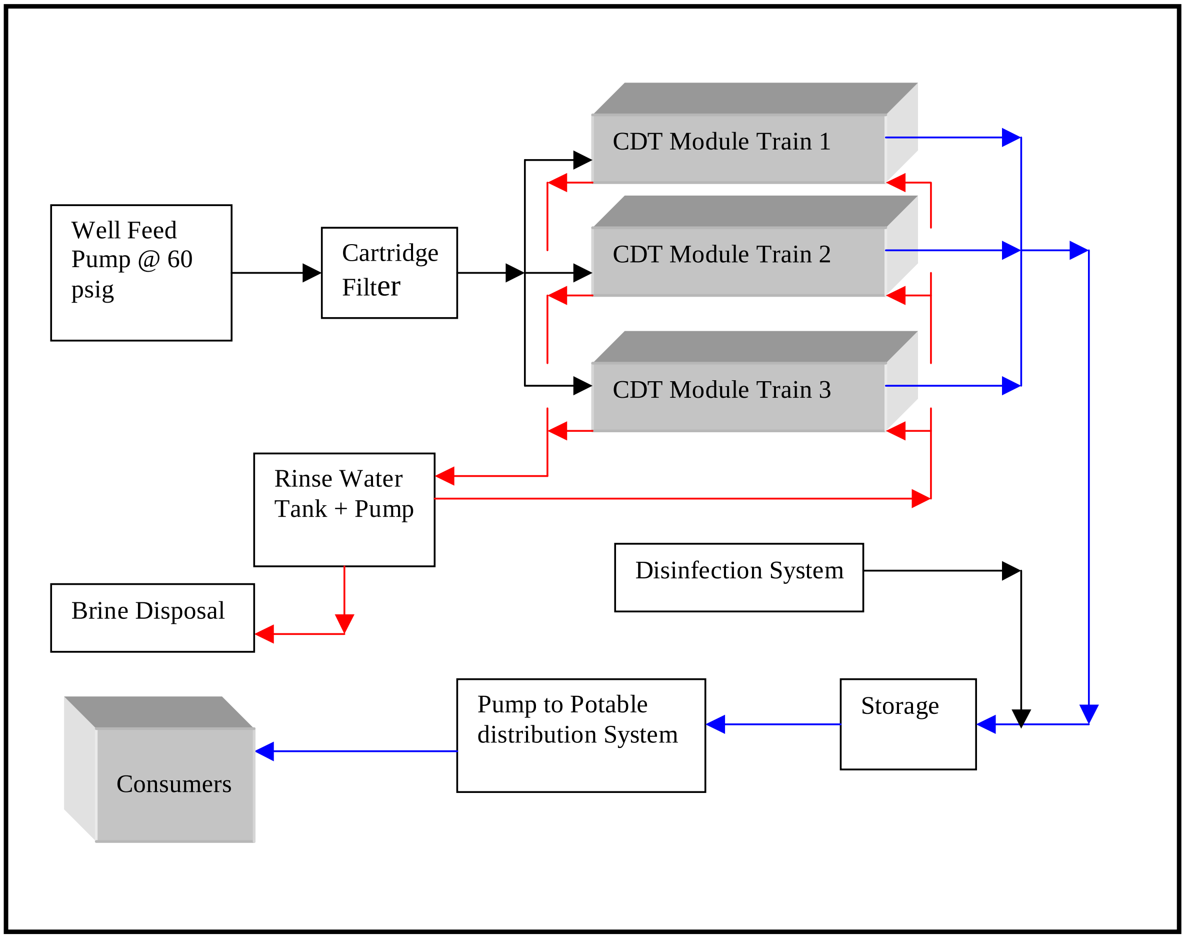

FIGURE 6.3: Typical CDT™ Brackish Water Process Flow Schematic

It must be noted that various site-specific factors could influence the final construction costs for both a RO and CDT™ facility. However for comparative purposes in this research it is assumed that both plants are to be constructed on similar sites, as described in the reference design (**Table 6.1**). **Table 6.4** presents a cost breakdown for the low-pressure RO system as illustrated in **Figure 6.2.**

TABLE 6.4: Estimated RO Costs for Reference Design.

ITEM	VALUE
Feed Salinity Content, TDS in mg/l	2 000
Flow Rate in Ml/d (mgd)	3 785 (1)
Capital/Construction Costs* (Direct and Indirect Costs)	$3 139 000
Annual Energy + O&M**	$296 535
15-Year Capital Amortization + 10% Residual	$188 340
Total Annual Costs	$484 875
Cost per 1000 gallons	**$1,33**
Cost per 1000 liters	**$0,35**

* See AWWA, M46 : p94 for a detailed breakdown of construction costs.

** Energy @ 3.83 kWh/1000 gal (AWWA, M46: p 98) typically is 33% of a RO facility's O&M costs (AWWA, M46: p 5). No Blending.

Table 6. 5 summarizes the costs as broken down in **Table 6.3** and **6.4**, for both CDT™ and a low pressure RO system, using the same reference design.

TABLE 6.5: Comparative Cost for Reference Design

CDT™			**RO**		
Capital	**O&M**	**Total**	**Capital**	**O&M**	**Total**
$0,26	**$0,14**	**$0,40**	**$0,52**	**$0,81**	**$1,33**
$0,11/1000 liters or $0,40/1000 gal			**$0,35/1000 liters or $1,33/1000 gal**		

Data Source:

CDT Systems, Inc for CDT data.

(AWWA M46, 1999) and (Gomez, 2004) for RO data.

As indicated in **Table 6.5**, significantly lower estimated capital cost of the CDT™ system and it's lower energy consumption (including an assumed 50% energy recovery) mean that that this system could be cost competitive compared to RO for brackish water applications (TDS < 10 000 mg/l). However, reverse osmosis would be more cost effective for the higher salinity waters and only by reducing the capital costs for the production of CDT™ modules, would capacitive deionization become a serious competitor for reverse osmosis in higher salinity brackish or seawater applications.

EDR is another competitive brackish water desalination technology. Without energy recovery test work on an industrial type CDT™ module indicated an energy requirement of 2,25 kWh/1000 gallons and EDR utilizes 7,7 kWh/1000 gallons (AWWA M46, 1999) for typical brackish water conditions. It is thus possible for future CDT™ plants to cut the costs to produce desalinated brackish water by 70%, as compared to existing EDR data.

CHAPTER 7

CONCLUSIONS AND RECOMMENDATIONS

7.1 CONCLUSIONS

The following conclusions can be made regarding the research conducted for this dissertation:

- **Aerogel manufacturing.**
  It is possible to cost effectively manufacture the carbon aerogel electrodes on a large/industrial scale, by designing and constructing a small model of a potential future manufacturing facility. To summarize, carbon aerogels are manufactured by poly-condensation of resorcinol and formaldehyde in a slightly basic medium, followed by supercritical drying and pyrolysis in an inert atmosphere. The impregnation of carbon cloth with the resorcinol-formaldehyde resin generates monolithic sheets. These monolithic sheets can easily be trimmed to produce the electrode sheets used in module assembly. Future carbon aerogels will be even more human and environmental friendly as material sciences advance.

- **Simple construction of industrial modules**
  CDT™ only requires simple double-sided planar electrodes, which can be stacked in a low-pressure housing (Plate-and-frame type module).

- **Enhanced energy efficiency for treatment of brackish water**.
  CDT™ can be used to treat brackish water (800 to 10 000 mg/l). The desalination of brackish source water is becoming increasingly more important.

Competing technologies for this application are electrodialysis 2,03 Wh/liter (7,7 Wh/gal) and reverse osmosis 2,25 Wh/liter (8,5 Wh/gal). CDT is more energy efficient at 0,13 to 0,59 Wh/liter (0,5 to 2,25 Wh/gal) depending on energy recovery and operation.

- **Elimination of wastes from chemical regeneration**.
  CDT™ uses electrical regeneration, thereby eliminating the need for handling secondary chemical wastes streams. A highly concentrated brine stream is the only waste stream produced.

- **Carbon Aerogel is resistant to chemical attack.**
  Aerogels are resistant to aggressive chemicals like HCl and resistant to oxidizing agents, should de-scaling or de-fouling be required in CDT™ desalination facilities.

- **Industrial treatment plants would be fully automated.**
  The capacitive deionization process is fully automatic. A typical industrial size plant would require a minimum of two treatment trains for continuous operation. While the one train produces desalinated water, the other would be regenerating. Energy captured from the regenerating train could be supplied to the train in production mode.

- **Potential to reduce treatment plant disposal costs.**
  Old membrane modules have no recycle value and thus present a disposal problem. CDT™ has the potential to reduce the overall disposal costs to a treatment plant, as the carbon aerogel electrode lifetime is conservatively estimated in excess of 10 years by LLNL.

In summary, simple design requirements and low energy costs could make CDT™ very competitive to existing membrane technologies such as reverse osmosis and electrodialysis for brackish water applications in the immediate future.

To be competitive for seawater applications, the production costs per capacitive deionization module needs to be reduced before the technology can cost effectively compete with reverse osmosis on such applications. CDT™ is a young, but very promising technology for the desalination of brackish and seawater sources.

7.2 RECOMMENDATIONS

Ongoing CDT™ industrial bench scale studies are important, however in order to prove long-term industrial scale operational effectiveness, it is vital to get a capacitive deionization industrial scale plant in operation. It is recommended to first use a pilot plant to verify design requirements for the larger industrial size plant.

Currently there are various ongoing research projects in the USA and Japan. The data from these projects would greatly accelerate the design and construction of industrial scale manufacturing plants. However, before an industrial size treatment plant can be built, an industrial scale manufacturing facility would be needed. CDT Systems, Inc is in the process of establishing such a facility.

With a manufacturing facility in place, this and LLNL research clearly indicates that CDT™ could cost effectively compete with existing industrial scale desalination technologies. Dedicated long-term planning, material science research and continued pilot scale testing will take this exciting water treatment technology to the industrial level. CDT™ has the potential to provide and order-of-magnitude step reduction in desalination costs and thus has the potential to provide not only potable water, but also agricultural and industrial water, from saline sources.

.

BIBLIOGRAPHY

AMERICAN WATER WORKS ASSOCIATION (1999). Reverse Osmosis and Nanofiltration. Manual for Water Supply Practices – M46. AWWA

CLARKE, R. (1991). Water: The International Crisis. London: Earthscan Publications.

DIETZ, S. (2004). Improved Electrodes for Capacitive Deionization. TDA Research, Inc.http://www.tda.com/Library/docs/Electr_Dietz_NSF_04_Proc.pdf Access: 23 August 2004.

DRAKE, W. (2001) "Take it without a grain of salt." *Environment*, 1, 2001.

FARMER[1], J (2000). Capacitive Deionization for the Elimination of Wastes. Strategic Environmental Research and Development Program. Livermore, CA: Lawrence Livermore National Laboratory.

FARMER[2] J.C., FIX D.V., MACK G.V., PEKALA R.W., POCO, J.F. (1995). Capacitive Deionization with Carbon Aerogel Electrodes: Carbonate, Sulfate, and Phosphate. LLNL. Internet: http:/www.llnl.gov/tid/lof/documents/pdf/228237.pdf .Access: 12 September 2003.

FARMER[3], J.C., FIX, D.V., MACK, G.V, PEKALA, R.W., POCO, J.F. (1996). Capacitive Deionization of NH_4ClO_4 Solutions with Carbon Aerogel Electrodes. LLNL. Internet: http:/www.llnl.gov/tid/lof/documents/pdf/228511.pdf .Access: 12 September 2003

FARMER[4], J.C., FIX, D., MACK, G., PEKALA, R., POCO, J. (1995). Capacitive Deionization of NaCl and $NaNO_3$ Solutions with Carbon Aerogel Electrodes. LLNL. Internet: http:/www.llnl.gov/tid/lof/documents/pdf/227653.pdf .Access: 12 September 2003

FARMER[5] J.C., J.K., PEKALA R.W., FIX D.V., MACK G.V, POCO J.F., GRANT W.J., POMERNACKI C.L., SAVOYE C.F. (1995). Capacitive Deionization with Carbon Aerogel Electrodes. LLNL. Internet: http:/www.llnl.gov/tid/lof/documents/pdf/226878.pdf .Access: 12 September 2003.

FARMER[6] J.C., TRAN T.D., RICHARDSON J.H., FIX D.V., MAY S.C., THOMSON S.L. (1997). The Application of Carbon Aerogel Electrodes to Desalination & Waste Treatment. LLNL. Internet: http:/www.llnl.gov/tid/lof/documents/pdf/231717.pdf .Access: 17 September 2003.

FARMER[7] J.C., FIX D.V., MACK G.V., POCO J.F., NIELSEN J.K., PEKALA R.W., RICHARDSON J.H. (1995). Capacitive Deionization of Seawater. LLNL.Internet: http:/www.llnl.gov/tid/lof/documents/pdf/121958.pdf .Access: 17 September 2003.

FARMER[8] J.C., RICHARDSON J.H., FIX D.V., DE PRUNDA J.A.H., MACK G.V., POCO J.F., NIELSEN J.K., PEKALA R.W. (1996). Capacitive Deionization System. LLNL. Internet: http:/www.llnl.gov/tid/lof/documents/pdf/231565.pdf . Access: 12 September 2003.

GOMEZ G.G. (2004). Design and Construction of a 7.5 mgd Desalination Plant for the City of Brownsville. Binasional Desalination Conference 2004 El Paso.

GLEICK P.H. (1993). Water in Crisis: A Guide to the World's Fresh Water Resources. New York: Oxford University Press.

GLEICK P.H. (2000). The World's Water*:* 2000-2001: The Biennial Report on Freshwater Resources. Washington D.C.: Island Press.

HALLIDAY D., RESNICK R. (1988). Fundamentals of Physics. 3rd ed. New York: Wiley, 1149p.

HEALD, C., SMITH, A.C.K. (1974). Applied Physical Chemistry. 1 st ed. London: Macmillan. 391p.

PACIFIC INSTITUTE. Report : Dirty Water: Estimated Deaths from Water Related Diseases 2000 – 2020. 2002.

POSTEL, S. (1992). Last Oasis: Facing Water Scarcity. New York: W.W. Norton & Company.

KING, J.D. (1980). Separation Processes. 2nd Ed. New York: McGraw-Hill : P 662

SIMON[1], P. (1998). Tapped Out: The Coming World Crisis in Water and What We Can Do About It. New York: Welcome Rain.

SIMON[2], P. "Desalinate Water." Water: Opposing Viewpoints", Ed. Carol Wekesser. San Diego: Greenhaven Press, 1994.

UNITED NATIONS. (1964), Water Desalination in Developing Countries. New York:

MONTAIGNE, F. (2002). Water Pressure. *National Geographic*, September: pp 2-32.

United States of America - Department of Interior, Bureau of Reclamation. (2004). Desalination and Water Purification Roadmap. Sandia National Laboratories. Report No. 95.

United Nations University News Release. (1999). World Day for Water. Nairobi, Kenya 18 March 1999. **http://www.unu.edu/env/water/2000-waterday.html**

WODRASKA, J. (2004). "National Convergence in the New Water Arena." CE News. Ed. Shanon Fauerbach. June 2004 : p. 34 – 37. Mercor Media, Inc. Atlanta.

APPENDIX A

AEROGEL QAULITY CONTROL AND INDUSTRIAL CDT™ PROTOTYPE TEST RUN DATA

Aerogel QAQC Test Procedure

The attached data file show a typical QAQC test procedure that was conducted by the researcher on each batch of carbon aerogel produced during the industrial module development phase.

- Two pieces of aerogel { 7.62 cm (3-inch) x 5.08 cm (2-inch) } was cut from a randomly selected aerogel sheet.
- The two pieces were then electrically connected in a 10 000 ppm NaCl solution as a capacitor.
- Computer measurements were taken of the applied voltage and current to the capacitor during a charge and discharge cycle. Three test runs was done per QAQC test.
- Voltage and current data was then used to calculate total energy used to charge the capacitor per test run and the total energy discharged by the capacitor, as measured through a shunt resistor.
- A summary sheet was then generated, via a macro program written by the researcher.
- The amount of energy stored by the mini aerogel capacitor is a direct link to the amount of ion storage to be expected by the industrial unit. Therefore a batch of produced aerogel was passed or failed by this procedure, before the aerogel was inserted into an industrial module.

Aerogel QAQC Test Data Run 1

Time (sec)	Voltage	Current	Energy J	Power W
0	0	0	0	0
10	0	0	0	0
20	1.42578	0.238525	3.400842	0.340084
30	1.31592	0.286621	7.172545	0.37717
40	1.30859	0.251953	10.46958	0.329703
50	1.30615	0.226318	13.42563	0.295605
60	1.30371	0.204102	16.08653	0.26609
70	1.30371	0.185791	18.5087	0.242218
80	1.30371	0.170654	20.73354	0.222483
90	1.30127	0.157715	22.78583	0.20523
100	1.30371	0.146484	24.69556	0.190973
110	1.30127	0.136475	26.47147	0.177591
120	1.30127	0.127686	28.13301	0.166154
130	1.30127	0.120117	29.69606	0.156305
140	1.30127	0.113037	31.16697	0.147092
150	1.30127	0.106689	32.55528	0.138831
160	1.30127	0.101563	33.87689	0.132161
170	1.30127	0.0964355	35.13178	0.125489
180	1.30127	0.0917969	36.3263	0.119453
190	1.29883	0.0876465	37.46468	0.113838
200	1.29883	0.0837402	38.55233	0.108764
210	1.30127	0.079834	39.59118	0.103886
220	1.29883	0.0766602	40.58687	0.099569
230	1.30127	0.0737305	41.5463	0.095943
240	1.30127	0.0710449	42.47079	0.092449
250	1.29883	0.0688477	43.365	0.089421
260	1.30127	0.065918	44.22277	0.085777
270	1.29883	0.0637207	45.0504	0.082762
280	1.29883	0.0612793	45.84631	0.079591
290	1.30127	0.0593262	46.6183	0.077199
300	1.29883	0.057373	47.36348	0.074518
310	1.29883	0.0556641	48.08646	0.072298
320	1.29883	0.0537109	48.78408	0.069761
330	1.30127	0.0522461	49.46394	0.067986
340	1.30127	0.0505371	50.12156	0.065762
350	1.30127	0.0493164	50.7633	0.064174
360	1.30127	0.0480957	51.38916	0.062585
370	1.30127	0.0463867	51.99277	0.060362
380	1.29883	0.045166	52.5794	0.058663
390	1.29883	0.0444336	53.15652	0.057712
400	1.30127	0.0432129	53.71884	0.056232
410	1.30127	0.0419922	54.26527	0.054643
420	1.29883	0.0412598	54.80116	0.053589
430	1.30127	0.0397949	55.319	0.051784
440	1.29883	0.0390625	55.82636	0.050736
450	1.29883	0.0380859	56.32103	0.049467
460	1.30127	0.0371094	56.80392	0.048289
470	1.29883	0.036377	57.2764	0.047248
480	1.30127	0.0356445	57.74023	0.046383
490	1.29883	0.034668	58.19051	0.045028
500	1.30127	0.0336914	58.62892	0.043842
510	1.29883	0.0332031	59.06018	0.043125
520	1.29883	0.0324707	59.48192	0.042174
530	1.30127	0.0322266	59.90127	0.041936
540	1.29883	0.0314941	60.31033	0.040905
550	1.30127	0.0307617	60.71062	0.040029
560	1.30127	0.0305176	61.10773	0.039712
570	1.30127	0.0297852	61.49532	0.038759
580	1.29883	0.0292969	61.87584	0.038052

590	1.29883	0.0285645	62.24684	0.0371
600	1.29883	0.0280762	62.6115	0.036466
610	1.29883	0.027832	62.97299	0.036149
620	1.29883	0.0273438	63.32814	0.035515
630	1.29883	0.0268555	63.67695	0.034881
640	1.29883	0.0266113	64.02259	0.034564
650	1.30127	0.0258789	64.35934	0.033675
660	1.30127	0.0256348	64.69292	0.033358
670	1.30127	0.0253906	65.02332	0.03304
680	1.30127	0.0249023	65.34737	0.032405
690	1.29883	0.0244141	65.66446	0.03171
700	1.29883	0.0244141	65.98156	0.03171
710	1.29883	0.0239258	66.29232	0.031076
720	1.30127	0.0234375	66.5973	0.030499
730	1.29883	0.0231934	66.89854	0.030124
740	1.29883	0.0229492	67.19661	0.029807
750	1.29883	0.0224609	67.48834	0.029173
760	1.29883	0.0224609	67.78007	0.029173
770	1.29883	0.0219727	68.06546	0.028539
780	1.30127	0.0214844	68.34503	0.027957
790	1.29883	0.0217285	68.62725	0.028222
800	1.29883	0.0212402	68.90312	0.027587
810	1.29883	0.0212402	69.179	0.027587
820	1.30127	0.0205078	69.44586	0.026686
830	1.29883	0.0205078	69.71222	0.026636
840	1.30127	0.0205078	69.97908	0.026686
850	1.30127	0.0202637	70.24277	0.026369
860	1.30127	0.0197754	70.5001	0.025733
870	1.30127	0.0197754	70.75743	0.025733
880	1.30127	0.0192871	71.00841	0.025098
890	1.30127	0.0192871	71.25938	0.025098
900	1.29883	0.0192871	71.50989	0.025051
910	0	0	0	0
920	0.866699	-0.0866699	0.751167	0.075117
930	0.839844	-0.0839844	1.456505	0.070534
940	0.817871	-0.0817871	2.125418	0.066891
950	0.795898	-0.0795898	2.758872	0.063345
960	0.773926	-0.0773926	3.357833	0.059896
970	0.751953	-0.0751953	3.923266	0.056543
980	0.732422	-0.0732422	4.459708	0.053644
990	0.715332	-0.0715332	4.971408	0.05117
1000	0.695801	-0.0695801	5.455547	0.048414
1010	0.67627	-0.067627	5.912888	0.045734
1020	0.656738	-0.0656738	6.344193	0.04313
1030	0.639648	-0.0639648	6.753343	0.040915
1040	0.622559	-0.0622559	7.140923	0.038758
1050	0.605469	-0.0605469	7.507515	0.036659
1060	0.588379	-0.0588379	7.853705	0.034619
1070	0.57373	-0.057373	8.182871	0.032917
1080	0.556641	-0.0556641	8.49272	0.030985
1090	0.541992	-0.0541992	8.786476	0.029376
1100	0.527344	-0.0527344	9.064567	0.027809
1110	0.512695	-0.0512695	9.327424	0.026286
1120	0.498047	-0.0498047	9.575474	0.024805
1130	0.48584	-0.048584	9.811515	0.023604
1140	0.471191	-0.0471191	10.03354	0.022202
1150	0.456543	-0.0456543	10.24197	0.020843
1160	0.444336	-0.0444336	10.4394	0.019743
1170	0.432129	-0.0432129	10.62614	0.018674
1180	0.41748	-0.041748	10.80043	0.017429
1190	0.405273	-0.0405273	10.96467	0.016425
1200	0.393066	-0.0393066	11.11917	0.01545
1210	0.383301	-0.0383301	11.26609	0.014692
1220	0.371094	-0.0371094	11.4038	0.013771

1230	0.358887	-0.0358887	11.5326	0.01288
1240	0.349121	-0.0349121	11.65449	0.012189
1250	0.339355	-0.0339355	11.76965	0.011516
1260	0.32959	-0.032959	11.87828	0.010863
1270	0.319824	-0.0319824	11.98057	0.010229
1280	0.310059	-0.0310059	12.07671	0.009614
1290	0.300293	-0.0300293	12.16688	0.009018
1300	0.290527	-0.0290527	12.25129	0.008441
1310	0.283203	-0.0283203	12.33149	0.00802
1320	0.273438	-0.0273438	12.40626	0.007477
1330	0.263672	-0.0263672	12.47578	0.006952
1340	0.256348	-0.0256348	12.5415	0.006571
1350	0.249023	-0.0249023	12.60351	0.006201
1360	0.239258	-0.0239258	12.66075	0.005724
1370	0.234375	-0.0234375	12.71568	0.005493
1380	0.227051	-0.0227051	12.76724	0.005155
1390	0.219727	-0.0219727	12.81552	0.004828
1400	0.212402	-0.0212402	12.86063	0.004511
1410	0.205078	-0.0205078	12.90269	0.004206
1420	0.197754	-0.0197754	12.9418	0.003911
1430	0.192871	-0.0192871	12.97899	0.00372
1440	0.185547	-0.0185547	13.01342	0.003443
1450	0.180664	-0.0180664	13.04606	0.003264
1460	0.17334	-0.017334	13.07611	0.003005
1470	0.168457	-0.0168457	13.10449	0.002838
1480	0.163574	-0.0163574	13.13124	0.002676
1490	0.15625	-0.015625	13.15566	0.002441
1500	0.153809	-0.0153809	13.17931	0.002366
1510	0.148926	-0.0148926	13.20149	0.002218
1520	0.144043	-0.0144043	13.22224	0.002075
1530	0.136719	-0.0136719	13.24093	0.001869
1540	0.134277	-0.0134277	13.25896	0.001803
1550	0.129395	-0.0129395	13.27571	0.001674
1560	0.126953	-0.0126953	13.29182	0.001612
1570	0.12207	-0.012207	13.30672	0.00149
1580	0.117188	-0.0117188	13.32046	0.001373
1590	0.114746	-0.0114746	13.33362	0.001317
1600	0.109863	-0.0109863	13.34569	0.001207
1610	0.107422	-0.0107422	13.35723	0.001154
1620	0.102539	-0.0102539	13.36775	0.001051
1630	0.100098	-0.0100098	13.37777	0.001002
1640	0.0976563	-0.00976563	13.3873	0.000954
1650	0.0927734	-0.00927734	13.39591	0.000861
1660	0.090332	-0.0090332	13.40407	0.000816
1670	0.0878906	-0.00878906	13.4118	0.000772
1680	0.0854492	-0.00854492	13.4191	0.00073
1690	0.0830078	-0.00830078	13.42599	0.000689
1700	0.078125	-0.0078125	13.43209	0.00061
1710	0.0756836	-0.00756836	13.43782	0.000573
1720	0.0756836	-0.00756836	13.44355	0.000573
1730	0.0732422	-0.00732422	13.44891	0.000536
1740	0.0708008	-0.00708008	13.45392	0.000501
1750	0.0683594	-0.00683594	13.4586	0.000467
1760	0.065918	-0.0065918	13.46294	0.000435
1770	0.0634766	-0.00634766	13.46697	0.000403
1780	0.0610352	-0.00610352	13.4707	0.000373
1790	0.0610352	-0.00610352	13.47442	0.000373
1800	0.0585938	-0.00585938	13.47786	0.000343
1810	0.0561523	-0.00561523	13.48101	0.000315

Aerogel QAQC Test Data Run 2

Time (sec)	Voltage	Current	Energy J	Power W
0	0	0	0	0
10	0	0	0	0
20	1.31592	0.389893	5.13068	0.513068
30	1.31104	0.326172	9.406925	0.427625
40	1.30859	0.284424	13.12887	0.372194
50	1.30615	0.252686	16.42933	0.330046
60	1.30371	0.227783	19.39896	0.296963
70	1.30371	0.207764	22.1076	0.270864
80	1.30371	0.190918	24.59661	0.248902
90	1.30371	0.176025	26.89147	0.229486
100	1.30127	0.163818	29.02318	0.213171
110	1.30371	0.151855	31.00293	0.197975
120	1.30371	0.14209	32.85537	0.185244
130	1.30127	0.133545	34.59316	0.173778
140	1.30127	0.125244	36.22292	0.162976
150	1.30127	0.118164	37.76055	0.153763
160	1.29883	0.111572	39.20968	0.144913
170	1.30127	0.105957	40.58847	0.137879
180	1.30127	0.100586	41.89736	0.13089
190	1.29883	0.0961914	43.14673	0.124936
200	1.29883	0.0913086	44.33267	0.118594
210	1.30127	0.0871582	45.46683	0.113416
220	1.30127	0.0834961	46.55334	0.108651
230	1.30127	0.079834	47.5922	0.103886
240	1.29883	0.0766602	48.58788	0.099569
250	1.29883	0.0734863	49.54235	0.095446
260	1.30127	0.0710449	50.46683	0.092449
270	1.30127	0.0678711	51.35002	0.088319
280	1.30127	0.0656738	52.20461	0.085459
290	1.29883	0.0639648	53.03541	0.083079
300	1.29883	0.0617676	53.83766	0.080226
310	1.29883	0.0600586	54.61772	0.078006
320	1.29883	0.0578613	55.36924	0.075152
330	1.29883	0.0559082	56.09539	0.072615
340	1.30127	0.0541992	56.80067	0.070528
350	1.29883	0.0527344	57.4856	0.068493
360	1.30127	0.0505371	58.14323	0.065762
370	1.29883	0.0495605	58.78693	0.064371
380	1.30127	0.0480957	59.41279	0.062585
390	1.29883	0.046875	60.02161	0.060883
400	1.30127	0.0456543	60.6157	0.059409
410	1.29883	0.0444336	61.19282	0.057712
420	1.29883	0.0437012	61.76042	0.05676
430	1.29883	0.0429688	62.31851	0.055809
440	1.30127	0.0412598	62.85541	0.05369
450	1.29883	0.0407715	63.38497	0.052955
460	1.29883	0.0397949	63.90184	0.051687
470	1.29883	0.0388184	64.40602	0.050419
480	1.30127	0.0378418	64.89844	0.049242
490	1.30127	0.0368652	65.37816	0.047972
500	1.29883	0.036377	65.85064	0.047248
510	1.29883	0.0356445	66.3136	0.046296
520	1.30127	0.034668	66.76472	0.045112
530	1.30127	0.0344238	67.21267	0.044795
540	1.29883	0.0339355	67.65343	0.044076
550	1.30127	0.0332031	68.08549	0.043206
560	1.30127	0.0327148	68.5112	0.042571
570	1.30127	0.0322266	68.93056	0.041936
580	1.30127	0.0317383	69.34356	0.0413

590	1.29883	0.03125	69.74944	0.040588
600	1.30127	0.0305176	70.14656	0.039712
610	1.30127	0.0300293	70.53732	0.039076
620	1.30127	0.029541	70.92173	0.038441
630	1.29883	0.029541	71.30542	0.038369
640	1.29883	0.0288086	71.67959	0.037417
650	1.29883	0.0288086	72.05377	0.037417
660	1.29883	0.0283203	72.4216	0.036783
670	1.30127	0.027832	72.78377	0.036217
680	1.29883	0.0273438	73.13892	0.035515
690	1.30127	0.0270996	73.49156	0.035264
700	1.30127	0.0266113	73.83784	0.034628
710	1.30127	0.026123	74.17777	0.033993
720	1.30127	0.0258789	74.51453	0.033675
730	1.29883	0.0256348	74.84748	0.033295
740	1.30127	0.0251465	75.1747	0.032722
750	1.30127	0.0251465	75.50193	0.032722
760	1.30127	0.0246582	75.8228	0.032087
770	1.30127	0.0244141	76.14049	0.031769
780	1.29883	0.0244141	76.45759	0.03171
790	1.29883	0.0241699	76.77151	0.031393
800	1.30127	0.0236816	77.07968	0.030816
810	1.29883	0.0236816	77.38726	0.030758
820	1.29883	0.0236816	77.69484	0.030758
830	1.30127	0.0231934	77.99665	0.030181
840	1.29883	0.0229492	78.29472	0.029807
850	1.30127	0.0224609	78.587	0.029228
860	1.30127	0.0222168	78.8761	0.02891
870	1.30127	0.0224609	79.16838	0.029228
880	1.30127	0.0224609	79.46065	0.029228
890	1.30127	0.0217285	79.7434	0.028275
900	1.30127	0.0214844	80.02297	0.027957
910	0	0	0	0
920	0.9375	-0.09375	0.878906	0.087891
930	0.908203	-0.0908203	1.703739	0.082483
940	0.878906	-0.0878906	2.476215	0.077248
950	0.856934	-0.0856934	3.210551	0.073434
960	0.830078	-0.0830078	3.89958	0.068903
970	0.808105	-0.0808105	4.552614	0.065303
980	0.783691	-0.0783691	5.166785	0.061417
990	0.761719	-0.0761719	5.747001	0.058022
1000	0.742188	-0.0742188	6.297844	0.055084
1010	0.717773	-0.0717773	6.813042	0.05152
1020	0.698242	-0.0698242	7.300584	0.048754
1030	0.678711	-0.0678711	7.761233	0.046065
1040	0.65918	-0.065918	8.195751	0.043452
1050	0.637207	-0.0637207	8.601784	0.040603
1060	0.620117	-0.0620117	8.986329	0.038455
1070	0.600586	-0.0600586	9.347032	0.03607
1080	0.583496	-0.0583496	9.6875	0.034047
1090	0.566406	-0.0566406	10.00832	0.032082
1100	0.549316	-0.0549316	10.31006	0.030175
1110	0.532227	-0.0532227	10.59333	0.028327
1120	0.515137	-0.0515137	10.8587	0.026537
1130	0.500488	-0.0500488	11.10918	0.025049
1140	0.483398	-0.0483398	11.34286	0.023367
1150	0.46875	-0.046875	11.56258	0.021973
1160	0.456543	-0.0456543	11.77102	0.020843
1170	0.441895	-0.0441895	11.96629	0.019527
1180	0.427246	-0.0427246	12.14883	0.018254
1190	0.415039	-0.0415039	12.32108	0.017226
1200	0.400391	-0.0400391	12.4814	0.016031
1210	0.388184	-0.0388184	12.63208	0.015069
1220	0.375977	-0.0375977	12.77344	0.014136

1230	0.36377	-0.036377	12.90577	0.013233
1240	0.354004	-0.0354004	13.03109	0.012532
1250	0.341797	-0.0341797	13.14791	0.011683
1260	0.332031	-0.0332031	13.25816	0.011024
1270	0.319824	-0.0319824	13.36045	0.010229
1280	0.310059	-0.0310059	13.45658	0.009614
1290	0.300293	-0.0300293	13.54676	0.009018
1300	0.290527	-0.0290527	13.63116	0.008441
1310	0.283203	-0.0283203	13.71137	0.00802
1320	0.270996	-0.0270996	13.78481	0.007344
1330	0.263672	-0.0263672	13.85433	0.006952
1340	0.253906	-0.0253906	13.9188	0.006447
1350	0.244141	-0.0244141	13.9784	0.00596
1360	0.236816	-0.0236816	14.03449	0.005608
1370	0.229492	-0.0229492	14.08715	0.005267
1380	0.219727	-0.0219727	14.13543	0.004828
1390	0.212402	-0.0212402	14.18055	0.004511
1400	0.205078	-0.0205078	14.2226	0.004206
1410	0.197754	-0.0197754	14.26171	0.003911
1420	0.192871	-0.0192871	14.29891	0.00372
1430	0.185547	-0.0185547	14.33334	0.003443
1440	0.178223	-0.0178223	14.3651	0.003176
1450	0.17334	-0.017334	14.39515	0.003005
1460	0.168457	-0.0168457	14.42352	0.002838
1470	0.161133	-0.0161133	14.44949	0.002596
1480	0.15625	-0.015625	14.4739	0.002441
1490	0.151367	-0.0151367	14.49681	0.002291
1500	0.144043	-0.0144043	14.51756	0.002075
1510	0.13916	-0.013916	14.53693	0.001937
1520	0.136719	-0.0136719	14.55562	0.001869
1530	0.131836	-0.0131836	14.573	0.001738
1540	0.126953	-0.0126953	14.58912	0.001612
1550	0.12207	-0.012207	14.60402	0.00149
1560	0.117188	-0.0117188	14.61775	0.001373
1570	0.114746	-0.0114746	14.63092	0.001317
1580	0.112305	-0.0112305	14.64353	0.001261
1590	0.107422	-0.0107422	14.65507	0.001154
1600	0.10498	-0.010498	14.66609	0.001102
1610	0.100098	-0.0100098	14.67611	0.001002
1620	0.0976563	-0.00976563	14.68565	0.000954
1630	0.0952148	-0.00952148	14.69471	0.000907
1640	0.0927734	-0.00927734	14.70332	0.000861
1650	0.0878906	-0.00878906	14.71105	0.000772
1660	0.0854492	-0.00854492	14.71835	0.00073
1670	0.0830078	-0.00830078	14.72524	0.000689
1680	0.0805664	-0.00805664	14.73173	0.000649
1690	0.078125	-0.0078125	14.73783	0.00061
1700	0.0732422	-0.00732422	14.7432	0.000536
1710	0.0732422	-0.00732422	14.74856	0.000536
1720	0.0708008	-0.00708008	14.75357	0.000501
1730	0.0683594	-0.00683594	14.75825	0.000467
1740	0.065918	-0.0065918	14.76259	0.000435
1750	0.0634766	-0.00634766	14.76662	0.000403
1760	0.0634766	-0.00634766	14.77065	0.000403
1770	0.0610352	-0.00610352	14.77438	0.000373
1780	0.0585938	-0.00585938	14.77781	0.000343
1790	0.0561523	-0.00561523	14.78096	0.000315
1800	0.0561523	-0.00561523	14.78412	0.000315
1810	0.0537109	-0.00537109	14.787	0.000288

Aerogel QAQC Test Data Run 3

Time (sec)	Voltage	Current	Energy J	Power W
0	0	0	0	0
10	0	0	0	0
20	1.30127	0.227295	2.957722	0.295772
30	1.30371	0.208496	5.675905	0.271818
40	1.30127	0.205322	8.347698	0.267179
50	1.30127	0.200684	10.95914	0.261144
60	1.30371	0.192627	13.47044	0.25113
70	1.30127	0.184082	15.86584	0.23954
80	1.30371	0.17334	18.12569	0.225985
90	1.30127	0.164307	20.26377	0.213808
100	1.30127	0.153809	22.26524	0.200147
110	1.30127	0.145752	24.16187	0.189663
120	1.30127	0.137207	25.9473	0.178543
130	1.30127	0.128906	27.62472	0.167742
140	1.30371	0.121582	29.20979	0.158508
150	1.30127	0.115723	30.71566	0.150587
160	1.30127	0.109375	32.13892	0.142326
170	1.30127	0.104492	33.49865	0.135972
180	1.30127	0.0991211	34.78848	0.128983
190	1.30127	0.0952148	36.02748	0.1239
200	1.30127	0.0910645	37.21248	0.1185
210	1.30127	0.0871582	38.34664	0.113416
220	1.29883	0.0837402	39.43428	0.108764
230	1.30127	0.0800781	40.47632	0.104203
240	1.30127	0.0773926	41.4834	0.100709
250	1.29883	0.074707	42.45372	0.097032
260	1.30127	0.0720215	43.39091	0.093719
270	1.29883	0.0693359	44.29147	0.090056
280	1.30127	0.0668945	45.16195	0.087048
290	1.30127	0.0646973	46.00383	0.084189
300	1.30127	0.0629883	46.82348	0.081965
310	1.29883	0.0603027	47.60671	0.078323
320	1.30127	0.0585938	48.36917	0.076246
330	1.30127	0.0568848	49.1094	0.074022
340	1.29883	0.0554199	49.82921	0.071981
350	1.30127	0.0537109	50.52813	0.069892
360	1.30127	0.0524902	51.21117	0.068304
370	1.29883	0.0517578	51.88342	0.067225
380	1.29883	0.0505371	52.53981	0.065639
390	1.30127	0.0490723	53.17837	0.063856
400	1.29883	0.0473633	53.79354	0.061517
410	1.30127	0.0458984	54.3908	0.059726
420	1.29883	0.045166	54.97743	0.058663
430	1.30127	0.0446777	55.55881	0.058138
440	1.30127	0.0437012	56.12748	0.056867
450	1.30127	0.0424805	56.68027	0.055279
460	1.30127	0.0419922	57.2267	0.054643
470	1.30127	0.0407715	57.75725	0.053055
480	1.30127	0.0402832	58.28144	0.052419
490	1.30127	0.0400391	58.80246	0.052102
500	1.30127	0.0388184	59.30759	0.050513
510	1.29883	0.0378418	59.79909	0.04915
520	1.30127	0.0375977	60.28834	0.048925
530	1.30127	0.0366211	60.76488	0.047654
540	1.29883	0.0358887	61.23101	0.046613
550	1.29883	0.0354004	61.6908	0.045979
560	1.29883	0.0349121	62.14425	0.045345
570	1.30127	0.0344238	62.5922	0.044795
580	1.29883	0.0339355	63.03296	0.044076

590	1.29883	0.0334473	63.46738	0.043442
600	1.30127	0.0327148	63.89309	0.042571
610	1.29883	0.0319824	64.30849	0.04154
620	1.29883	0.0319824	64.72389	0.04154
630	1.29883	0.0314941	65.13294	0.040905
640	1.29883	0.0310059	65.53565	0.040271
650	1.30127	0.0305176	65.93277	0.039712
660	1.30127	0.0300293	66.32353	0.039076
670	1.30127	0.029541	66.70794	0.038441
680	1.29883	0.0292969	67.08846	0.038052
690	1.30127	0.0285645	67.46016	0.03717
700	1.30127	0.0283203	67.82868	0.036852
710	1.30127	0.0283203	68.19721	0.036852
720	1.30127	0.027832	68.55938	0.036217
730	1.30127	0.0275879	68.91837	0.035899
740	1.30127	0.0273438	69.27419	0.035582
750	1.30127	0.0270996	69.62683	0.035264
760	1.30127	0.0266113	69.97311	0.034628
770	1.29883	0.0263672	70.31558	0.034247
780	1.30127	0.0256348	70.64915	0.033358
790	1.29883	0.0256348	70.98211	0.033295
800	1.30127	0.0251465	71.30933	0.032722
810	1.30127	0.0251465	71.63655	0.032722
820	1.29883	0.0251465	71.96316	0.032661
830	1.29883	0.0249023	72.2866	0.032344
840	1.29883	0.0244141	72.6037	0.03171
850	1.29883	0.0244141	72.9208	0.03171
860	1.29883	0.0244141	73.2379	0.03171
870	1.29883	0.0239258	73.54865	0.031076
880	1.30127	0.0236816	73.85681	0.030816
890	1.29883	0.0236816	74.1644	0.030758
900	1.29883	0.0231934	74.46564	0.030124
910	0	0	0	0
920	0.83252	-0.083252	0.69309	0.069309
930	0.78125	-0.078125	1.303441	0.061035
940	0.756836	-0.0756836	1.876242	0.05728
950	0.737305	-0.0737305	2.419861	0.054362
960	0.722656	-0.0722656	2.942092	0.052223
970	0.708008	-0.0708008	3.443368	0.050128
980	0.693359	-0.0693359	3.924114	0.048075
990	0.673828	-0.0673828	4.378158	0.045404
1000	0.65918	-0.065918	4.812677	0.043452
1010	0.64209	-0.064209	5.224956	0.041228
1020	0.622559	-0.0622559	5.612536	0.038758
1030	0.60791	-0.060791	5.982091	0.036955
1040	0.593262	-0.0593262	6.33405	0.035196
1050	0.578613	-0.0578613	6.668843	0.033479
1060	0.561523	-0.0561523	6.984151	0.031531
1070	0.541992	-0.0541992	7.277907	0.029376
1080	0.534668	-0.0534668	7.563777	0.028587
1090	0.517578	-0.0517578	7.831664	0.026789
1100	0.505371	-0.0505371	8.087063	0.02554
1110	0.490723	-0.0490723	8.327873	0.024081
1120	0.478516	-0.0478516	8.55685	0.022898
1130	0.466309	-0.0466309	8.774294	0.021744
1140	0.45166	-0.045166	8.978291	0.0204
1150	0.437012	-0.0437012	9.16927	0.019098
1160	0.424805	-0.0424805	9.34973	0.018046
1170	0.415039	-0.0415039	9.521987	0.017226
1180	0.405273	-0.0405273	9.686233	0.016425
1190	0.393066	-0.0393066	9.840734	0.01545
1200	0.383301	-0.0383301	9.987654	0.014692
1210	0.371094	-0.0371094	10.12536	0.013771
1220	0.361328	-0.0361328	10.25592	0.013056

1230	0.351563	-0.0351563	10.37952	0.01236
1240	0.339355	-0.0339355	10.49468	0.011516
1250	0.332031	-0.0332031	10.60493	0.011024
1260	0.322266	-0.0322266	10.70878	0.010386
1270	0.3125	-0.03125	10.80644	0.009766
1280	0.302734	-0.0302734	10.89808	0.009165
1290	0.29541	-0.029541	10.98535	0.008727
1300	0.285645	-0.0285645	11.06695	0.008159
1310	0.275879	-0.0275879	11.14305	0.007611
1320	0.266113	-0.0266113	11.21387	0.007082
1330	0.258789	-0.0258789	11.28084	0.006697
1340	0.249023	-0.0249023	11.34285	0.006201
1350	0.244141	-0.0244141	11.40246	0.00596
1360	0.236816	-0.0236816	11.45854	0.005608
1370	0.229492	-0.0229492	11.51121	0.005267
1380	0.222168	-0.0222168	11.56057	0.004936
1390	0.214844	-0.0214844	11.60672	0.004616
1400	0.209961	-0.0209961	11.65081	0.004408
1410	0.205078	-0.0205078	11.69286	0.004206
1420	0.200195	-0.0200195	11.73294	0.004008
1430	0.192871	-0.0192871	11.77014	0.00372
1440	0.187988	-0.0187988	11.80548	0.003534
1450	0.183105	-0.0183105	11.83901	0.003353
1460	0.175781	-0.0175781	11.86991	0.00309
1470	0.170898	-0.0170898	11.89911	0.002921
1480	0.166016	-0.0166016	11.92668	0.002756
1490	0.161133	-0.0161133	11.95264	0.002596
1500	0.153809	-0.0153809	11.9763	0.002366
1510	0.148926	-0.0148926	11.99848	0.002218
1520	0.144043	-0.0144043	12.01922	0.002075
1530	0.144043	-0.0144043	12.03997	0.002075
1540	0.13916	-0.013916	12.05934	0.001937
1550	0.136719	-0.0136719	12.07803	0.001869
1560	0.131836	-0.0131836	12.09541	0.001738
1570	0.126953	-0.0126953	12.11153	0.001612
1580	0.124512	-0.0124512	12.12703	0.00155
1590	0.119629	-0.0119629	12.14134	0.001431
1600	0.114746	-0.0114746	12.15451	0.001317
1610	0.112305	-0.0112305	12.16712	0.001261
1620	0.109863	-0.0109863	12.17919	0.001207
1630	0.107422	-0.0107422	12.19073	0.001154
1640	0.10498	-0.010498	12.20175	0.001102
1650	0.100098	-0.0100098	12.21177	0.001002
1660	0.0976563	-0.00976563	12.22131	0.000954
1670	0.0952148	-0.00952148	12.23037	0.000907
1680	0.090332	-0.0090332	12.23853	0.000816
1690	0.0878906	-0.00878906	12.24626	0.000772
1700	0.0854492	-0.00854492	12.25356	0.00073
1710	0.0830078	-0.00830078	12.26045	0.000689
1720	0.078125	-0.0078125	12.26655	0.00061
1730	0.078125	-0.0078125	12.27266	0.00061
1740	0.0756836	-0.00756836	12.27839	0.000573
1750	0.0732422	-0.00732422	12.28375	0.000536
1760	0.0683594	-0.00683594	12.28842	0.000467
1770	0.065918	-0.0065918	12.29277	0.000435
1780	0.065918	-0.0065918	12.29711	0.000435
1790	0.0634766	-0.00634766	12.30114	0.000403
1800	0.0610352	-0.00610352	12.30487	0.000373
1810	0.0610352	-0.00610352	12.30859	0.000373

Energy Data Used for Graph

Time s	Run 1 - Energy J	Run 2 - Energy J	Run 3 - Energy J
0	0	0	0
10	0	0	0
20	3.400841745	5.130679966	2.957721647
30	7.172544808	9.406925354	5.675904848
40	10.46957657	13.12886938	8.347698438
50	13.42562913	16.42932757	10.95913912
60	16.08652731	19.39895731	13.47043659
70	18.50870316	22.10759736	15.86584043
80	20.73353642	24.59661442	18.12569134
90	22.7858344	26.89146994	20.26376904
100	24.69556096	29.02318443	22.26523941
110	26.47146919	31.00293325	24.16186647
120	28.1330088	32.85537479	25.94729999
130	29.69605529	34.59315581	27.6247151
140	31.16697186	36.22291841	29.20979179
150	32.55528381	37.7605511	30.71566047
160	33.87689266	39.2096817	32.13892454
170	35.13177889	40.58846836	33.49864759
180	36.32630441	41.8973638	34.78848072
190	37.46468345	43.14672656	36.02748235
200	38.55232629	44.33267005	37.21247737
210	39.59118218	45.46683356	38.34664088
220	40.58686785	46.55334326	39.43428372
230	41.54630073	47.59219915	40.47631601
240	42.4707867	48.58788483	41.4834027
250	43.36500128	49.54234694	42.45371963
260	44.22277244	50.46683291	43.3909138
270	45.05039601	51.35001917	44.29146927
280	45.84630994	52.20461263	45.16194733
290	46.61830398	53.03540664	46.00383388
300	47.36348172	53.83766276	46.82348174
310	48.08646375	54.61772187	47.60671129
320	48.78407703	55.36924179	48.36917484
330	49.46393986	56.09539427	49.10939967
340	50.12156398	56.8006722	49.82920996
350	50.7633035	57.48560241	50.52813379
360	51.38915841	58.14322653	51.21117301
370	51.99277462	58.78693317	51.88341885
380	52.57940418	59.41278808	52.53980986
390	53.15652111	60.02161465	53.17837298
400	53.71883761	60.61570036	53.79354173
410	54.26526951	61.19281728	54.39080384
420	54.80116417	61.76042158	54.9774334
430	55.31900327	62.31851324	55.5588109
440	55.82635874	62.85541464	56.12748151
450	56.32102983	63.38496712	56.68026751
460	56.80392332	63.90183522	57.22669941
470	57.27639871	64.40602024	57.75724671
480	57.7402299	64.89844423	58.28143991
490	58.19050828	65.37816002	58.8024567
500	58.62892436	65.85063541	59.3075889
510	59.06017619	66.31359687	59.79908955
520	59.48191538	66.76472115	60.28833714
530	59.90127046	67.21266774	60.76487653
540	60.31032528	67.65343219	61.23100973
550	60.71061805	68.08549417	61.69080075
560	61.10773442	68.51120205	62.14424957
570	61.49532029	68.93055713	62.59219616
580	61.87583722	69.3435581	63.03296061

590	62.24684152	69.74944248	63.46738418
600	62.61150362	70.14655885	63.89309206
610	62.97299399	70.53732112	64.30848906
620	63.32814347	70.92172929	64.72388607
630	63.67695076	71.30541666	65.13294089
640	64.02258631	71.6795914	65.53565482
650	64.35934067	72.05376614	65.93277119
660	64.69291863	72.42159869	66.32353346
670	65.02331889	72.78376816	66.70794163
680	65.34736505	73.13891764	67.08845856
690	65.66446271	73.4915566	67.46015983
700	65.98156036	73.83784147	67.8286834
710	66.29231583	74.17777223	68.19720696
720	66.59730098	74.51452659	68.55937643
730	66.89854382	74.84747906	68.9183695
740	67.19661492	75.17470292	69.27418616
750	67.48834382	75.50192678	69.62682513
760	67.78007273	75.82279654	69.97310999
770	68.06546075	76.1404899	70.3155751
780	68.3450308	76.45758756	70.64915306
790	68.62724708	76.77151347	70.98210553
800	68.90312117	77.07967503	71.30932939
810	69.17899526	77.38725875	71.63655325
820	69.44585711	77.69484248	71.96316354
830	69.71221857	77.99665123	72.28660208
840	69.97908042	78.29472233	72.60369974
850	70.24276586	78.58699928	72.92079739
860	70.50009721	78.87609983	73.23789505
870	70.75742856	79.16837679	73.54865051
880	71.00840581	79.46065374	73.85681207
890	71.25938305	79.74340019	74.1643958
900	71.50988969	80.02297025	74.46563863
910	0	0	0
920	0.751167157	0.87890625	0.69308955
930	1.456505101	1.703738939	1.303441113
940	2.125418074	2.476214696	1.876241844
950	2.7588717	3.210550576	2.419860507
960	3.357833153	3.899580062	2.942092201
970	3.923266468	4.552613754	3.443367529
980	4.459708454	5.166785337	3.924114232
990	4.971408324	5.747001172	4.378158406
1000	5.455547356	6.297844199	4.812676678
1010	5.912888468	6.813042279	5.224956246
1020	6.344193269	7.300584169	5.612535955
1030	6.753342833	7.761232791	5.982090523
1040	7.140922542	8.195751063	6.334050323
1050	7.507515251	8.601783824	6.668843327
1060	7.853705099	8.986328918	6.984151407
1070	8.182871212	9.347032461	7.277906735
1080	8.492720415	9.687500043	7.563776605
1090	8.786475743	10.0083158	7.831663591
1100	9.064567437	10.31006387	8.087063439
1110	9.3274236	10.59332945	8.327872501
1120	9.575474415	10.85869558	8.556850064
1130	9.81151492	11.10918381	8.774294147
1140	10.03353588	11.34285744	8.978290903
1150	10.24196739	11.562584	9.169270391
1160	10.43940187	11.77101551	9.349729679
1170	10.62613734	11.96628671	9.52198705
1180	10.80042689	12.14882585	9.686233255
1190	10.9646731	12.32108322	9.840734135
1200	11.11917398	12.48139617	9.987653792

1210	11.26609363	12.63208299	10.12536455
1220	11.40380439	12.7734417	10.25592247
1230	11.53260427	12.90577031	10.37951902
1240	11.65448974	13.03108914	10.49468083
1250	11.76965156	13.14791433	10.60492542
1260	11.87828113	13.25815892	10.70878079
1270	11.98056852	13.36044631	10.80643704
1280	12.0767051	13.45658289	10.89808492
1290	12.16688099	13.54675878	10.98535198
1300	12.25128693	13.63116471	11.06694505
1310	12.33149086	13.71136865	11.14305427
1320	12.4062592	13.78480748	11.2138704
1330	12.47578213	13.85433041	11.28084215
1340	12.54149643	13.91879867	11.3428546
1350	12.60350888	13.97840349	11.40245943
1360	12.66075327	14.03448531	11.45854125
1370	12.71568491	14.08715189	11.51120783
1380	12.76723707	14.13543184	11.56056645
1390	12.81551702	14.18054645	11.60672439
1400	12.86063163	14.22260344	11.65080801
1410	12.90268862	14.26171008	11.692865
1420	12.94179526	14.29890931	11.73294304
1430	12.97899448	14.333337	11.77014226
1440	13.01342217	14.36510043	11.80548175
1450	13.04606165	14.39514719	11.83900919
1460	13.07610841	14.42352495	11.86990815
1470	13.10448617	14.44948879	11.89911427
1480	13.13124262	14.47390286	11.92667559
1490	13.15565669	14.49681482	11.95263943
1500	13.1793139	14.51756321	11.97629664
1510	13.20149285	14.53692872	11.99847559
1520	13.22224124	14.5556208	12.01922398
1530	13.24093332	14.57300153	12.03997236
1540	13.25896363	14.5891186	12.05933787
1550	13.2757067	14.60401968	12.07802995
1560	13.29182376	14.61775271	12.09541069
1570	13.30672485	14.63091935	12.11152775
1580	13.32045788	14.64353177	12.12703099
1590	13.33362452	14.65507125	12.14134209
1600	13.3456944	14.66609205	12.15450873
1610	13.35723388	14.67611166	12.16712114
1620	13.36774813	14.68564841	12.17919102
1630	13.37776774	14.69471427	12.19073051
1640	13.38730449	14.70332118	12.20175131
1650	13.3959114	14.71104593	12.21177092
1660	13.40407127	14.7183475	12.22130767
1670	13.41179603	14.7252378	12.23037353
1680	13.41909759	14.73172874	12.2385334
1690	13.42598789	14.73783226	12.24625816
1700	13.4320914	14.74319668	12.25355972
1710	13.43781941	14.7485611	12.26045002
1720	13.44354742	14.75357385	12.26655353
1730	13.44891184	14.75824686	12.27265705
1740	13.45392459	14.76259204	12.27838506
1750	13.4585976	14.76662132	12.28374948
1760	13.46294278	14.7706506	12.28842248
1770	13.46697206	14.77437589	12.29276767
1780	13.47069735	14.77780913	12.29711285
1790	13.47442265	14.78096221	12.30114213
1800	13.47785588	14.78411529	12.30486742
1810	13.48100896	14.78700015	12.30859272

SUMMARY SHEET

AEROGEL MANUFACTURING: QUALITY CONTROL TEST

Technician: T.Welgemoed

BATCH SERIAL NUMBER: QA071900edge

REMARK : Aerogel received from CCAT on 071900
Test Pieces from edge of sample sheet.

PHYSICAL PARAMETERS

	Length in inches "	Width in inches "	Thickness "x.001	Dry Mass in g	Length in cm	Width in cm	Thickness in cm	Density in g/cm3
Plate1	3	2	34	2.35	7.62	5.08	0.08636	0.703
Plate2	3	2	34	2.3	7.62	5.08	0.08636	0.688

CAPACITY TEST

	Datafile	Energy In - J	Energy Out - J	Ratio out/In	Energy out per g of Aerogel (J/g)	Energy out per cm^2 (J/cm^2)
Run 1	QAmini071900A	71.51	13.48	0.1885195	5.737	0.348
Run 2	QAmini071900B	80.02	14.79	0.18478445	6.292	0.382
Run 3	QAmini071900C	74.47	12.31	0.16529225	5.238	0.318
	Average	75.33	13.53	0.17953207	5.756	0.349

GRAPH FOR BATCH SERIAL NUMBER : **QA071900edge**

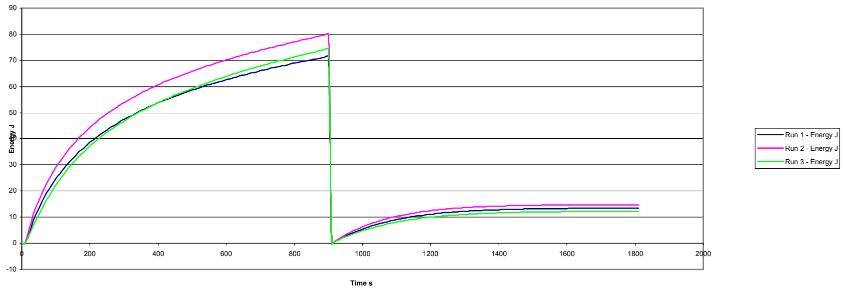

	YES/NO	Supervisor	Action Taken
Batch Approved For Manufacturing	Yes	TW	None

Preliminary Source Water Desalination Efficiency Test

Once an industrial module prototype was completed a basic desalination efficiency test was conducted for a specific source water. The attached sheet illustrates typical data collected during a basic desalination efficiency test.

DATA FOR ENCINA PILOT PLANT TESTING

Capacitive Deionization Technology: Encina Water Pollution Control Facility
2-Apr-01
Experimental setup: Recirculating Flow .
Objective: Determine Ion Storage Capacity of 1/4 scale Cell
Feed Water: Encina Brackish Groundwater
Technician: T.Welgemoed

Time	Flow (liters/min)	Cell Voltage (V)	Current (A)	Conductivity IN (uS/cm)	Conductivity OUT (uS/cm)
0	1.50	0.60	110.00	4591	5806
1	1.50	0.60	110.00	4620	5848
2	1.50	0.73	110.00	4614	5804
3	1.50	0.83	110.00	4611	5730
4	1.50	0.92	110.00	4598	5673
5	1.50	1.00	110.00	4567	5525
6	1.50	1.06	110.00	4539	5401
7	1.50	1.10	110.00	4480	5287
8	1.50	1.17	110.00	4424	5154
9	1.50	1.20	93.00	4355	5045
10	1.50	1.20	69.00	4286	4941
12	1.50	1.20	60.00	4215	4852
13	1.50	1.20	40.00	4058	4714
15	1.50	1.20	37.00	3925	4630
17	1.50	1.20	30.00	3798	4557
19	1.50	1.20	29.00	3711	4498
22	1.50	1.20	22.00	3640	4448
24	1.50	1.20	19.00	3501	4421
30	1.50	1.20	20.00	3467	4459
36	1.50	1.20	17.00	3384	4462
40	1.50	1.20	17.00	3348	4493
41	**1.50**	**0.00**	**0.00**	**3344**	**4489**
42	1.50	0.00	0.00	3340	4505
43	1.50	0.00	0.00	3332	4664
44	1.50	0.00	0.00	3328	4599
45	1.50	0.00	0.00	3332	4664
46	1.50	0.90	0.00	3342	4721
47	1.50	0.89	0.00	3353	4781
48	1.50	0.86	0.00	3385	4827
49	1.50	0.84	0.00	3409	4878
50	1.50	0.82	0.00	3429	4917
55	1.50	0.71	0.00	3571	5140
60	1.50	0.63	0.00	3665	5297
70	1.50	0.48	0.00	3832	5602
80	1.50	0.37	0.00	3932	5842
85	1.50	0.32	0.00	3955	5921
91	1.50	0.28	0.00	3988	5967
93	1.50	0.27	0.00	3971	5978
94	1.50	0.26	0.00	4004	5974
96	1.50	0.25	0.00	4005	5970
97	1.50	0.24	0.00	4008	5989
98	1.50	0.23	0.00	4009	6008
100	1.50	0.22	0.00	4015	6019
101	1.00	0.00	0.00	4015	6019
102	1.00	0.22	0.00	4022	6028
105	1.00	0.20	0.00	4044	6044

107	0.10	0.00	0.00	4058	6049
109	0.10	0.18	0.00	4072	6053
112	0.10	0.17	0.00	4072	6075

FARWEST GROUP, INC
Water Analysis Report
Client : CBMA
Date of Test Run: 21 June, 2000
Datafile: C:\Temp\cbma062100
Prepared by : T. Welgemoed

Sample No	Description	Conductivity in microsiemans/cm	Iron as mg/l Fe	Sodium as mg/l Na	Bicarbonate as mg/l $CaCO_3$	Total Alk as mg/l $CaCO_3$	Sulfate as mg/l SO_4	pH
CBMA 1	Feed To Brick after 50 % dilution	1140.1	ND	280	520	520	ND	8.2
CBMA 2	After Physi-sorbsion	980	ND	230	370	410	5.1	8.5
CBMA 3	After 40 min Charge - Once Through Flow	285	ND	68	72	120	ND	9
CBMA 4	Rinse Water at Stabilization		ND	84	140	140	ND	8.2
	% Reduction of Component with regards to feed		NA	75.71%	86.15%	76.92%	NA	NA

ND = None Detected
NA = Not Applicable

Comments

Total Rinse volume was 6.15 liters from which a combined sample (CBMA 4) was taken.
The rinse cycle was started at the end of the 40 min charge cycle by changing polarity, shorting the brick and switching of the power. The feed water for the rinse cycle was as for CBMA 1 sample.

Conclusion

This source water is mostly contaminated by Na_2HCO_3 (Sodium Bicarbonate)
Raw Water Quality :
pH = 8.0
Conductivity = 2490 microsiemans/cm
Turbidity = 200 NTU (Must be filtered before entering CDT system)
DO = 1.33 mg/l
HCO_3^- = 1040 mg/l
Na^+ = 560 mg/l
No iron was detected and very little sulfate
CDT would be able to treat this source water effectively to produce potable and or irrigation standard water.

APPENDIX B

INDUSTRIAL PROTOTYPE DEVELEPMENT PHASE: TECHNICAL BULLITENS

Graphite Bus - Mk-8A Brick

Initial Testing

FarWest Group, Inc
Engineering and Development Center
701 Palomar Airport Road, Suite 300
Carlsbad, CA 92009

Phone: (760)931-4784 Fax: (760)931-4850
Email: c_sheppard@msn.com

Introduction

Due to the high costs of experimental graphite components, the electrode internal electrical connections have been made via metallic bus elements. This has been adequate to obtain short term performance data but has never been the long term design objective.

A prototype brick incorporating a psuedo graphite bus has been construced using the same housings and electrode geometry as the Mk-8 brick. The electrical bus is constructed at each end by reaming and press fitting four 1/4 inch diameter graphite rods through a stack of aerogel electrodes and aerogel spacers at each end of the brick.

Redundant electrical connection is made by parallel connection to three of the graphite rods at each pole. The fourth is used to monitor electrode voltage.

Coupling to the graphite rods is made by wraping the post with stripped multistrand copper wire and installing a metal "P" clamp over the wire. The copper wire provides improved coupling between the clamp and rod.

The results of two single pass tests at different flow rates are presented here and compared with the previous Mk-8 brick containing metallic separators...

Objectives

1. Determine ion storage capacity.
2. Compare performance of the new Mk-8A graphite bus brick with the older Mk-8 metal bus brick.
3. Study effect of flow rate on ion adsorption and energy use.

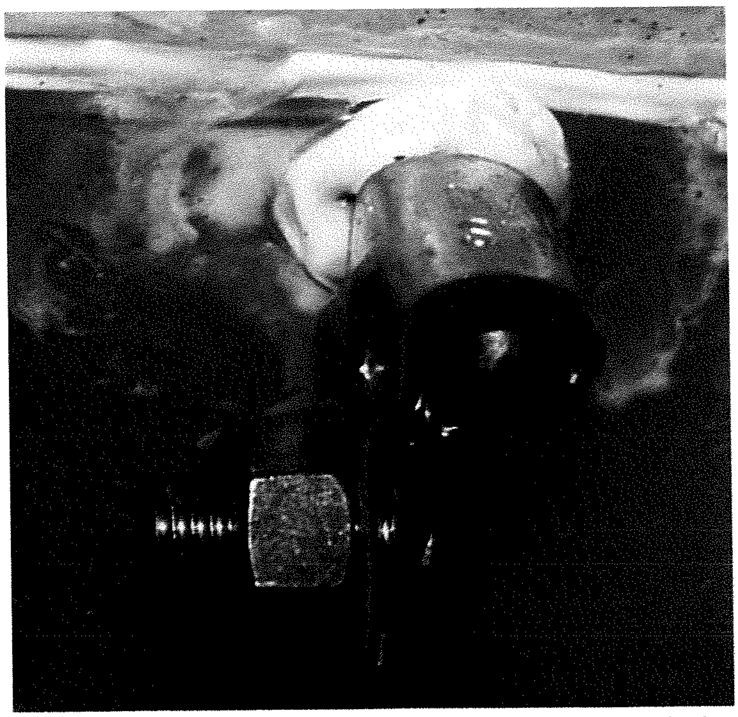

Figure 1 - Graphite rod connection. Metal clamp makes good electrical connection to graphite rod through stranded copper wires.

Test Equipment

1. Mk-8A brick serial number 3
2. Mk-8 brick serial number 1 (tested June 2000)
3. Pulsafeeder metering pumps set at 52.6 ml/min and 157.6 ml/min flow rates
4. Input reservoir containing 500 ppm NaCl
5. Signet conductivity probe K=1
6. Signet conductivity readout model 8850 - full scale 20mA output value set to 5000 uS/cm
7. Industrial computer ADIO interface board mounted in Compaq Presario 4880
8. FarWest test interface control box
9. Fluke 89 mk IV True RMS Multimeter
10. Ohaus 2610g triple beam balance
11. Plastic tubing and connectors

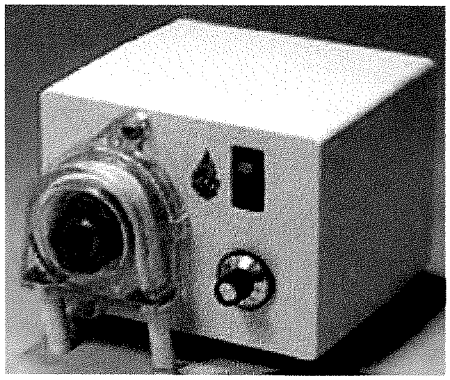

Figure 2 - Metering Pump

Figure 3 - Experimental setup - the fourth, non connected terminal at each end of the brick is used to measure the voltage in the bus. To reach the non connected terminals, current must flow through the internal bus.

Test Results

Variables and Constants

Aerogel electrode dimensions,

$l_{electrode} := 11.86 \cdot in$ $w_{electrode} := 6.25 \cdot in$ $t_{electrode} := .032 \cdot in$

Aerogel Density

$\rho_{aerogel} := .78 \cdot \frac{gm}{cm^3}$

Note: the density is adjusted for the aerogel sheets used in the MK8A brick which were more compressed than usual during pyrolization.

Water Density

$\rho_{water} := 1 \cdot \frac{kg}{liter}$

Number of electrodes,

$n_{electrodeMK8} := 20$ $n_{electrodeMK8A} := 24$

Total electrode area,

$A_{totalelectrodeMK8} := w_{electrode} \cdot l_{electrode} \cdot n_{electrodeMK8}$ $A_{totalelectrodeMK8} = 10.295\ ft^2$

$A_{totalelectrodeMK8A} := w_{electrode} \cdot l_{electrode} \cdot n_{electrodeMK8A}$ $A_{totalelectrodeMK8A} = 12.354\ ft^2$

Brick scale compared to 1000 square foot version

$Scale_{MK8} := \frac{A_{totalelectrodeMK8}}{1000 \cdot ft^2}$ $Scale_{MK8} = 0.01$

$Scale_{MK8A} := \frac{A_{totalelectrodeMK8A}}{1000 \cdot ft^2}$ $Scale_{MK8A} = 0.012$

Flow rates,

$Flow_{low} := 52.6 \cdot 10^{-3} \cdot \frac{liter}{min}$ $Flow_{low} = 0.014\ \frac{gal}{min}$

$Flow_{moderate} := 157.6 \cdot 10^{-3} \cdot \frac{liter}{min}$ $Flow_{moderate} = 0.042\ \frac{gal}{min}$

TDS to Conductivity Ratio

$TDS_{conversion} := \frac{500 \cdot 10^{-6}}{1032 \cdot 10^{-6} \cdot \frac{S}{cm}}$ $TDS_{conversion} = 0.484\ \frac{cm}{S}$

Input conductivity

$Conductivity_{Input} := 1032 \cdot 10^{-6} \cdot \frac{S}{cm}$ $TDS_{Input} := Conductivity_{Input} \cdot TDS_{conversion}$

$TDS_{Input} = 5 \times 10^{-4}$

Results Tables

Data is arranged in the following column order - Time(sec), Conductivity (uS/cm), PS Voltage(V), Current (A)

Low Flow Test - Mk-8A Brick

$Data_{Mk8Asn3\_4} :=$

	0	1	2	3
0	0	1004.77	0	0
1	10	997.82	0	0
2	20	1001.3	0	0
3	30	1008.25	0	0.05
4	40	1008.25	0	0
5	50	1008.25	0	0.05
6	60	56.31	0	0.05
7	70	164.01	0	0.05
8	80	191.8	0	0
9	90	125.79	0	0.05

$i := 0, 1 .. 779$

$j1 := 125, 126 .. 512$

$k1 := 120, 121 .. 475$

Table 1 - Mk-8A Graphite bus S/N 3 brick test 4 data, 52 ml/min flow (only 10 table entries visible).

Moderate Flow Results - Mk-8A Brick

$Data_{Mk8Asn3\_5} :=$

	0	1	2	3
0	0	35.46	0	0.05
1	10	31.99	0	0.05
2	20	28.51	0	0
3	30	25.04	0	0
4	40	1008.25	0	0.05
5	50	1015.19	0	0.05
6	60	98	0	0.05
7	70	139.69	0	0.05
8	80	35.46	0	0.05
9	90	18.09	0	0

Table 2 - Mk-8A Graphite bus S/N 3 brick test 5 data, 157 ml/min (only 10 table entries visible)

Time increment for integration

$$dT := \left(Data_{Mk8Asn3\_5_{1,0}} - Data_{Mk8Asn3\_5_{0,0}}\right)\cdot sec \qquad dT = 10\,s$$

Low Flow Test - Mk-8 Brick

This data for the Mk-8 brick with the metallic bus was collected May 9, 2000. The brick is now at Kurita.

$Data_{Mk8sn1\_060900a} :=$

	0	1	2	3
0	0	1088.15	0	0.07
1	10	1084.68	0	0.02
2	20	1091.63	0	0
3	30	1077.73	0	0.02
4	40	1088.15	-0	-0.02
5	50	1084.68	0	0.07
6	60	1254.92	0.01	0.05
7	70	-13.18	0.01	0
8	80	-2.75	0	0.05
9	90	1025.62	-0	0.05

Table 3 - Mk-8 metallic bus brick S/N 1 test data collected May 9, 2000, 157.6 ml/min (only 10 table entries visible)

Graphical Data

Data is collected at 10 second intervals using the Industrial Computer ADIO 1600 I/O board and stored in ASCII format delineated by commas. Tables 1,2 and 3 contain the raw data. Only 10 values are shown and the full data set can be viewed using Mathcad.
The graphs presented here compare the following;

- Effect of flow rates on output conductivity/ion adsorption and power requirements
- Effect of improved electrical connections on output conductivity/ion adsorption and power requirements

Offsets and Counters

For correct alignment of graphical data offsets should be applied,

- Time Offsets - adjust the ellapsed time to align the trigger event horizontally
- Measured Quantity Offsets - adjust the Y axis value to account for such things as measurement offset or summation starting point correction

Time counter offset for the Mk-8A graphite bus brick low flow test time axis

$$dNT_{Mk8Asn3\_4} \equiv 70$$

Moves data to left by 70 time increments 11.7 minutes.

Time counter offset for the Mk-8A graphite bus brick moderate flow test time axis

$$dNT_{Mk8Asn3\_5} \equiv 0$$

Time counter offset for the Mk-8 metal bus brick test results at 52.6 ml/min from 06/09/00

$$dNT_{Mk8sn1\_060900a} := 20$$

Ion mass offset for the Mk-8A graphite bus brick low flow test

$$dIon_{Mk8Asn3\_4} \equiv -.35$$

Ion mass offset for the Mk-8A graphite bus brick moderate flow test

$$dIon_{Mk8Asn3\_5} \equiv -.35$$

Ion mass offset for the Mk-8 metal bus brick test results at 52.6 ml/min from 06/09/00

$$dIon_{Mk8sn1\_060900a} \equiv 0$$

Effect of Flow Rate on Performance

The data presented here compares results from two tests performed on the Mk-8A brick containing the graphite bus. Slow flow results at 52.6 ml/min are shown in red and the moderate flow of 157 ml/min is shown in blue.

Conductivity Reduction

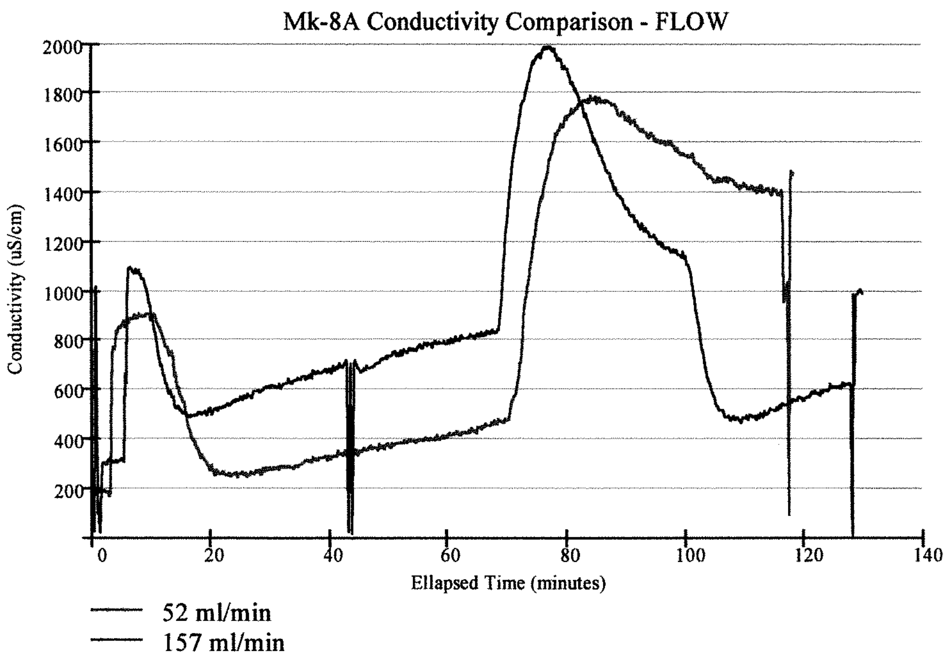

Figure 4 - Output conductivity of Mk-8A s/n 1 graphite bus brick for one charge/discharge cycle of single pass 1032 uS/cm NaCl. Two flow rates are presented.

Notes on Flow Comparison Conductivity Graph Above

- For the low flow rate test, conductivity at start is not at full level due to physisorbtion, longer stabilization would have brought it to the 1032 uS/cm level - does not significantly affect validity of results.
- At approximately 100 minutes the 157 ml/min flow conductivity starts to fall since a second cycle was initiated.
- The higher flow velocity produced more rapid removal of ions during rinse.

Power Use

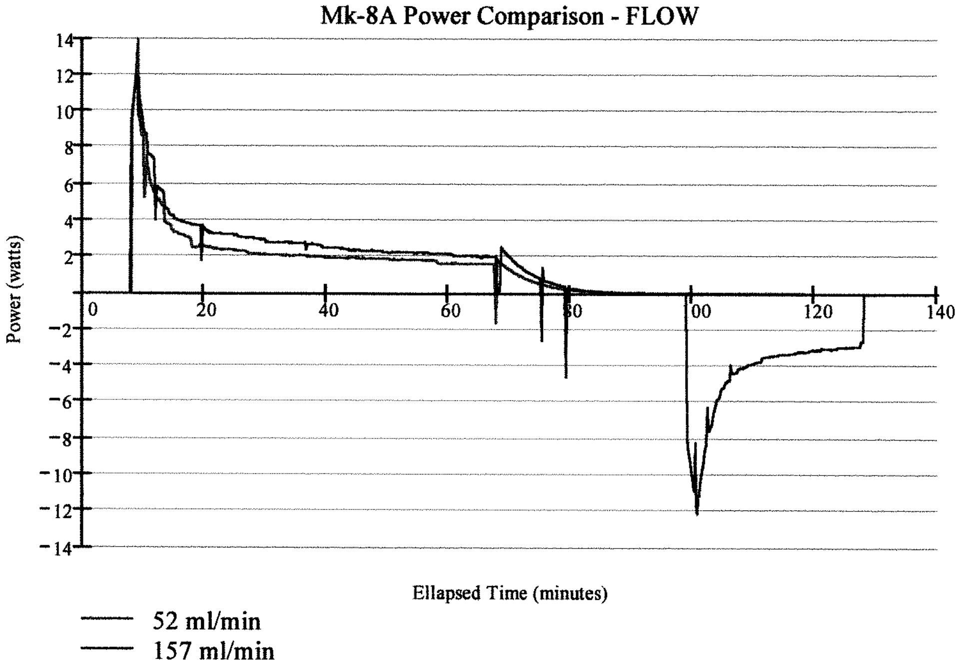

Figure 5 - Power use of Mk-8A s/n 1 graphite bus brick for one charge/discharge cycle of single pass 1032 uS/cm NaCl. Two flow rates presented

Notes on Flow Comparison Power Graph Above

- Power is obtained by multiplying voltage by current
- A second charge cycle of reversed polarity was started on the moderate flow test but not the low flow test
- Curves to the between the discontinuities at about 72.5 minutes and 100 minutes represent energy recovered from the shorted cell - discharge through the small shunt resistor may give an unrealistic value of recovered energy
- Both curves are of the type expected - capacitor charging

Ion Adsorption

Cummulative ion adsorption can be calculated by integrating the product of TDS reduction, water density, and flow rate over time.

$$IonMass_{low}(i1) := dT \cdot \rho_{water} \cdot Flow_{low} \cdot TDS_{conversion} \cdot \sum_{j=0}^{i1} \left(Conductivity_{Input} - Data_{Mk8Asn3\_4_{j,1}} \cdot 10^{-6} \cdot \frac{S}{cm} \right)$$

$$IonMass_{moderate}(i1) := dT \cdot \rho_{water} \cdot Flow_{moderate} \cdot TDS_{conversion} \cdot \sum_{j=0}^{i1} \left(Conductivity_{Input} - Data_{Mk8Asn3\_5_{j,1}} \cdot 10^{-6} \cdot \frac{S}{cm} \right)$$

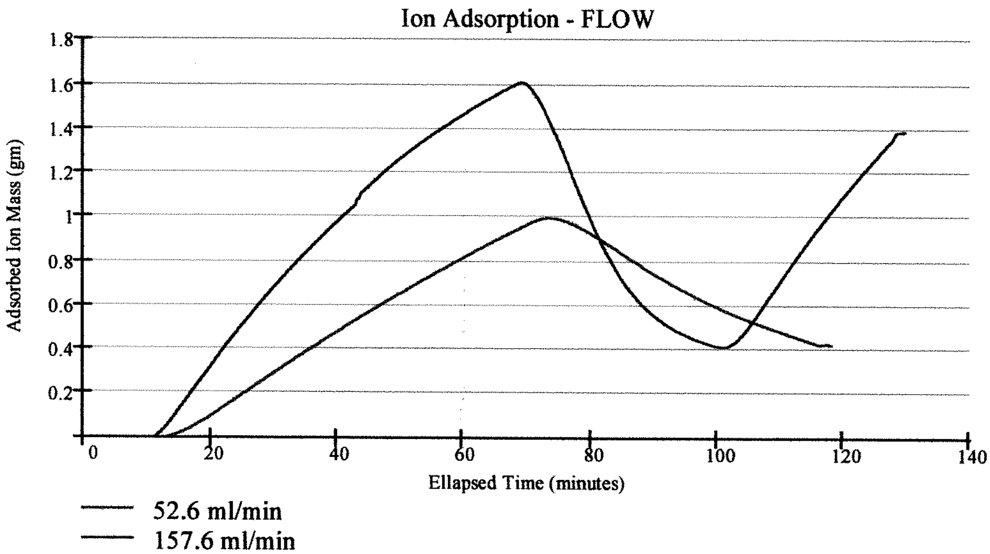

Figure 6 - Cummulative ion adsorption of Mk-8A s/n 1 graphite bus brick for one charge/discharge cycle of single pass 1032 uS/cm NaCl. Two flow rates are presented

Notes on Ion adsorption mass graph above

- Adsorbed mass was adjusted to be zero at the power on start time
- The release of ions during regeneration for the 157.6 ml/min flow case was incomplete when another cycle was started at 100 minutes.

Resistive Losses

At low voltages, resistive losses have been a significant problem resulting in low voltage at the aerogel electrode surface.
During the 52.6 ml/min flow experiment, voltages were measured at several points for evaluation of resistive losses through the system;

- Brick terminal posts on FarWest switch box - voltage going into the brick attachment cables.
- End of brick attachment cables after last brick attachment clip - this is the voltage reaching the clips attached to the graphite terminal rods on the brick.
- Vacant (unconnected) brick graphite terminal posts - current has travelled into and out of the bus to reach these points so this is the voltage on the aerogel at the bus end.

To determine the resistance of the control box to brick cables, the difference in potential at the control box and at the brick cable clamps is multiplied by the current. Simtoilarly the resistance of the bus is determined by comparing the potential differences between the cable clamps and vacant graphite post.

Five samples are used to improve accuracy.

$\text{Voltages}_{\text{Mk8Asn3\_4}} :=$

	0	1	2	3
0	4.5	1.3	1.23	1.1
1	1.95	1.28	1.24	1.17
2	1.5	1.3	1.27	1.22
3	1.4	1.31	1.28	1.23
4	1.3	1.3	1.27	0

$n_{\text{voltage}} := 0, 1 .. 4$

Table 4 - Voltage and current measurements at various points in the system. Columns represent Current(A), Control Box Voltage(V), Voltage at Cable Ends (V), Voltage Accross Vacant Posts (V)

Cable Resistance (total, both cables)

$$R_{\text{cable}} := \sum_{n_{\text{voltage}}} \frac{\left[\dfrac{\left(\text{Voltages}_{\text{Mk8Asn3\_4}_{n_{\text{voltage}},1}} - \text{Voltages}_{\text{Mk8Asn3\_4}_{n_{\text{voltage}},2}}\right)\cdot \text{volt}}{\text{Voltages}_{\text{Mk8Asn3\_4}_{n_{\text{voltage}},0}}\cdot \text{amp}}\right]}{5}$$

$R_{\text{cable}} = 0.02\,\Omega$

Bus Resistance (total, both poles)

$$R_{\text{bus}} := \sum_{n_{\text{voltage}}} \frac{\left[\dfrac{\left(\text{Voltages}_{\text{Mk8Asn3\_4}_{n_{\text{voltage}},2}} - \text{Voltages}_{\text{Mk8Asn3\_4}_{n_{\text{voltage}},3}}\right)\cdot \text{volt}}{\text{Voltages}_{\text{Mk8Asn3\_4}_{n_{\text{voltage}},0}}\cdot \text{amp}}\right]}{5}$$

$R_{\text{bus}} = 0.222\,\Omega$

Performance Comparison to MK8 Metallic Bus Brick

To quantify improvements realized by the graphite bus system and multiple terminal connections, results obtained at 52.6 ml/min flow rate are compared to those obtained at the same flow from a Mk-8 brick containing metallic bus parts. Data for the Mk-8 metallic bus brick was collected on June 9, 2000.

Conductivity Reduction

The data presented here compares results from the tests performed on the Mk-8A brick containing the graphite bus and the Mk-8 brick containing a metal bus. Both tests were conducted at 52.6 ml/min. The Mk-8A graphite bus brick results are shown in red and the Mk-8 metallic bus brick results in green.

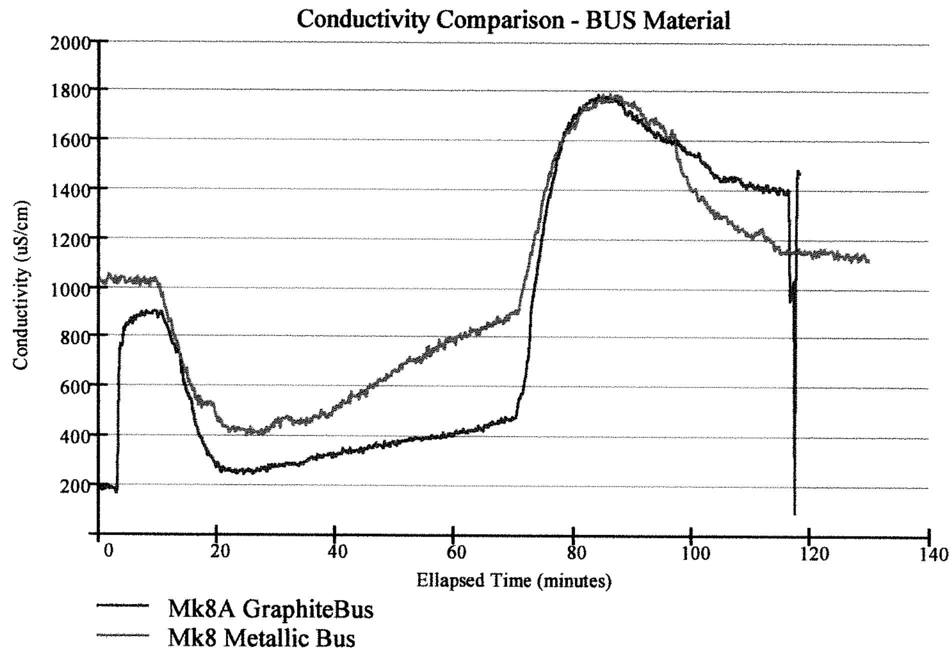

Figure 7 - Output conductivity for one charge/discharge cycle of single pass 1032 uS/cm NaCl at 52.6 ml/min. Data for the Mk-8A graphite bus brick (red) and Mk-8 metal bus brick (green) are presented.

Notes on Flow Comparison Conductivity Graph Above

- For the low flow rate test, conductivity at start is not at full level due to physisorbtion, longer stabilization would have brought it to the 1032 uS/cm level - does not significantly affect validity of results.
- Regeneration started at around 72.5 minutes.
- The Mk-8 metallic bus brick was almost saturated by the time regeneration began, the Mk-8A graphite bus brick was a long way from saturation.

Power Use

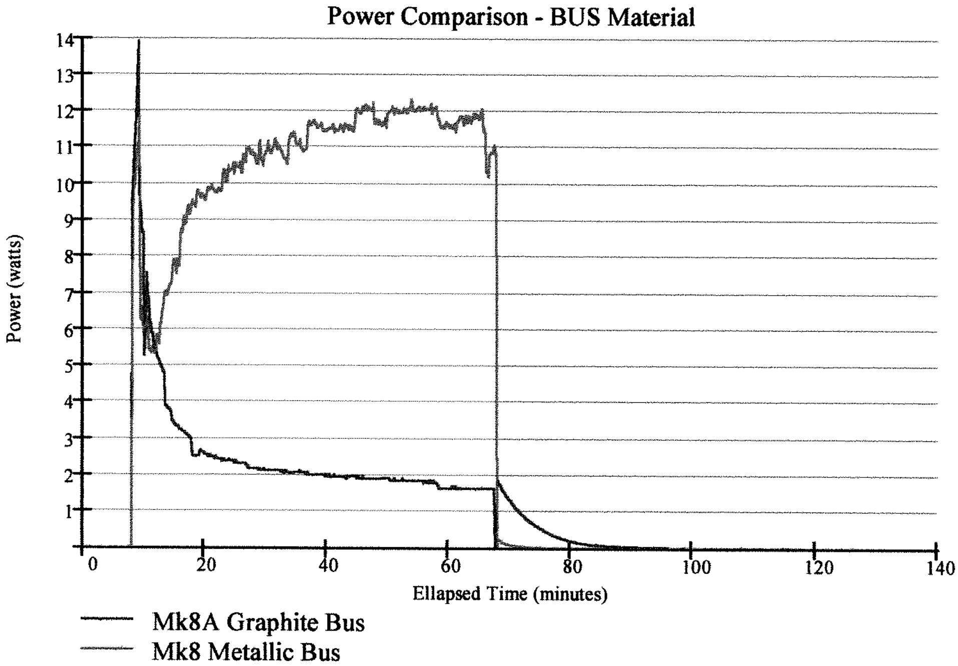

Figure 8 - Power use for one charge/discharge cycle of single pass 1032 uS/cm NaCl at 52.6 ml/min. Data for the Mk-8A graphite bus brick (red) and Mk-8 metal bus brick (green) are presented.

Notes on Flow Comparison Power Graph Above

- Power is obtained by multiplying voltage by current
- The Mk8 metallic bus brick developed an increased current draw at approximately 12 minutes - it is not a direct short since the voltage was maintained at 1.3 volts by the power supply.
- Power draw measurements for the Mk8 metallic bus brick should be viewed with caution, however other data should be considered reliable since voltage was maintained.

Ion Adsorption

Cummulative ion adsorption can be calculated by integrating the product of TDS reduction, water density, and flow

$$IonMass_{metallic}(i1) := dT \cdot \rho_{water} \cdot Flow_{low} \cdot TDS_{conversion} \cdot \sum_{j=0}^{i1} \left(Conductivity_{Input} - Data_{Mk8sn1\_060900a_{j,1}} \cdot 10^{-6} \cdot \frac{S}{cm} \right)$$

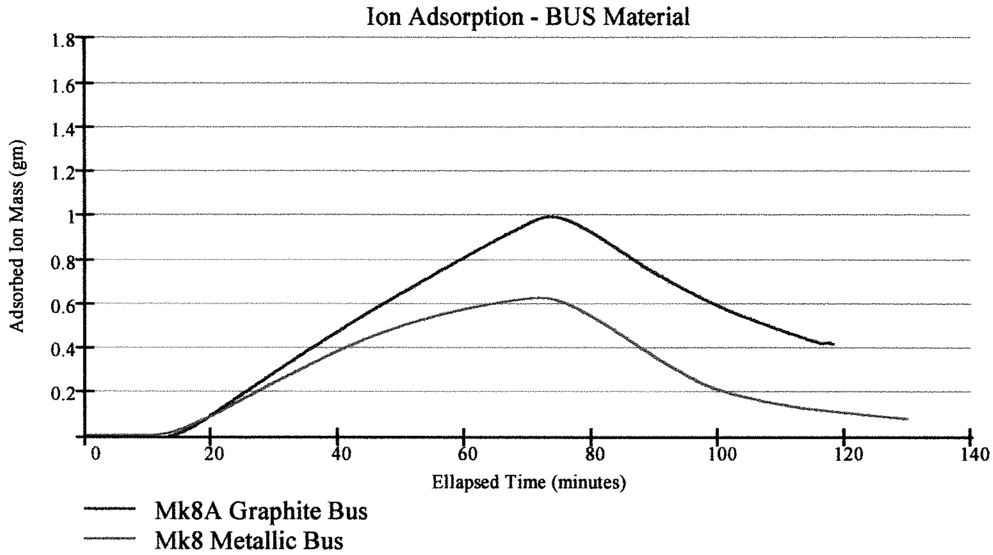

Figure 9 - Cummulative ion adsorption for one charge/discharge cycle of single pass 1032 uS/cm NaCl at 52.6 ml/min. Data for the Mk-8A graphite bus brick (red) and Mk-8 metal bus brick (green) are presented.

Notes on Ion adsorption mass graph above

- Adsorbed mass was adjusted to be zero at the power on start time
- The release of ions during regenerationwas not complete in either case
- The Mk8A Graphite bus brick clearly had greater ion adsorption capacity.

Conclusions

- Electrical losses in the new Mk-8A graphite bus based brick are lower.
- Increased flow rates improve ion adsorption
- The graphite bus configuration adsorbs 1.6 times the ions of the metallic configuration - probably more at the higher flow rate but no data is available for the metal bus brick.

Graphite Bus - Mk-8A Brick

2 Bricks in Series - Mountain Spring Water

FarWest Group, Inc
Engineering and Development Center
701 Palomar Airport Road, Suite 300
Carlsbad, CA 92009

Phone: (760)931-4784 Fax: (760)931-4850
Email: c_sheppard@msn.com

Introduction

A demonstration was prepared for two representatives from Hankook Jungsoo Industries of Korea to demonstrate suitability of CDT for water polishing. An application of interest to the company is production of high purity water for the electronics and other manufacturing industries.

As input, bottled mountain spring water with a conductivity of 282 micro Seimen/centimeters was chosen. We had no analytical data on the sample but felt it was a good random selection.

The test system chosen to demonstrate the process incorporated two Mk-8A connected in series. This setup had been configured earlier for determining maximum rinse concentration levels attainable when processing water from coal beds.

Arrangement of the system components was such that complete drainage of tubes and bricks could be accomplished through computer control between production and rinse cycles.

Objectives

1. Demonstrate ion removal at low TDS.
2. Determine effect of output conductivity on flow rate.
3. Evaluate efficiency of electrical series connection to bricks.

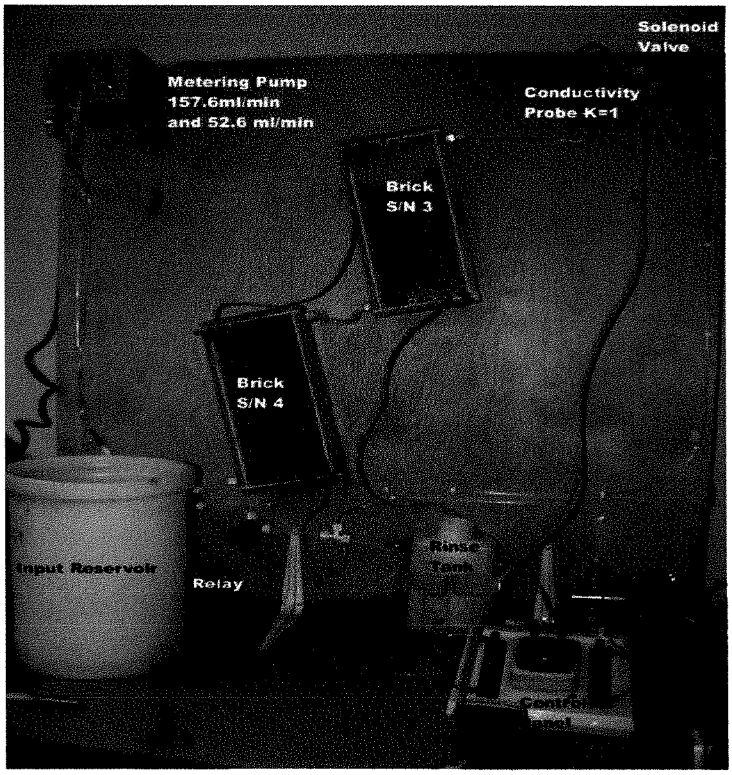

Figure 1 - Rinse concentration system setup incorporating 2 Mk-8A bricks.

Test Equipment

1. Mk-8A bricks serial numbers 3 and 4
2. Pulsafeeder metering pumps set at 52.6 ml/min and 157.6 ml/min flow rates
3. Input reservoir containing 9.46 litres of 282 uS/cm "Sparklets" mountain spring water
4. Additional 9.46 litres of mountain spring water for top up during experiment
5. Signet conductivity probe K=1
6. Signet conductivity readout model 8850 - full scale 20mA output value set to 5000 uS/cm
7. Industrial computer ADIO interface board mounted in Compaq Presario 4880
8. FarWest test interface control box
9. Fluke 89 mk IV True RMS Multimeter
10. Plastic tubing and connectors

Input Data

Variables and Constants

Aerogel electrode dimensions,

$l_{electrode} := 11.86 \cdot in$ $w_{electrode} := 6.25 \cdot in$ $t_{electrode} := .032 \cdot in$

Aerogel Density

$\rho_{aerogel} := .78 \cdot \frac{gm}{cm^3}$

Note: the density is adjusted for the aerogel sheets used in the MK8A brick which were more compressed than usual during pyrolization.

Water Density

$\rho_{water} := 1 \cdot \frac{kg}{liter}$

Number of electrodes per brick,

$n_{electrodeMK8} := 20$ $n_{electrodeMK8A} := 24$

Number of bricks in system,

$n_{bricks} := 2$

Total electrode area,

$A_{totalelectrodeMK8A} := w_{electrode} \cdot l_{electrode} \cdot n_{electrodeMK8A} \cdot n_{bricks}$ $A_{totalelectrodeMK8A} = 24.708\,ft^2$

Brick scale compared to 1000 square foot version

$$Scale_{MK8A} := \frac{A_{totalelectrodeMK8A}}{1000 \cdot ft^2} \qquad Scale_{MK8A} = 0.025$$

Flow rates,

$$Flow_{low} := 52.6 \cdot 10^{-3} \cdot \frac{liter}{min} \qquad Flow_{low} = 0.014 \frac{gal}{min}$$

$$Flow_{moderate} := 157.6 \cdot 10^{-3} \cdot \frac{liter}{min} \qquad Flow_{moderate} = 0.042 \frac{gal}{min}$$

TDS to Conductivity Ratio based on 500ppm NaCl Solution

$$TDS_{conversion} := \frac{500 \cdot 10^{-6}}{1032 \cdot 10^{-6} \cdot \frac{S}{cm}} \qquad TDS_{conversion} = 0.484 \frac{cm}{S}$$

Input conductivity

$$Conductivity_{Input} := 282 \cdot 10^{-6} \cdot \frac{S}{cm} \qquad TDS_{Input} := Conductivity_{Input} \cdot TDS_{conversion}$$

$$TDS_{Input} = 1.366 \times 10^{-4}$$

Results Tables

Initially the run time for the experiment was set at 1 hour so the data collection terminated after that time. Since the results were encouraging, a second data collection file was started and ran for an additional hour.
Both files were concatenated into a single file.
There was approximatey 5 minutes (300 seconds) between the last data point of the first file and the first data point of the second file.
Data is arranged in the following column order - Time(sec), Conductivity (uS/cm), PS Voltage(V), Current (A)

$Data_{MSC} :=$

	0	1	2	3
286	2860	-145.2	-3.18	1.12
287	2870	-134.77	-3.18	1.12
288	2880	-134.77	-3.03	0.93
289	2890	-6.23	-2.93	0.98
290	2900	31.99	-2.93	0.98
291	2910	18.09	-2.93	0.98
292	2920	28.51	-2.92	1.07
293	2930	31.99	-2.92	1.07
294	2940	14.62	-2.92	1.07
295	2950	35.46	-2.92	1.02

$i := 0, 1 .. 720$

Table 1 - Combined data from 2 files - only the first 10 out of 720 entries are shown.

Time increment for integration

$$dT := \left(Data_{MSC_{1,0}} - Data_{MSC_{0,0}}\right) \cdot sec \qquad dT = 10\,s$$

Graphical Data

Data is collected at 10 second intervals using the Industrial Computer ADIO 1600 I/O board and stored in ASCII format delineated by commas. The previous table was produced by concatenating two output files from the data collection system;

- MountainSpring.TXT - first 60 minutes of data collection
- MountainSpringContd1.TXT - second 60 minutes of data collection

The graphs presented here show the results obtained over the total 120 minutes data collection period;

- Output conductivity
- Instantaneous power consumptioin
- Cummulative ion storage

Output Conductivity

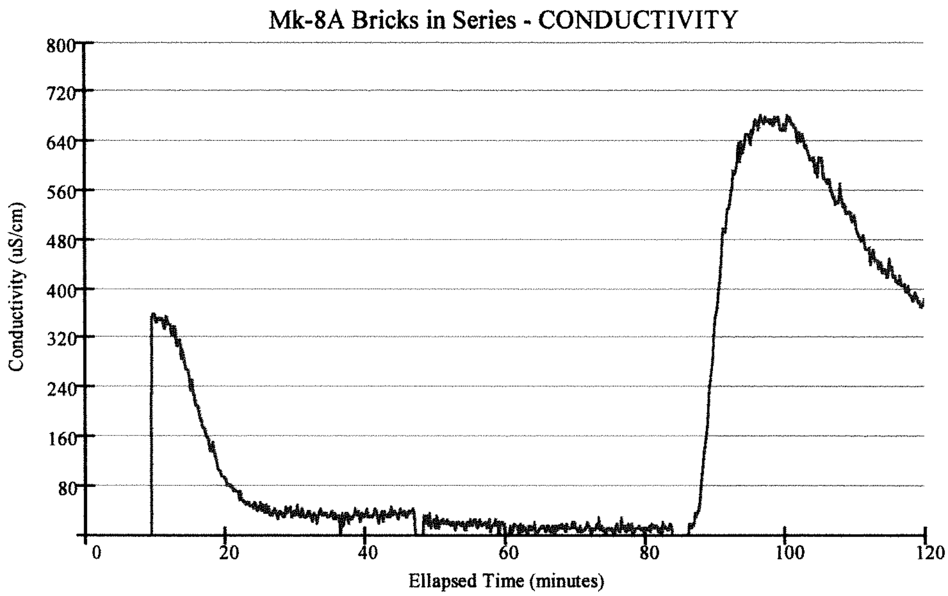

Figure 2 - Output conductivity of two Mk-8A s/n 3 and 4 graphite bus brick for one charge/partial discharge cycle of single pass of 282uS/cm "Sparklets Bottled Mountain Spring Water"

Notes on Graph Above

- Flow rate was 157.6 ml/min except between t=48 minutes and t=85 minutes when it was switched to 52.6 ml/min.
- Fluctuations of measurement are due to the computer recording sensitivity which was set to 5000 uS/cm full range with 8 bit full rrange. In other words, one count represented 19.5 uS/cm (looking at the conductivity meter during the last part of the production cycle it was stable at 20-25 uS/cm)

Power Consumption

The two bricks were wired in series and a voltage of 2.8 - 3.0 volts applied at the control panel end of the cables. Voltages were measured at several points in the system within a few minutes of start up.

- Power supply voltage at control panel end of cable: 3.0 volts
- Power supply voltage at brick end of cable: 2.9 volts
- Voltage drop across brick S/N 3 bus measured at vacant terminal posts: 1.22 volts
- Voltage drop across brick S/N 4 bus measured at vacant terminal posts: 1.03 volts

From the above measurements it can be assumed that an applied voltage of 3 volts yields the correct bus voltage in each brick. Further into the test, the difference in voltages between S/N 3 and S/N 4 increased but weren't recorded.

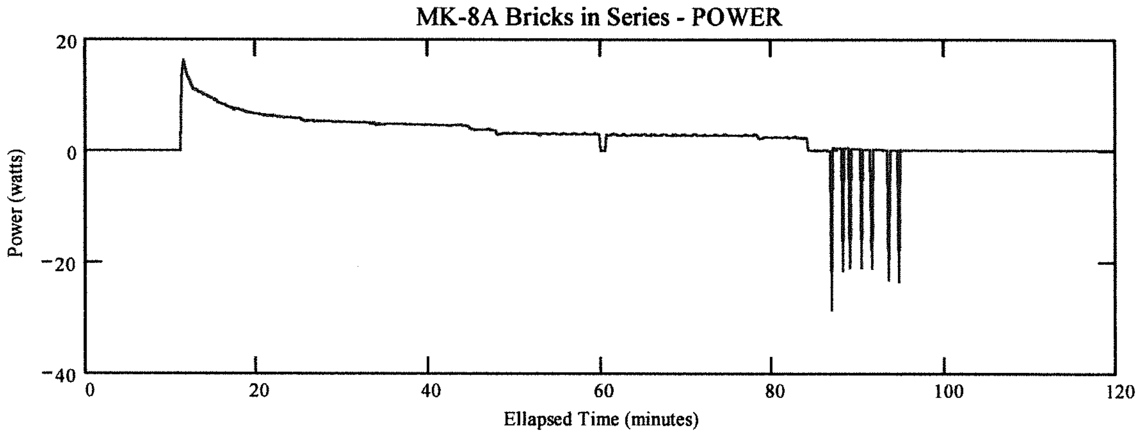

Figure 3 - Power use of two Mk-8A s/n 3 and 4 graphite bus brick for one charge/partial discharge cycle of single pass 232 μS/cm "Sparklets Bottled Mountain Spring Water"

Notes on Power Graph Above

- Power is obtained by multiplying voltage by current
- Spikes at around 88 minutes are given during regeneration to force ions off electrodes (10A for 10 seconds)

Ion Adsorption

Cumulative ion adsorption can be calculated by integrating the product of TDS reduction, water density, and flow rate over time. Since there was a change in flow rate during the test, the equation is a little more complex than for a single flow rate.

The record number at which flow changed from 157.6 to 52.6 ml/min,

$$j_{low} := 283$$

Similarly, the record number at which flow reverted back to 157.6 ml/min is;

$$j_{moderate} := 505$$

The equation for the flow rate as a function of the record number is;

$$\mathrm{Flow}(i2) := \mathrm{if}\left(i2 < j_{low}, \mathrm{Flow}_{moderate}, \mathrm{if}\left(i2 < j_{moderate}, \mathrm{Flow}_{low}, \mathrm{Flow}_{moderate}\right)\right)$$

Cumulative ion adsorption is defined by the following equation;

$$\mathrm{IonMass}_{MSC}(i1) := dT \cdot \rho_{water} \cdot \mathrm{TDS}_{conversion} \cdot \sum_{j=0}^{i1} \left[\left(\mathrm{Conductivity}_{Input} - \mathrm{Data}_{MSC_{j,1}} \cdot 10^{-6} \cdot \frac{S}{cm}\right) \cdot \mathrm{Flow}(j)\right]$$

$$\mathrm{Offset}_{ionmass} := .3 \cdot gm$$

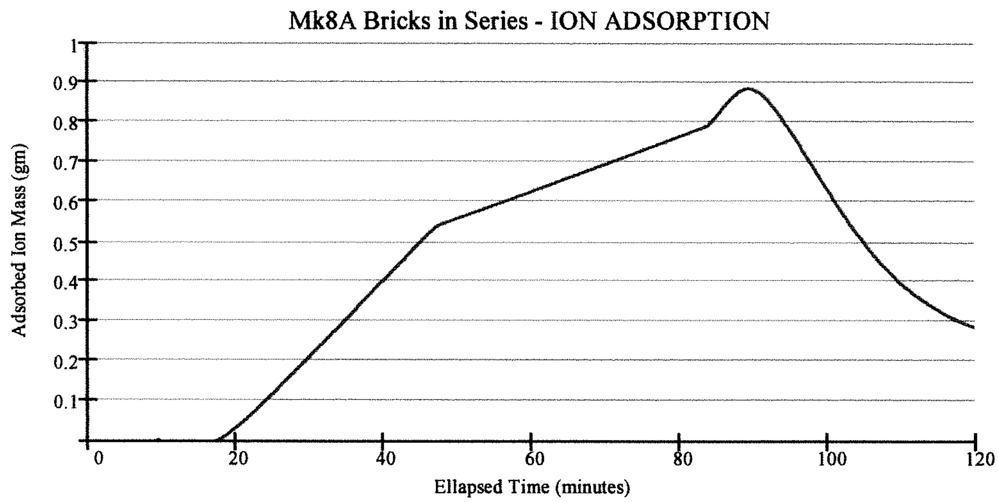

Figure 4 - Cummulative ion adsorption of Mk-8A s/n 3 and 4 graphite bus brick for one charge/discharge cycle of single pass 282 uS/cm "Sparklets Bottled Mountain Spring Water".

Notes on Ion adsorption mass graph above

- The first 18 minutes of integration were prior to output flow so the conductivity probe was at zero. This caused the integration to accumulate .3 g of ion adsorption during the period there was no output flow (filling). To correct for this .3g was subtracted from the ion adsorption mass values when plotted in figure 4.
- Change in slope at 47 minutes was due to the flow rate change from 157.6 to 52.6 ml/min.
- Regeneration was not completed and the bricks were not drained.

Conclusions

- the ion adsorption limit was not reached during this test since the input conductivity was low. If the production cycle had been extended, the output would have remained low for an hour or more (based on the knowledge that two bricks should adsorb a minimum of 3 g).
- series electrical connection produced unequal voltage drops accross the bricks due to variations in instantaneous resistance. Resistance variations arise from the capacitive nature of the device and the variations in water conductivity as is progresses through the system.

Dual Brick Concentrator

Coalbed Methane Application

FarWest Group, Inc
Engineering and Development Center
701 Palomar Airport Road, Suite 300
Carlsbad, CA 92009

Phone: (760)931-4784 Fax: (760)931-4850
Email: c_sheppard@msn.com

Introduction

For certain applications of CDT the goal is to produce a waste stream with the highest concentration of impurities and a product stream of adequate quality for reintroduction to the ground water system. Undoubtedly there is a reduction in the efficiency of the CDT system as rinse stream concentrations are increased due to residual impurities depositing themselves on the electrode surfaces between rinse and production cycles.

It is not adequate to demonstrate removal of ions from the product output but more importantly one must show the level of concentration that can be achieved in the waste stream. Depending on the regulations, it may be necessary to turn the contaminants into solid before storage in a long term closed landfill. Under this scenario, there will be an economic cutoff at which concentration is taken over by a secondary process such as distillation or other dewatering techniques.

A special series arrangement of two Mk-8A bricks was configured with elevations and flow paths oriented such that bricks and lines could be drained between cycles. This minimizes mixing between the product and rinse volumes thereby allowing the maximum concentrations to be achieved.

The Mk-8A fill volume is only 800ml which means that a rinse reservoir of 2 litres is sufficient to provide circulation for the two bricks.

Objectives

1. Produce sample of output with low TDS for lab testing - below 300 uS/cm to determine which, if any elements remain untouched by CDT
2. Produce rinse sample of high TDS for lab testing to ensure constituents removed by CDT are placed in rinse stream.
3. Determine limits of rinse concentration - economic and physical

Experimental Arrangement

To produce the highest concentration of rinse water with the lowest total sample use, a two brick system was constructed with plumbing arranged for complete drainage between cycles. Solenoid valves open the lines and allow them to be drained into either rinse or product tank.

1. Mk-8A bricks serial numbers 3 and 4
   Plumbed in series
   Wired in parallel
2. Pulsafeeder metering pumps
   52.6 ml/min for production
   157.6 ml/min for rinse
3. Input reservoir containing water sample from Wyoming Coal bed methane well Red13M 3190 - conductivity 2095 uS/cm
4. Additional water sample to top up input tank
5. 2 litre rinse reservoir
6. Signet conductivity probe K=1
7. Signet conductivity readout model 8850 - full scale 20mA output value set to 5000 uS/cm, increased further into test as TDS level of rinse increases
8. Industrial computer ADIO interface board mounted in Compaq Presario 4880
9. FarWest test interface control box
10. Fluke 89 mk IV True RMS Multimeter
11. Four Teqcom 3 way solenoid valves - M423W1ATS
12. Lambda regulated power supply - 9A, 0-30Vdc
13. 5 Crydom D1210 solid state relays - TTL control, 110Vac x 10A load

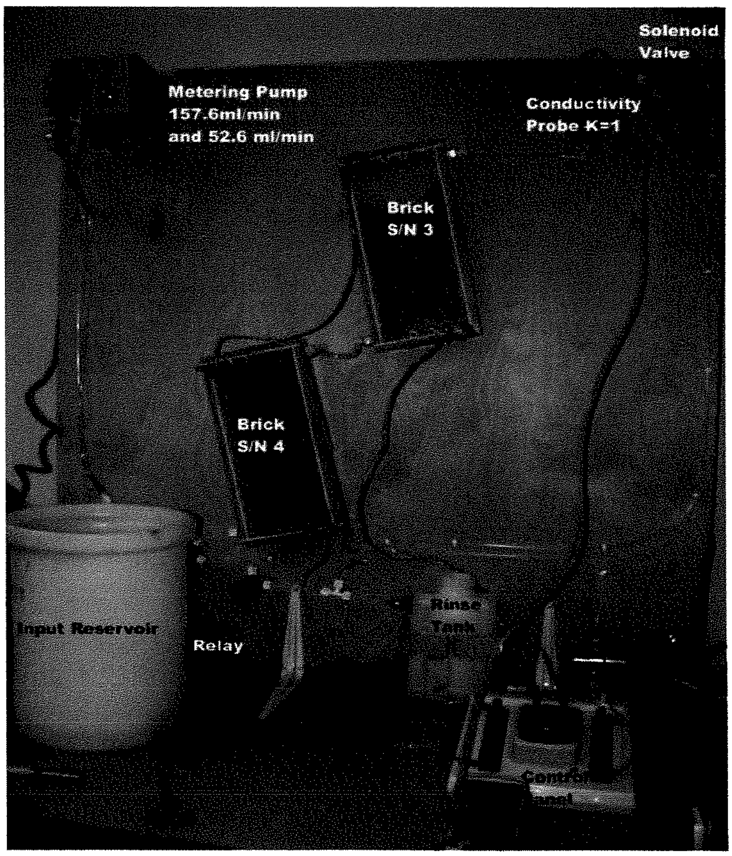

Figure 1: Dual brick concentrator setup. Note: wiring shown is series. It was changed to parallel for the tests since the capacitative nature of the load would not allow equal voltage distribution in a series connection.

System Diagram

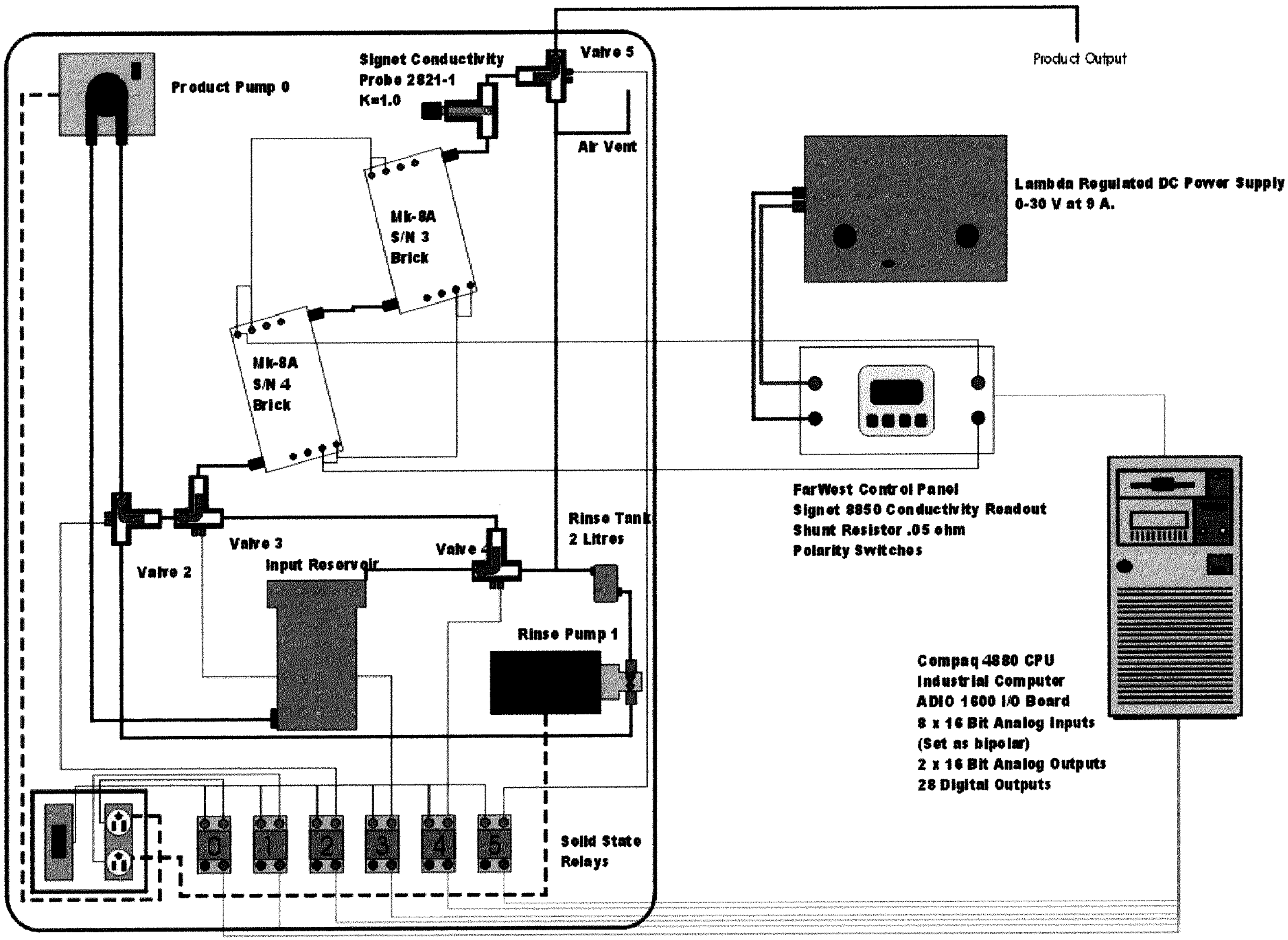

Results

The system operation mode is still not optimized to produce the desired results, to date these are the items that were discovered during testing -

- During the early portion of the charge cycle 1.3V on the terminal input lines did not produce the required 1.2V on the bus. On later runs voltage was adjusted according to the voltage measured across the vacant bus terminals.
- The initial product water following a rinse cycle had a higher TDS than the input water due to residuals from the rinse. This got worse as the rinse TDS increased.

Data Files

A data file is collected for each cycle and given the name Red13M3190"x" where "x" is a letter representing the cycle.
Each record in the data file contains time (sec), conductivity (uS/cm), Voltage (V), and Current (A). The data is recorded at 10 second intervals and the record number at which power is turned off and the rinse started is different for each file.
The following table lists the first record at which power is turned off (column 0) and the total number of records in the file. The first row corresponds to file A, the second to B and so on.

The number of cycles in this study is $N_{cycles} := 7$ $\quad n_{cycle} := 0, 1 .. N_{cycles} - 1$

$Data_{Red13M3190} :=$

	0	1	2	3
0	0	167.48	0	0.05
1	10	160.53	0	0
2	20	160.53	0	0
3	30	157.06	0	0
4	40	160.53	0	0.05
5	50	164.01	0	0.05
6	60	167.48	0	0.05
7	70	160.53	0.18	0.93
8	80	174.43	0.22	0.93
9	90	167.48	0.23	11.44

$Nrecord :=$

	0	1
0	252	720
1	264	720
2	562	720
3	592	900
4	560	900

$$N_{Records} := \sum_{i=0}^{(N_{cycles}-1)} Nrecord_{i,1}$$

$N_{Records} = 5.76 \times 10^3$ $\quad n := 0, 1 .. N_{Records}$

A second matrix can be constructed giving the starting record, power off, and ending record for each cycle from the table above

$$N_{Records} := \sum_{i=0}^{(N_{cycles}-1)} Nrecord_{i,1}$$

$$N_{Records} = 5.76 \times 10^{3}$$

$$n := 0,1..N_{Records}$$

A second matrix can be constructed giving the starting record, power off, and ending record for each cycle from the table above

$$N_{Event_{n_{cycle},0}} := \text{if}\left(n_{cycle} < 1, 0, \sum_{i=0}^{n_{cycle}-1} Nrecord_{i,1}\right)$$

$$N_{Event_{n_{cycle},1}} := N_{Event_{n_{cycle},0}} + Nrecord_{n_{cycle},0}$$

$$N_{Event_{n_{cycle},2}} := N_{Event_{n_{cycle},0}} + Nrecord_{n_{cycle},1}$$

$$N_{Event} = \begin{pmatrix} 0 & 252 & 720 \\ 720 & 984 & 1.44 \times 10^{3} \\ 1.44 \times 10^{3} & 2.002 \times 10^{3} & 2.16 \times 10^{3} \\ 2.16 \times 10^{3} & 2.752 \times 10^{3} & 3.06 \times 10^{3} \\ 3.06 \times 10^{3} & 3.62 \times 10^{3} & 3.96 \times 10^{3} \\ 3.96 \times 10^{3} & 4.577 \times 10^{3} & 4.86 \times 10^{3} \\ 4.86 \times 10^{3} & 5.416 \times 10^{3} & 5.76 \times 10^{3} \end{pmatrix}$$

Multiple Cycle Conductivity Plot

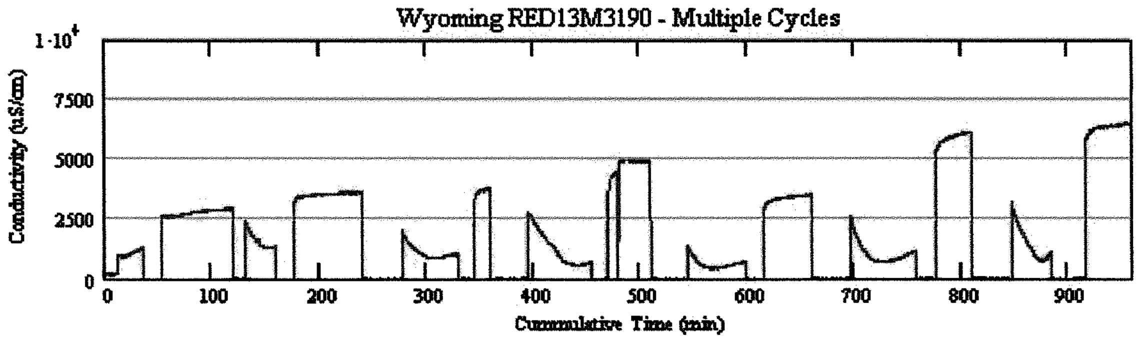

Notes on graph above

1. First two cycles used low rinse velocity S/A production
2. Decreasing portions of curve are production
3. Rinse conductivity values increase with time as more ions are accumulated on subsequent runs
4. Time to remove residual rinse ions increases with rinse conductivity

Sample Plot From Cycle 4 Using 4078 uS/cm Rinse

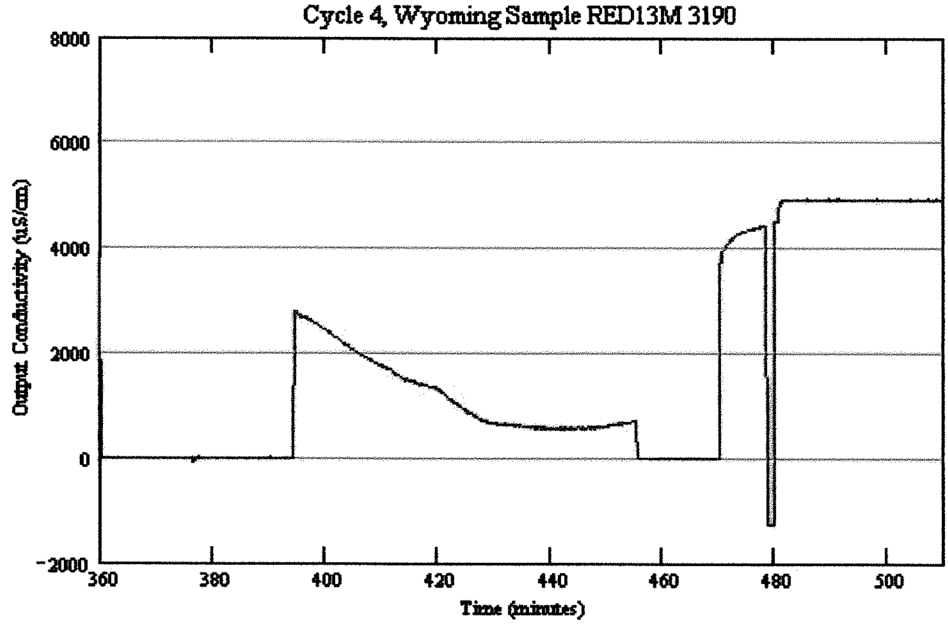

Comments on the graph above

- During the period from 360 to roughly 390 minutes, the brick was filling so there was no output from the conductivity probe located on the brick output
- The input water conductivity was 2095 uS/cm at 20.5 C.
- The output conductivity at the start of the cycle was above the input value due to residual rinse water being pushed out the system
- The rinse began at roughly 470 minutes, the zero conductivity occurs during the fill time and is 1/3 the time of the production fill since the rinse flow rate is 3 times the production flow rate
- Rinse conductivity saturated at 5000 uS/cm since this was the maximum range set on the meter - it was increased for subsequent runs

Conclusion

Testing is still in progress and the system cycles are being optimized to produce the desired high TDS rinse.

- The system consistently reduced the input conductivity from 2095 uS/cm to below 800 uS/cm in a single pass.
  Surface area in the system is 1/80th that in a full size brick
- Rinse water residuals are a problem, the new aerogel without the cracks of the current material will help this. The cracks in the current aerogel account for 20-40% of the total aerogel volume.
- Product water should be recycled to bring TDS down further and increase ions available for transfer into the rinse water.

Carlsbad Demonstrator

Preliminary Data - 1/4 Scale Bricks Fixed Volume Test 4.1.1

FarWest Group, Inc.
Engineering and Development Center
701 Palomar Airport Road, Suite 300
Carlsbad, CA 92009

Phone: (760)931-4784 Fax: (760)931-4850
Email: c_sheppard@msn.com

Introduction

This document provides a sample of test results obtained from the Carlsbad demonstration system during testing of single 1/4 scale CDT bricks - MK-9 running in recirculating mode.

The purpose of the tests was to determine the ion storage limits for single 1/4 scale bricks using the ground water from the Encina wastewater site. This information will be used to predict performance of the system when multiple bricks are in operation.

These tests also provided insight into the operating scenarios best suited to the 1/4 scale bricks and Encina water source - shown right.

Objectives

The objectives for the test are in line with the test plan. Also included are some operation parameter experimentation as the performance of the brick on the ground water source is understood.

- Determine ion storage capacity of single 1/4 scale brick
- Determine optimum flow rates for ion adsorption and release (rinse)
- Determine effects of voltage on ion removal rates

ENCINA WASTEWATER AUTHORITY LABORATORY
ENVIRONMENTAL LABORATORY CERTIFICATION #1441

SAMPLE NAME: CARLSBAD WATER PROJECT , EAST WELL
SAMPLE DATE & TIME : 9/5/2000 @ 10:10 AM

ANALYSIS	RESULTS	METHOD#	TESTED BY:
Alkalinity	283 mg/l	SM 2320 B	PH
Ammonia N	0.44 mg/l	SM 4500 NH₃ C	JL
Boron	0.56 mg/l	SM 4500 B-B	JL
COD	86.2 mg/l	HACH 8000	JP
Chloride	1,722 mg/l	SM 4500-Cl⁻ B	JL
Total Hardness	1440 mg/l	SM 2340 C	DC
Nitrate N	7.38 mg/l	USEPA 352.1	JL
Nitrite N	<0.1 mg/l	SM 4500 NO₂-B	JL
Grease & Oil	0.2 mg/l	SM 5520 B	PH
pH	7.20 units	SM 4500 H-B	PH
o-Phosphate	0.063 mg/l	SM 4500 E	JL
t-Phosphate	0.067 mg/l	HACH 8190	JL
TDS	4,598 mg/l	SM 2540 C	JP
TSS	1.9 mg/l	SM 2540 C	PH
VSS	1.3 mg/l	SM 2540 E	PH
Specific Conductance	6370 umhos/cm	SM 2510 B	JP
Sulfate	630 mg/l	USEPA 375.4	JL
Temperature	25.2 °C	SM 2550	PH
Turbidity	0.194 NTU	SM 2130 B	PH
Aluminum	0.18 mg/l	USEPA 6010 B	DEL MAR
Antimony	0.002 mg/l	SM 3113 B	DC
Arsenic	0.003 mg/l	SM 3113 B	DC
Barium	0.073 mg/l	SM 2130 B	DEL MAR
Beryllium	<0.0005 mg/l	SM 3113 B	DC
Cadmium	0.006 mg/l	SM 3111 B	DC
Calcium	70.8 mg/l	SM 3111 B	DC
t-Chromium	<0.1 mg/l	SM 3111 B	DC
Copper	<0.05 mg/l	SM 3111 B	DC
Iron	0.093 mg/l	SM 3111 B	DC
Lead	0.1 mg/l	SM 3111 B	DC
Magnesium	177.8 mg/l	SM 3111 B	DC
Manganese	0.109 mg/l	SM 3111 B	DC
Mercury	0.0004 mg/l	SM 3112 B	DC
Molybdenum	<0.01 mg/l	SM 3113 B	DC
Nickel	0.056 mg/l	SM 3111 B	DC
Potassium	15.4 mg/l	SM 3500 D	DC
Selenium	<0.015 mg/l	SM 3113 B	DC
Silver	<0.025 mg/l	SM 3111 B	DC
Sodium	977 mg/l	SM 3500 D	DC
Thallium	<0.005 mg/l	USEPA 279.2	DC
Zinc	0.046 mg/l	SM 3111 B	DC
Heterotrophic Plate Count	7,700 cfu/1ml	SM 9215 D	JL
Total Coliform m-F	8,800 cfu/100ml	SM 9222 B	JL
Fecal Coliform m-F	<10 cfu/100ml	SM 9222 D	JL
Enterococcus m-F	140 cfu/100 ml	SM 9230 C	JL
Color	2.0 color units	SM 2120 B	JL
Odor	2.9 TON	SM 2150 B	JL

Data Files

Each cycle is recorded in a separate data file. Each column from left to right represents Time (minutes), Flow (litres or litres/min), Voltage (V), Current (A), Probe 1 Conductivity (uS/cm), Probe 2 Conductivity (uS/cm)

$Data_{Sn2C} :=$

0	2.20	1.30	0.00	6539	6333
10	2.20	1.30	0.00	6487	6666
21	2.20	1.30	100.00	6502	6677
22	2.20	1.30	100.00	6499	6695
23	2.20	1.30	100.00	6514	6717
25	2.20	1.30	85.00	6047	6725
26	2.20	1.30	80.00	6042	6719
27	2.20	1.30	75.00	6037	6696
28	2.20	1.30	70.00	6026	6661
29	2.20	1.30	67.00	6026	6611
30	2.20	1.30	55.00	6024	6592
32	2.20	1.30	50.00	5988	6512
34	2.20	1.30	50.00	5943	6432
36	2.20	1.30	50.00	5723	6336
38	2.20	1.30	50.00	5354	6307
40	2.20	1.30	50.00	5282	6270
48	2.20	1.30	38.00	4023	6083
50	2.20	1.30	37.00	3987	6066
60	1.00	1.30	32.00	3125	5931
70	1.00	1.30	25.00	5193	5669
80	2.00	1.30	25.00	5048	5663
90	2.00	1.30	20.00	4956	5597
100	2.00	1.30	20.00	4583	5541
101	2	0	0	4575	5558
107	2.00	0.00	0.00	4566	5675
108	1.80	0.00	0.00	4573	5718
109	1.80	0.00	0.00	4582	5763
110	1.80	0.00	0.00	4598	5802
111	1.80	0.00	0.00	4616	5841
112	1.80	0.00	0.00	4626	5875
113	1.80	0.00	0.00	4654	5903
114	1.80	0.00	0.00	4679	5929
115	1.80	0.00	0.00	4680	5953
116	1.80	0.00	0.00	4709	5977
117	1.80	0.00	0.00	4717	5997
118	1.80	0.00	0.00	4744	6019
119	1.80	0.00	0.00	4756	6034
120	1.80	0.00	0.00	4746	6044
121	1.80	0.00	0.00	4779	6038
122	1.80	0.00	0.00	4799	6042
123	1.80	0.00	0.00	4811	6042
124	1.80	0.00	0.00	4825	6043
125	1.80	0.00	0.00	4837	6048

$Data_{Sn4A} :=$

0	1.00	1.30	0.00	5700	5788
1	1.00	1.30	40.00	5692	5804
2	1.00	1.30	40.00	5688	5812
3	1.00	1.30	37.00	5688	5830
4	1.00	1.30	35.00	5681	5832
5	1.00	1.30	34.00	5680	5825
6	1.00	1.30	32.00	5676	5816
7	1.00	1.30	31.00	5671	5810
8	1.00	1.30	30.00	5663	5795
9	1.00	1.30	30.00	5665	5775
10	1.00	1.30	29.00	5652	5753
12	1.00	1.30	27.00	5632	5709
14	1.00	1.30	25.00	5602	5663
16	1.00	1.30	25.00	5581	5617
18	1.00	1.30	24.00	5550	5569
20	1.00	1.30	23.00	5517	5526
25	1.00	1.30	21.00	5422	5426
30	1.00	1.30	20.00	5333	5341
35	1.00	1.30	19.00	5237	5271
40	1.00	1.30	17.00	5141	5189
45	1.00	1.30	16.00	5054	5174
50	1.00	1.30	16.00	4983	5101
55	1.00	1.30	15.00	4910	5054
60	1.00	1.30	15.00	4841	5004
65	1.00	1.30	15.00	4769	4958
75	1.00	1.30	14.00	4653	4889
80	1.00	1.30	12.00	4600	4863
85	1.00	1.30	12.00	4549	4827
100	1.00	1.30	11.00	4444	4753
107	1.00	1.30	10.00	4420	4744
108	1.00	0.00	0	4417	4760
109	1.00	0.00	0.00	4414	4775
110	1.00	0.00	0.00	4408	4812
111	1.50	0.00	0.00	4406	4860
112	1.50	0.00	0.00	4399	4897
113	1.50	0.00	0.00	4401	4922
114	1.50	0.00	0.00	4403	4947
115	1.50	0.00	0.00	4410	4972
120	1.50	0.00	0.00	4466	5123
140	1.50	0.00	0.00	4673	5413
168	1.50	0.00	0.00	4689	5582
174	1.50	0.00	0.00	4660	5638
178	1.50	0.00	0.00	4648	5652
186	1.50	0.00	0.00	4604	5681

$Data_{Sn4B} :=$

0	1.50	0.60	110.00	4591	5806
1	1.50	0.60	110.00	4620	5848
2	1.50	0.73	110.00	4614	5804
3	1.50	0.83	110.00	4611	5730
4	1.50	0.92	110.00	4598	5673
5	1.50	1.00	110.00	4567	5525
6	1.50	1.06	110.00	4539	5401
7	1.50	1.10	110.00	4480	5287
8	1.50	1.17	110.00	4424	5154
9	1.50	1.20	93.00	4355	5045
10	1.50	1.20	69.00	4286	4941
12	1.50	1.20	60.00	4215	4852
13	1.50	1.20	40.00	4058	4714
15	1.50	1.20	37.00	3925	4630
17	1.50	1.20	30.00	3798	4557
19	1.50	1.20	29.00	3711	4498
22	1.50	1.20	22.00	3640	4448
24	1.50	1.20	19.00	3501	4421
30	1.50	1.20	20.00	3467	4459
36	1.50	1.20	17.00	3384	4462
40	1.50	1.20	17.00	3348	4493
41	1.50	0.00	0.00	3344	4489
42	1.50	0.00	0.00	3340	4505
43	1.50	0.00	0.00	3331	4536
44	1.50	0.00	0.00	3328	4599
45	1.50	0.00	0.00	3332	4664
46	1.50	0.90	0.00	3342	4721
47	1.50	0.89	0.00	3353	4781
48	1.50	0.86	0.00	3385	4827
49	1.50	0.84	0.00	3409	4878
50	1.50	0.82	0.00	3429	4917
55	1.50	0.71	0.00	3571	5140
60	1.50	0.63	0.00	3665	5297
70	1.50	0.48	0.00	3832	5602
80	1.50	0.37	0.00	3932	5842
85	1.50	0.32	0.00	3955	5921
91	1.50	0.28	0.00	3988	5967
93	1.50	0.27	0.00	3971	5978
94	1.50	0.26	0.00	4004	5974
96	1.50	0.25	0.00	4005	5970
97	1.50	0.24	0.00	4008	5989
98	1.50	0.23	0.00	4009	6008
100	1.50	0.22	0.00	4015	6019
101	1.00	0.00	0.00	4019	6024
102	1.00	0.22	0.00	4022	6028
105	1.00	0.20	0.00	4044	6044
107	0.10	0.00	0.00	4058	6049
109	0.10	0.18	0.00	4072	6053
112	0.10	0.17	0.00	4072	6075

$Cond2Multiplier :=$

0
0
0
0
0
1

Effects of Control Voltage and Flow Rate

Early single brick tests were conducted with 1.3 vdc controlled at the power supply terminals.

Ion removal and removal levels were slow under this operating condition - electrical losses through the bus connections resulted in inadequate potential differences between aerogel electrode pairs.

For tests later than S/N 2D and S/N 4B, voltage control was implemented by sensing the voltage at two open terminals on the brick. The bricks have six terminals at each end alternating in polarity - 1,3,5 positive, 2,4,6 negative. Like terminals are connected internally through the aerogel electrodes. The supply cables were removed from terminals 5 and 6 at each end of the brick and they became the voltage sense points

The following graph demonstrates the dramatic performance accomplished by using bus feedback to regulate the applied voltage

$i := 0, 1 .. 50$

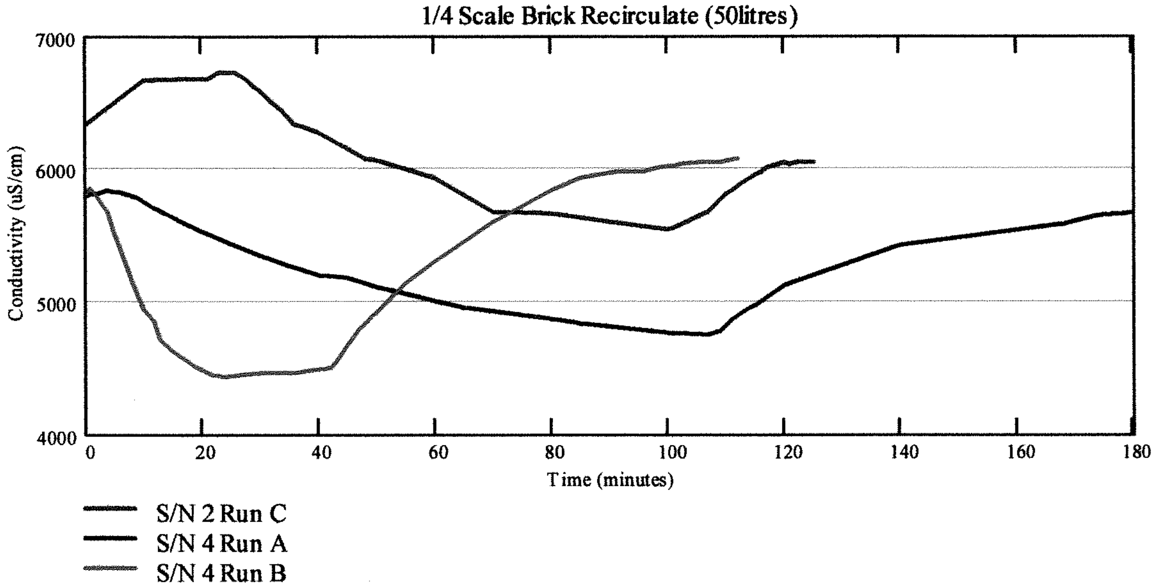

Comments on the previous graph

- Flow rates were 2, 1, and 1.5 litres/minute for runs S/N 2C, S/N 4A, and S/N 4B respectively
- Voltage control for run S/N 4B utilized feedback from vacant bus terminals on the brick, the other two runs controlled the voltage at the power supply.
- The S/N 2C brick was not completely rinsed on a prior rinse cycle and therefore increased conductivity of the water above input levels due to transfer of ions.
- Grounding occurred at 40 minutes for S/N 4B and approximately 100 minutes for the other two runs

Ion Storage Capacity

Using the conversion from conductivity to PPM given in the water analysis at the introduction, the mass of contaminants adsorbed and released can be predicted.

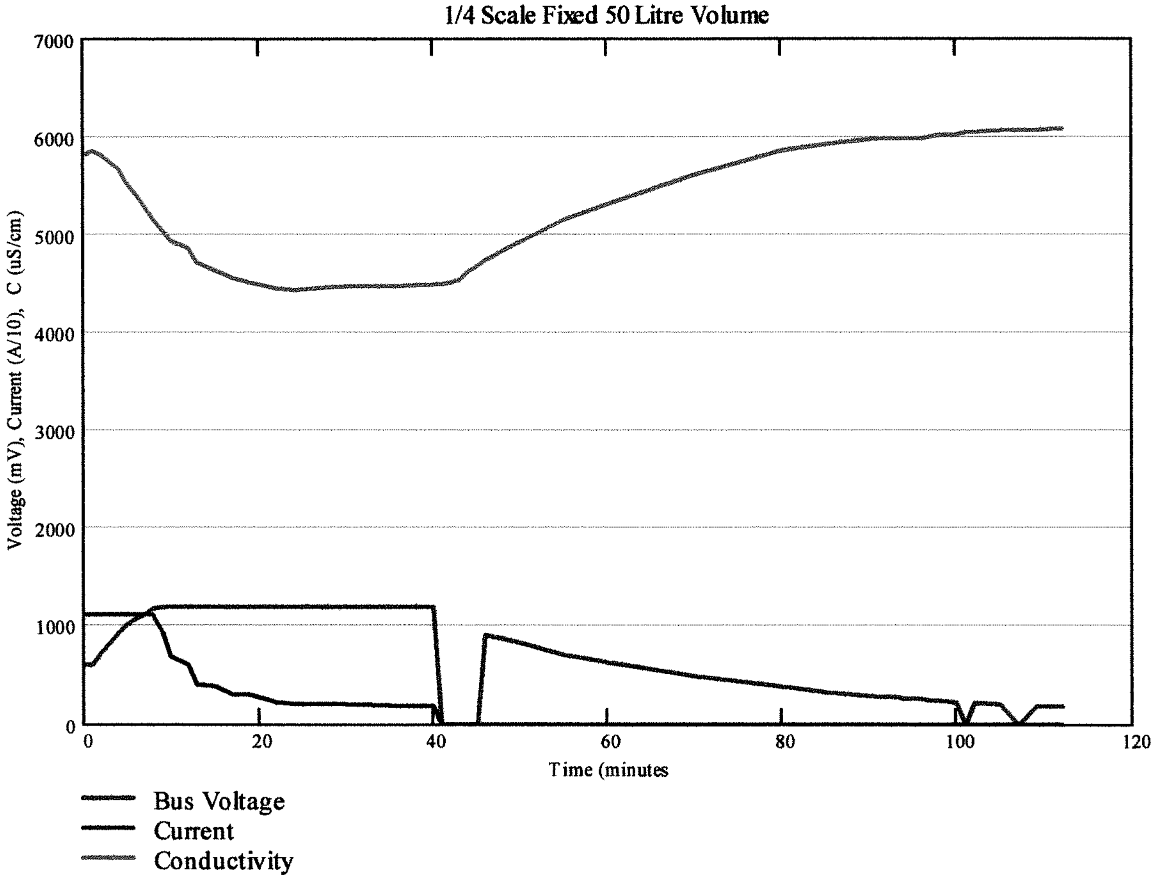

Notes on previous Graph

- Voltage not recorded from 41 to 46 minutes - hence dip in curve
- Discharge current not measured.
- System shorted at 40 minutes.
- Maximum current 110 A
- Maximum voltage 1.2 V

Water analysis conductivity, $C_{WaterAnal} := 6370 \cdot 10^{-6} \cdot \frac{S}{cm}$

Water analysis TDS, $TDS_{WaterAnal} := 4598 \cdot 10^{-6}$ (PPM expressed as a decimal)

Conversion factor - conductivity to TDS $Convert_{CondTDS} := \frac{TDS_{WaterAnal}}{C_{WaterAnal}}$ $Convert_{CondTDS} = 0.722 \frac{cm}{S}$

For S/N 4 run B the volume of water treated was $\quad Vol_{Water} := 50 \cdot liter$

Water density, $\quad \rho_{Water} := 1 \cdot \frac{kg}{liter}$

The approximate mass of ions adsorbed is calculated by looking at the change in conductivity accomplished

$MaxCond2 := max(Data_{Sn4B} \cdot Cond2Multiplier) \qquad MaxCond2 = 6.075 \times 10^3$

$MinCond2 := min(Data_{Sn4B} \cdot Cond2Multiplier) \qquad MinCond2 = 4.421 \times 10^3$

The absorbed ion mass is obtained thus,

$$M_{Ions} := (MaxCond2 - MinCond2) \cdot 10^{-6} \cdot \frac{S}{cm} \cdot Convert_{CondTDS} \cdot Vol_{Water} \cdot \rho_{Water}$$

$$M_{Ions} = 59.695\,gm$$

Benchmark

The goals for full scale CDT bricks are simple. A full size brick nominally contains 1000 square feet of aerogel and should accomplish a 1000 PPM TDS reduction at a flow rate of 1000 gallons per day.

This is considered the benchmark during development and brick performance is evaluated in terms of production gallons per day at 1000 ppm TDS reduction.

Initial results on the 1/4 scale brick S/N 4 suggest the following daily production at 1000 ppm TDS reduction

$CycleTime := 110 \cdot min \qquad BrickScale := \frac{1}{4}$

$$ScaledDailyProduction_{Sn4B} := \frac{24 \cdot hr}{CycleTime} \cdot \frac{M_{Ions}}{10^{-3} \cdot \rho_{Water}} \cdot \frac{1}{BrickScale}$$

$$ScaledDailyProduction_{Sn4B} = 825.756\,gal$$

Conclusions

- Applied voltage must be controlled using feedback from the bus for best performance
- Single brick scaled performance seems to be better than 80% of the goal
- A cycle time of approximately 100 minutes (production and rinse) is effective

Ion storage and scaled daily production (based on 1000 ppm reduction per full sized brick) are as follows

$$M_{Ions} = 59.695\,gm$$

$$ScaledDailyProduction_{Sn4B} = 825.756\,gal$$

ElectrodE Performance Measurements

Sample S1 - Reduced Cost Material

FarWest Group, Inc
Engineering and Development Center
701 Palomar Airport Road, Suite 300
Carlsbad, CA 92009

Phone: (760)931-4784 Fax: (760)931-4850
Email: c_sheppard@msn.com

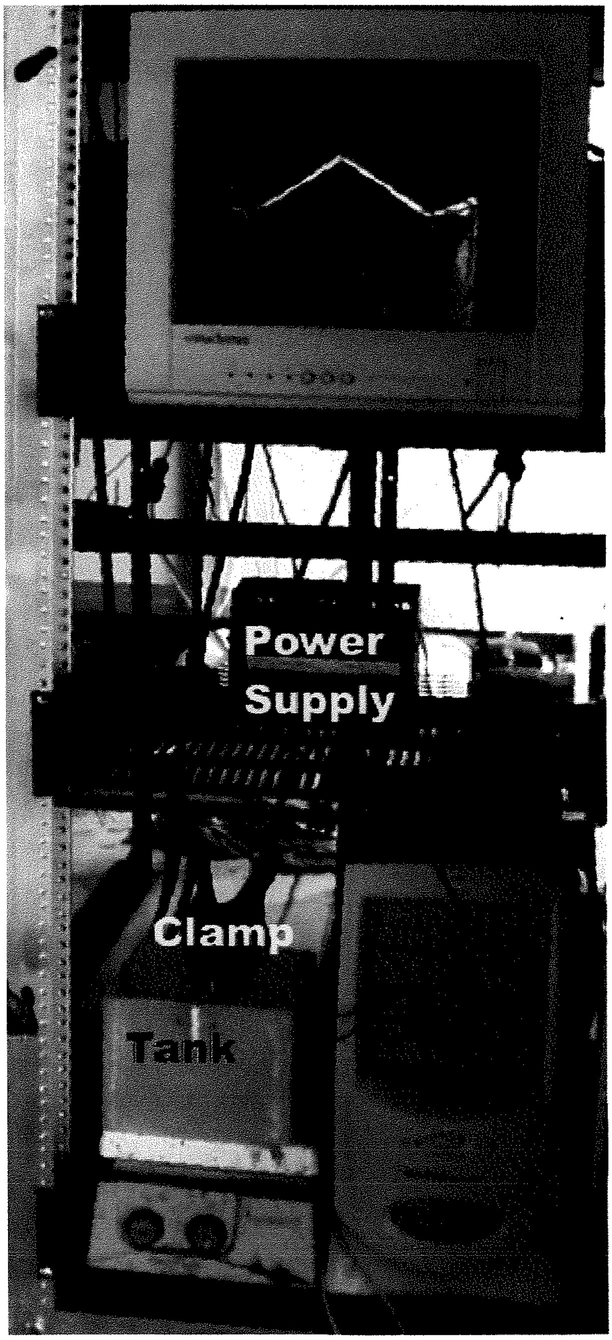

Introduction

There is ongoing development between FarWest and TDA to reduce the manufacturing costs of Aerogel and Aerogel type materials. As part of this development, materials are compared by charging and discharging a capacitor made of two 3" x 2" samples submerged in 10,000 ppm NaCl solution.

This document compares the following materials;

- Calibration run on same sample 071900Edge performed March 23, 2001
- Material P1 on Pan veil
- Material S1 on Carbon veil
- Material used in Mk-8A graphite bus bricks

Objectives

Objectives of these tests are two fold

- Quantify electrical conductivity improvement realized by changing from alligator connectors to spring loaded graphite rods for electrode coupling.

- Evaluate the P1 and S1 materials as a possible substitute for the current material due to their lower manufacturing cost.

Test Equipment

1. Polypropylene reservoir - 2.0 litre fill level
2. 2 litres of 10,000 ppm NaCl solution
3. Plastic clamp with 1/4 diameter graphite rods bonded to tips for contact with electrode samples
4. Kepco power supply PAT 7-2 computer controlled 0-7 vdc at 0-2 A.
5. Industrial Computer ADIO 1600 I/O board mounted in Compaq 5304 computer
6. FarWest interface board containing relays and power supply control resistors.
   Relays are used to switch from power supply to discharge resistor during discharge portion of test cycle
7. Thermolyne Cimarec 2 hot plate/magnetic mixer
8. Various test electrode pairs measuring 2" x 3"
9. FarWest visual c++ control software "geltest"

Test Sequence

1. Mix 10,000 ppm NaCl solution and fill reservoir with 2.0 litres
2. Mount test samples in tank such that a 2" x 2" area remains under the water.
3. Set program for 15 minutes charge and 15 minutes discharge with an initial 10 second settling time
4. Assign filename
5. Start mixer
6. Start test
7. At end of test, record data.
8. Perform second cycle with new file name
9. Reverse clamp such that polarity is reversed relative to samples
10. Repeat two more cycles with new filenames

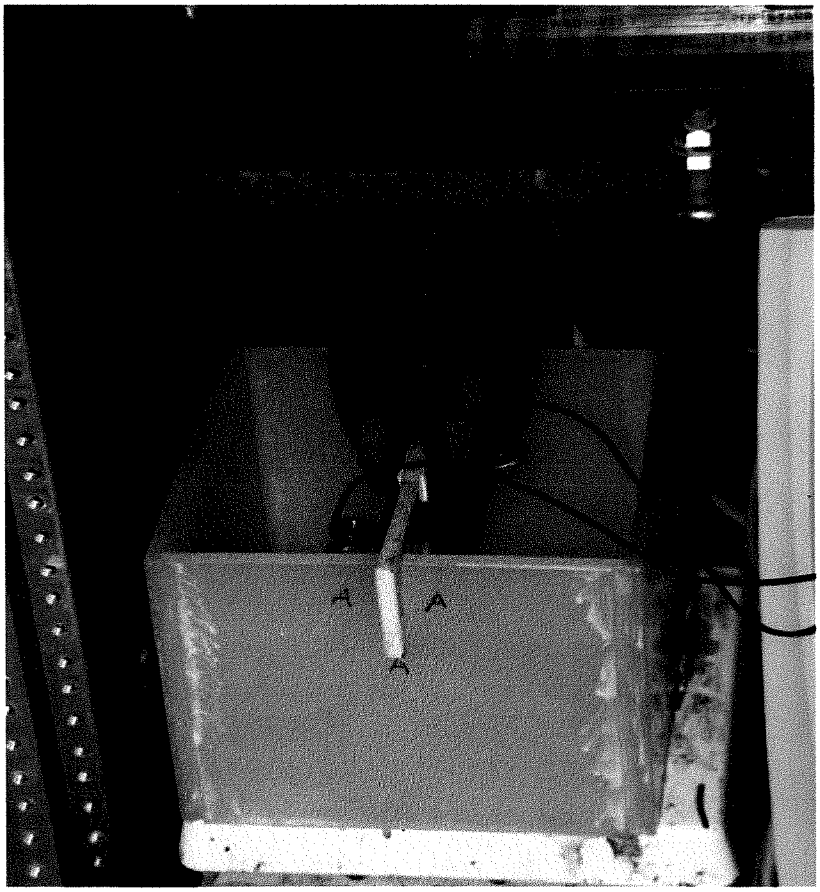

Test Data

Raw test data is presented in the same format for each run. The three columns represent Time (sec), Voltage Across Samples (V), Current (A).

Since this is a Mathcad document, the entire table of 181 entries is stored for each data set but only the first few are visible.

Old Test Results - Q/A 071900Edge

From the Q/A tests performed on 07-19-00, the average input and output energies for these samples was

- Average input energy = 75.33 J
- Average output energy = 13.53 J
- Ratio of output to input = 18%

$AvEnergyIn_{071900Edge} := 75.33 \cdot J$

$AvEnergyOut_{071900Edge} := 13.53 \cdot J$

Calibration Run 071900Edge Sample

These results have been obtained by performing the capacitor test on the same samples tested in Tucson immediately after production of the aerogel.

The only difference is the method of electrical connection to the electrode samples

$Data_{071900EdgeCalA} :=$

	0	1	2
0	10	0	0
1	20	1.22	0.38
2	30	1.21	0.3
3	40	1.21	0.25
4	50	1.21	0.21
5	60	1.2	0.18
6	70	1.2	0.16

$Data_{071900EdgeCalB} :=$

	0	1	2
0	10	0	0
1	20	1.23	0.39
2	30	1.21	0.31
3	40	1.21	0.25
4	50	1.21	0.21
5	60	1.2	0.18
6	70	1.2	0.16

Sample Physical Data

Plate 1

$t_{071900Edge\_1} := .034 \cdot in$

$L_{071900Edge\_1} := 3 \cdot in$

$w_{071900Edge\_1} := 2 \cdot in$

$M_{071900Edge\_1} := 2.35 \cdot gm$

Plate 2

$t_{071900Edge\_2} := .034 \cdot in$

$L_{071900Edge\_2} := 3 \cdot in$

$w_{071900Edge\_2} := 2 \cdot in$

$M_{071900Edge\_2} := 2.3 \cdot gm$

$Data_{071900EdgeCalC} :=$

	0	1	2
0	10	0	0
1	20	1.23	0.41
2	30	1.21	0.32
3	40	1.21	0.26
4	50	1.2	0.23
5	60	1.21	0.2
6	70	1.2	0.17

$Data_{071900EdgeCalD} :=$

	0	1	2
0	10	0	0
1	20	1.23	0.42
2	30	1.22	0.32
3	40	1.2	0.25
4	50	1.21	0.22
5	60	1.21	0.18
6	70	1.2	0.16

Material P1 on Carbon Veil

$Data_{P1\_082800B} :=$

	0	1	2
0	10	0	0
1	20	1.21	0.3
2	30	1.21	0.27

$Data_{P1\_082800C} :=$

	0	1	2
0	10	0	0
1	20	1.2	0.21
2	30	1.2	0.2

$Data_{P1\_082800D} :=$

	0	1	2
0	10	0	0
1	20	1.2	0.31
2	30	1.21	0.29

Sample Physical Data

Plate 1

$t_{P1\_082800\_1} := .033 \cdot in$

$L_{P1\_082800\_1} := 3. \cdot in$

$w_{P1\_082800\_1} := 2 \cdot in$

$M_{P1\_082800\_1} := 1.75 \cdot gm$

$Data_{P1\_082800E} :=$

	0	1	2
0	10	0	0
1	20	1.21	0.27
2	30	1.2	0.25

Plate 2

$t_{P1\_082800\_2} := .033 \cdot in$

$L_{P1\_082800\_2} := 3 \cdot in$

$w_{P1\_082800\_2} := 2 \cdot in$

$M_{P1\_082800\_2} := 1.75 \cdot gm$

$Data_{P1\_082800F} :=$

	0	1	2
0	10	0	0
1	20	1.2	0.3
2	30	1.2	0.28

Material S1 on Carbon Veil

Four 2" x 3" samples were produced using the S1 formulation on carbon veil. These are the test results from the second pair tested.
The first pair gave almost identical results.

$Data_{S1\_032901A} :=$

	0	1	2
0	10	0.31	-0.01
1	20	1.21	0.24
2	30	1.2	0.21

$Data_{S1\_032901B} :=$

	0	1	2
0	10	0.22	-0.01
1	20	1.21	0.27
2	30	1.2	0.24

Sample Physical Data

Plate 1

$t_{S1\_032901\_1} := .036 \cdot in$

$L_{S1\_032901\_1} := 3 \cdot in$

$w_{S1\_032901\_1} := 2 \cdot in$

$M_{S1\_032901\_1} := 1.59 \cdot gm$

$Data_{S1\_032901C} :=$

	0	1	2
0	10	0.24	-0.01
1	20	1.21	0.26
2	30	1.2	0.24

$Data_{S1\_032901D} :=$

	0	1	2
0	10	0	0
1	20	1.21	0.46
2	30	1.21	0.41

Plate 2

$t_{S1\_032901\_2} := .036 \cdot in$

$L_{S1\_032901\_2} := 3 \cdot in$

$w_{S1\_032901\_2} := 2 \cdot in$

$M_{S1\_032901\_2} := 1.59 \cdot gm$

$Data_{S1\_032901E} :=$

	0	1	2
0	10	0.07	-0.01
1	20	1.21	0.35
2	30	1.21	0.31

$Data_{S1\_032901F} :=$

	0	1	2
0	10	0.1	-0.01
1	20	1.21	0.34
2	30	1.21	0.3

MK 8A Graphite Bus Brick Samples

These samples were taken from material used in the construction of MK 8A serial number 6. They are from the same batch of material used to construct serial numbers 3, 4, and 5.

$Data_{Mk8ASn6A} :=$

	0	1	2
0	10	0.89	-0.02
1	20	1.2	0.09
2	30	1.2	0.08

$Data_{Mk8ASn6B} :=$

	0	1	2
0	10	0.07	-0.01
1	20	1.22	0.35
2	30	1.21	0.27

$Data_{Mk8ASn6C}$:=

	0	1	2
0	10	0.08	-0.01
1	20	1.22	0.36
2	30	1.21	0.28

$Data_{Mk8ASn6D}$:=

	0	1	2
0	10	0	0
1	20	1.23	0.47
2	30	1.22	0.37

$Data_{Mk8ASn6E}$:=

	0	1	2
0	10	0.06	-0.01
1	20	1.23	0.38
2	30	1.21	0.3

$Data_{Mk8ASn6F}$:=

	0	1	2
0	10	0.08	-0.01
1	20	1.22	0.38
2	30	1.21	0.29

Graphical Results

Calibration Sample

$i := 0, 1 .. 181$ $\qquad i_{charge} := 0, 1 .. 90$

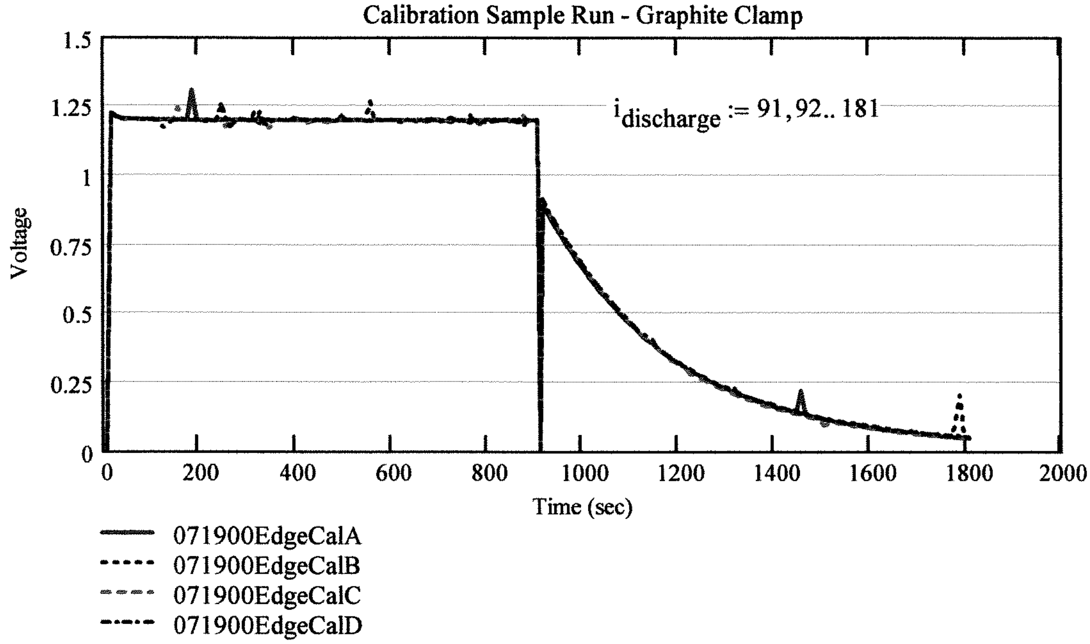

Material P1 on Carbon Veil

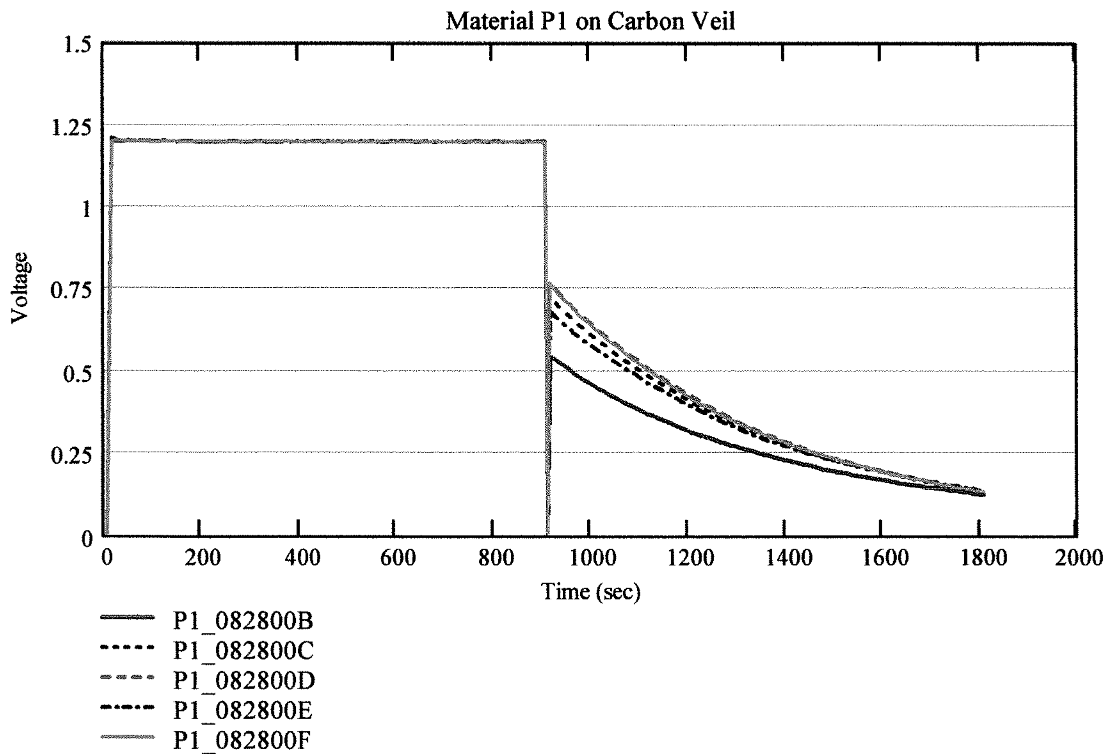

Material S1 on Carbon Veil

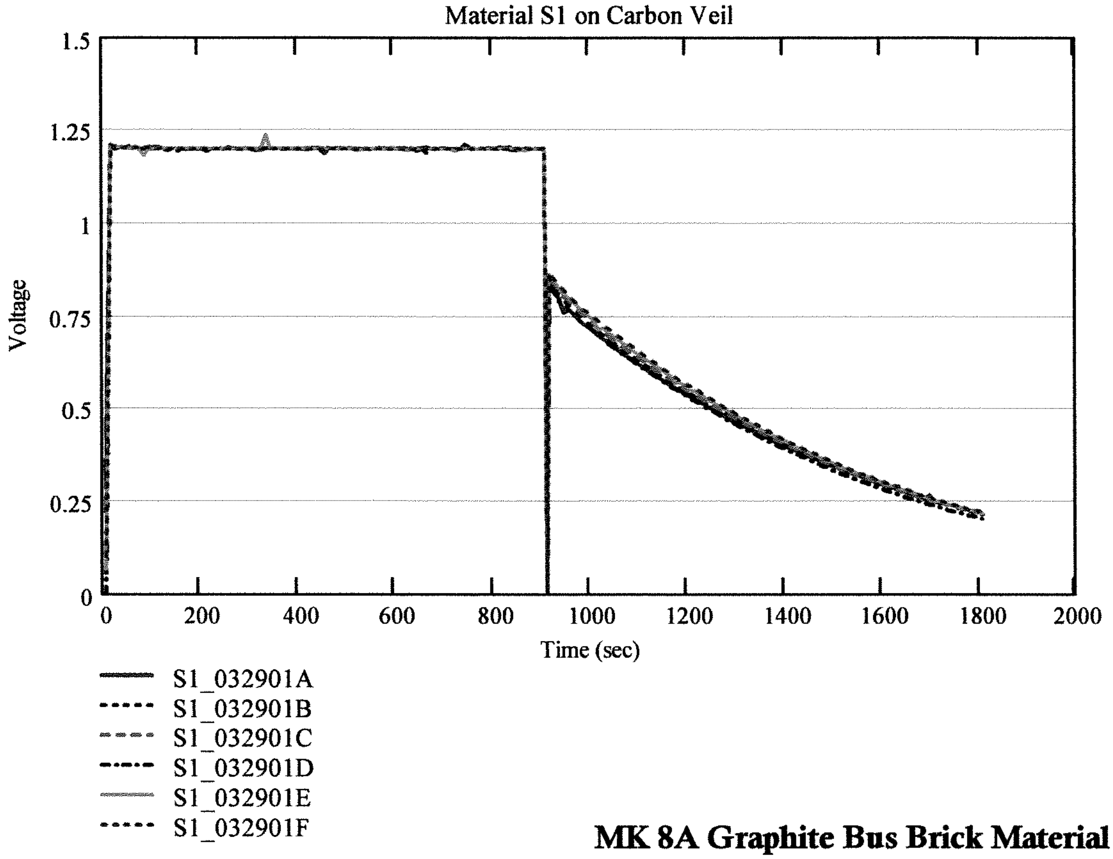

MK 8A Graphite Bus Brick Material

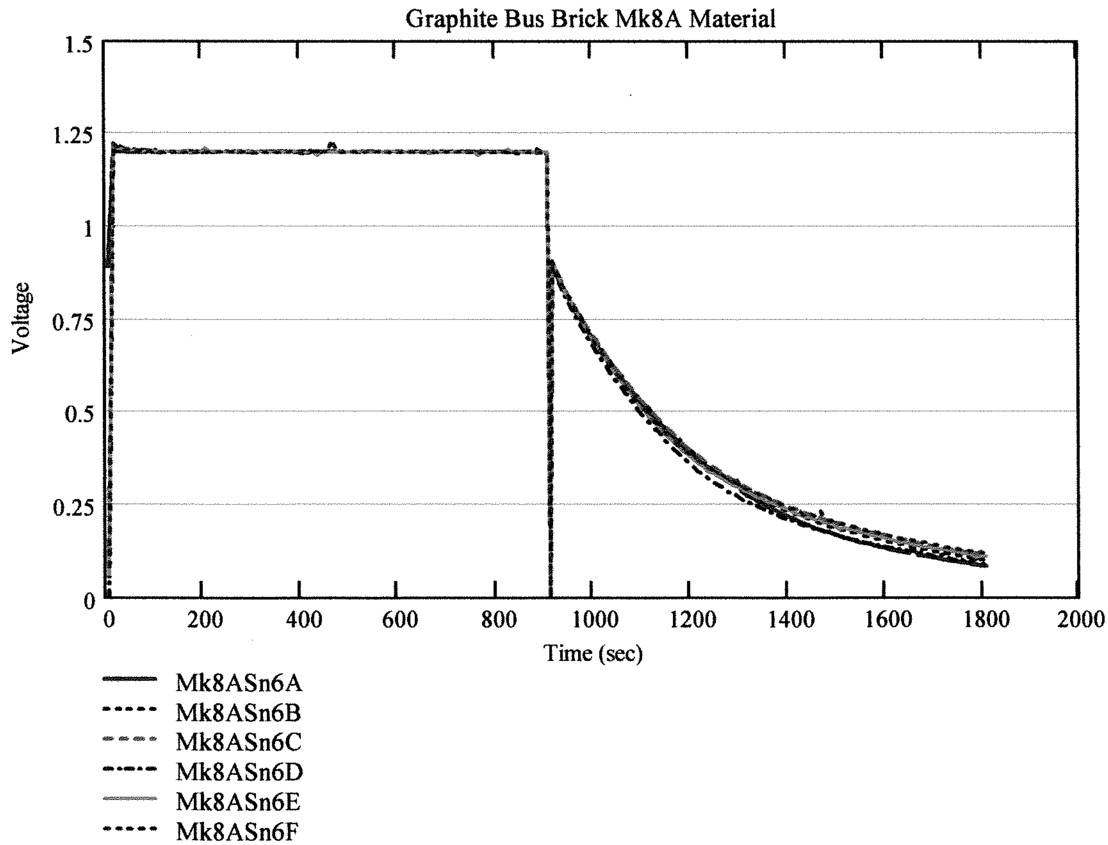

Energy Calculations

Before the energy input and output can be determined from the data tables (matrices), the tables must be split into two sub matrices - input and output

$Input_{071900EdgeCalA} := submatrix(Data_{071900EdgeCalA}, 0, 90, 0, 2)$

$Input_{071900EdgeCalB} := submatrix(Data_{071900EdgeCalB}, 0, 90, 0, 2)$

$Input_{071900EdgeCalC} := submatrix(Data_{071900EdgeCalC}, 0, 90, 0, 2)$

$Input_{071900EdgeCalD} := submatrix(Data_{071900EdgeCalD}, 0, 90, 0, 2)$

$Output_{071900EdgeCalA} := submatrix(Data_{071900EdgeCalA}, 91, 181, 0, 2)$

$Output_{071900EdgeCalB} := submatrix(Data_{071900EdgeCalB}, 91, 181, 0, 2)$

$Output_{071900EdgeCalC} := submatrix(Data_{071900EdgeCalC}, 91, 181, 0, 2)$

$Output_{071900EdgeCalD} := submatrix(Data_{071900EdgeCalD}, 91, 181, 0, 2)$

$Input_{P1\_082800B} := submatrix(Data_{P1\_082800B}, 0, 90, 0, 2)$

$Input_{P1\_082800C} := submatrix(Data_{P1\_082800C}, 0, 90, 0, 2)$

$Input_{P1\_082800D} := submatrix(Data_{P1\_082800D}, 0, 90, 0, 2)$

$Input_{P1\_082800E} := submatrix(Data_{P1\_082800E}, 0, 90, 0, 2)$

$Input_{P1\_082800F} := submatrix(Data_{P1\_082800F}, 0, 90, 0, 2)$

$Output_{P1\_082800B} := submatrix(Data_{P1\_082800B}, 91, 181, 0, 2)$

$Output_{P1\_082800C} := submatrix(Data_{P1\_082800C}, 91, 181, 0, 2)$

$Output_{P1\_082800D} := submatrix(Data_{P1\_082800D}, 91, 181, 0, 2)$

$Output_{P1\_082800E} := submatrix(Data_{P1\_082800E}, 91, 181, 0, 2)$

$Output_{P1\_082800F} := submatrix(Data_{P1\_082800F}, 91, 181, 0, 2)$

$$VoltageExtract := \begin{pmatrix} 0 \\ volt \\ 0 \end{pmatrix}$$

$$CurrentExtract := \begin{pmatrix} 0 \\ 0 \\ amp \end{pmatrix}$$

$\Delta t := 10 \cdot sec$

$Input_{S1\_032901A} := submatrix(Data_{S1\_032901A}, 0, 90, 0, 2)$

$Input_{S1\_032901B} := submatrix(Data_{S1\_032901B}, 0, 90, 0, 2)$

$Input_{S1\_032901C} := submatrix(Data_{S1\_032901C}, 0, 90, 0, 2)$

$Input_{S1\_032901D} := submatrix(Data_{S1\_032901D}, 0, 90, 0, 2)$

$Input_{S1\_032901E} := submatrix(Data_{S1\_032901E}, 0, 90, 0, 2)$

$Input_{S1\_032901F} := submatrix(Data_{S1\_032901F}, 0, 90, 0, 2)$

$Output_{S1\_032901A} := submatrix(Data_{S1\_032901A}, 91, 181, 0, 2)$

$Output_{S1\_032901B} := submatrix(Data_{S1\_032901B}, 91, 181, 0, 2)$

$Output_{S1\_032901C} := submatrix(Data_{S1\_032901C}, 91, 181, 0, 2)$

$Output_{S1\_032901D} := submatrix(Data_{S1\_032901D}, 91, 181, 0, 2)$

$Output_{S1\_032901E} := submatrix(Data_{S1\_032901E}, 91, 181, 0, 2)$

$Output_{S1\_032901F} := submatrix(Data_{S1\_032901F}, 91, 181, 0, 2)$

$Input_{Mk8ASn6A} := submatrix(Data_{Mk8ASn6A}, 0, 90, 0, 2)$

$Input_{Mk8ASn6B} := submatrix(Data_{Mk8ASn6B}, 0, 90, 0, 2)$

$Input_{Mk8ASn6C} := submatrix(Data_{Mk8ASn6C}, 0, 90, 0, 2)$

$Input_{Mk8ASn6D} := submatrix(Data_{Mk8ASn6D}, 0, 90, 0, 2)$

$Input_{Mk8ASn6E} := submatrix(Data_{Mk8ASn6E}, 0, 90, 0, 2)$

$Input_{Mk8ASn6F} := submatrix(Data_{Mk8ASn6F}, 0, 90, 0, 2)$

$Output_{Mk8ASn6A} := submatrix(Data_{Mk8ASn6A}, 91, 181, 0, 2)$

$Output_{Mk8ASn6B} := submatrix(Data_{Mk8ASn6B}, 91, 181, 0, 2)$

$Output_{Mk8ASn6C} := submatrix(Data_{Mk8ASn6C}, 91, 181, 0, 2)$

$Output_{Mk8ASn6D} := submatrix(Data_{Mk8ASn6D}, 91, 181, 0, 2)$

$Output_{Mk8ASn6E} := submatrix(Data_{Mk8ASn6E}, 91, 181, 0, 2)$

$Output_{Mk8ASn6F} := submatrix(Data_{Mk8ASn6F}, 91, 181, 0, 2)$

Energy Calibration Sample

$$EnergyIn_{071900EdgeCal_0} := (Input_{071900EdgeCalA} \cdot VoltageExtract) \cdot (Input_{071900EdgeCalA} \cdot CurrentExtract) \cdot \Delta t$$

$$EnergyIn_{071900EdgeCal_1} := (Input_{071900EdgeCalB} \cdot VoltageExtract) \cdot (Input_{071900EdgeCalB} \cdot CurrentExtract) \cdot \Delta t$$

$$EnergyIn_{071900EdgeCal_2} := (Input_{071900EdgeCalC} \cdot VoltageExtract) \cdot (Input_{071900EdgeCalC} \cdot CurrentExtract) \cdot \Delta t$$

$$EnergyIn_{071900EdgeCal_3} := (Input_{071900EdgeCalD} \cdot VoltageExtract) \cdot (Input_{071900EdgeCalD} \cdot CurrentExtract) \cdot \Delta t$$

$$AvEnergyIn_{071900EdgeCal} := mean(EnergyIn_{071900EdgeCal})$$

$$AvEnergyIn_{071900EdgeCal} = 48.938\,J$$

$$EnergyOut_{071900EdgeCal_0} := (Output_{071900EdgeCalA} \cdot VoltageExtract) \cdot (Output_{071900EdgeCalA} \cdot CurrentExtract) \cdot \Delta t$$

$$EnergyOut_{071900EdgeCal_1} := (Output_{071900EdgeCalB} \cdot VoltageExtract) \cdot (Output_{071900EdgeCalB} \cdot CurrentExtract) \cdot \Delta t$$

$$EnergyOut_{071900EdgeCal_2} := (Output_{071900EdgeCalC} \cdot VoltageExtract) \cdot (Output_{071900EdgeCalC} \cdot CurrentExtract) \cdot \Delta t$$

$$EnergyOut_{071900EdgeCal_3} := (Output_{071900EdgeCalD} \cdot VoltageExtract) \cdot (Output_{071900EdgeCalD} \cdot CurrentExtract) \cdot \Delta t$$

$$AvEnergyOut_{071900EdgeCal} := mean(EnergyOut_{071900EdgeCal})$$

$$AvEnergyOut_{071900EdgeCal} = -11.767\,J$$

Energy - Material P1 on Carbon Veil

$$EnergyIn_{P1\_082800_0} := (Input_{P1\_082800B} \cdot VoltageExtract) \cdot (Input_{P1\_082800B} \cdot CurrentExtract) \cdot \Delta t$$

$$EnergyIn_{P1\_082800_1} := (Input_{P1\_082800C} \cdot VoltageExtract) \cdot (Input_{P1\_082800C} \cdot CurrentExtract) \cdot \Delta t$$

$$EnergyIn_{P1\_082800_2} := (Input_{P1\_082800D} \cdot VoltageExtract) \cdot (Input_{P1\_082800D} \cdot CurrentExtract) \cdot \Delta t$$

$$EnergyIn_{P1\_082800_3} := (Input_{P1\_082800E} \cdot VoltageExtract) \cdot (Input_{P1\_082800E} \cdot CurrentExtract) \cdot \Delta t$$

$$EnergyIn_{P1\_082800_4} := (Input_{P1\_082800F} \cdot VoltageExtract) \cdot (Input_{P1\_082800F} \cdot CurrentExtract) \cdot \Delta t$$

$$AvEnergyIn_{P1\_082800} := mean(EnergyIn_{P1\_082800})$$

$$AvEnergyIn_{P1\_082800} = 70.3\,J$$

$$EnergyOut_{P1\_082800_0} := (Output_{P1\_082800B} \cdot VoltageExtract) \cdot (Output_{P1\_082800B} \cdot CurrentExtract) \cdot \Delta t$$

$$EnergyOut_{P1\_082800_1} := (Output_{P1\_082800C} \cdot VoltageExtract) \cdot (Output_{P1\_082800C} \cdot CurrentExtract) \cdot \Delta t$$

$$EnergyOut_{P1\_082800_2} := (Output_{P1\_082800D} \cdot VoltageExtract) \cdot (Output_{P1\_082800D} \cdot CurrentExtract) \cdot \Delta t$$

$$\text{EnergyOut}_{\text{P1\_082800}_3} := \left(\text{Output}_{\text{P1\_082800E}}\cdot\text{VoltageExtract}\right)\cdot\left(\text{Output}_{\text{P1\_082800E}}\cdot\text{CurrentExtract}\right)\cdot\Delta t$$

$$\text{EnergyOut}_{\text{P1\_082800}_4} := \left(\text{Output}_{\text{P1\_082800F}}\cdot\text{VoltageExtract}\right)\cdot\left(\text{Output}_{\text{P1\_082800F}}\cdot\text{CurrentExtract}\right)\cdot\Delta t$$

$$\text{AvEnergyOut}_{\text{P1\_082800}} := \text{mean}\left(\text{EnergyOut}_{\text{P1\_082800}}\right)$$

$$\text{AvEnergyOut}_{\text{P1\_082800}} = -12.396\ \text{J}$$

Energy - Material S1 on Carbon Veil

$$\text{EnergyIn}_{\text{S1\_032901}_0} := \left(\text{Input}_{\text{S1\_032901A}}\cdot\text{VoltageExtract}\right)\cdot\left(\text{Input}_{\text{S1\_032901A}}\cdot\text{CurrentExtract}\right)\cdot\Delta t$$

$$\text{EnergyIn}_{\text{S1\_032901}_1} := \left(\text{Input}_{\text{S1\_032901B}}\cdot\text{VoltageExtract}\right)\cdot\left(\text{Input}_{\text{S1\_032901B}}\cdot\text{CurrentExtract}\right)\cdot\Delta t$$

$$\text{EnergyIn}_{\text{S1\_032901}_2} := \left(\text{Input}_{\text{S1\_032901C}}\cdot\text{VoltageExtract}\right)\cdot\left(\text{Input}_{\text{S1\_032901C}}\cdot\text{CurrentExtract}\right)\cdot\Delta t$$

$$\text{EnergyIn}_{\text{S1\_032901}_3} := \left(\text{Input}_{\text{S1\_032901D}}\cdot\text{VoltageExtract}\right)\cdot\left(\text{Input}_{\text{S1\_032901D}}\cdot\text{CurrentExtract}\right)\cdot\Delta t$$

$$\text{EnergyIn}_{\text{S1\_032901}_4} := \left(\text{Input}_{\text{S1\_032901E}}\cdot\text{VoltageExtract}\right)\cdot\left(\text{Input}_{\text{S1\_032901E}}\cdot\text{CurrentExtract}\right)\cdot\Delta t$$

$$\text{AvEnergyIn}_{\text{S1\_032901}} := \text{mean}\left(\text{EnergyIn}_{\text{S1\_032901}}\right)$$

$$\text{AvEnergyIn}_{\text{S1\_032901}} = 87.075\ \text{J}$$

$$\text{EnergyOut}_{\text{S1\_032901}_0} := \left(\text{Output}_{\text{S1\_032901A}}\cdot\text{VoltageExtract}\right)\cdot\left(\text{Output}_{\text{S1\_032901A}}\cdot\text{CurrentExtract}\right)\cdot\Delta t$$

$$\text{EnergyOut}_{\text{S1\_032901}_1} := \left(\text{Output}_{\text{S1\_032901B}}\cdot\text{VoltageExtract}\right)\cdot\left(\text{Output}_{\text{S1\_032901B}}\cdot\text{CurrentExtract}\right)\cdot\Delta t$$

$$\text{EnergyOut}_{\text{S1\_032901}_2} := \left(\text{Output}_{\text{S1\_032901C}}\cdot\text{VoltageExtract}\right)\cdot\left(\text{Output}_{\text{S1\_032901C}}\cdot\text{CurrentExtract}\right)\cdot\Delta t$$

$$\text{EnergyOut}_{\text{S1\_032901}_3} := \left(\text{Output}_{\text{S1\_032901D}}\cdot\text{VoltageExtract}\right)\cdot\left(\text{Output}_{\text{S1\_032901D}}\cdot\text{CurrentExtract}\right)\cdot\Delta t$$

$$\text{EnergyOut}_{\text{S1\_032901}_4} := \left(\text{Output}_{\text{S1\_032901E}}\cdot\text{VoltageExtract}\right)\cdot\left(\text{Output}_{\text{S1\_032901E}}\cdot\text{CurrentExtract}\right)\cdot\Delta t$$

$$\text{AvEnergyOut}_{\text{S1\_032901}} := \text{mean}\left(\text{EnergyOut}_{\text{S1\_032901}}\right)$$

$$\text{AvEnergyOut}_{\text{S1\_032901}} = -21.73\ \text{J}$$

Energy - Mk 8A Graphite Bus Brick Material

$$\text{EnergyIn}_{\text{Mk8ASn6}_0} := \left(\text{Input}_{\text{Mk8ASn6A}}\cdot\text{VoltageExtract}\right)\cdot\left(\text{Input}_{\text{Mk8ASn6A}}\cdot\text{CurrentExtract}\right)\cdot\Delta t$$

$$\text{EnergyIn}_{\text{Mk8ASn6}_1} := \left(\text{Input}_{\text{Mk8ASn6B}}\cdot\text{VoltageExtract}\right)\cdot\left(\text{Input}_{\text{Mk8ASn6B}}\cdot\text{CurrentExtract}\right)\cdot\Delta t$$

$$\text{EnergyIn}_{\text{Mk8ASn6}_2} := \left(\text{Input}_{\text{Mk8ASn6C}}\cdot\text{VoltageExtract}\right)\cdot\left(\text{Input}_{\text{Mk8ASn6C}}\cdot\text{CurrentExtract}\right)\cdot\Delta t$$

$$EnergyIn_{Mk8ASn6_3} := \left(Input_{Mk8ASn6D} \cdot VoltageExtract\right) \cdot \left(Input_{Mk8ASn6D} \cdot CurrentExtract\right) \cdot \Delta t$$

$$EnergyIn_{Mk8ASn6_4} := \left(Input_{Mk8ASn6E} \cdot VoltageExtract\right) \cdot \left(Input_{Mk8ASn6E} \cdot CurrentExtract\right) \cdot \Delta t$$

$$EnergyIn_{Mk8ASn6_5} := \left(Input_{Mk8ASn6F} \cdot VoltageExtract\right) \cdot \left(Input_{Mk8ASn6F} \cdot CurrentExtract\right) \cdot \Delta t$$

$$AvEnergyIn_{Mk8ASn6} := mean\left(EnergyIn_{Mk8ASn6}\right)$$

$$AvEnergyIn_{Mk8ASn6} = 53.394\ J$$

$$EnergyOut_{Mk8ASn6_0} := \left(Output_{Mk8ASn6A} \cdot VoltageExtract\right) \cdot \left(Output_{Mk8ASn6A} \cdot CurrentExtract\right)$$

$$EnergyOut_{Mk8ASn6_1} := \left(Output_{Mk8ASn6B} \cdot VoltageExtract\right) \cdot \left(Output_{Mk8ASn6B} \cdot CurrentExtract\right)$$

$$EnergyOut_{Mk8ASn6_2} := \left(Output_{Mk8ASn6C} \cdot VoltageExtract\right) \cdot \left(Output_{Mk8ASn6C} \cdot CurrentExtract\right)$$

$$EnergyOut_{Mk8ASn6_3} := \left(Output_{Mk8ASn6D} \cdot VoltageExtract\right) \cdot \left(Output_{Mk8ASn6D} \cdot CurrentExtract\right)$$

$$EnergyOut_{Mk8ASn6_4} := \left(Output_{Mk8ASn6E} \cdot VoltageExtract\right) \cdot \left(Output_{Mk8ASn6E} \cdot CurrentExtract\right)$$

$$EnergyOut_{Mk8ASn6_5} := \left(Output_{Mk8ASn6F} \cdot VoltageExtract\right) \cdot \left(Output_{Mk8ASn6F} \cdot CurrentExtract\right)$$

$$AvEnergyOut_{Mk8ASn6} := mean\left(EnergyOut_{Mk8ASn6}\right) \cdot \Delta t$$

$$AvEnergyOut_{Mk8ASn6} = -14.202\ J$$

CONCLUSIONS

- The electrical connections implemented on the test setup provide improved conductivity and therefore lower losses as seen by the ratios of output to input energies on identical samples.

$$EnergyRatio_{071900Edge} := \frac{AvEnergyOut_{071900Edge}}{AvEnergyIn_{071900Edge}} \qquad EnergyRatio_{071900EdgeCal} := \frac{AvEnergyOut_{071900EdgeCal}}{AvEnergyIn_{071900EdgeCal}}$$

$EnergyRatio_{071900Edge} = 17.961\ \%$ Old Setup $EnergyRatio_{071900EdgeCal} = -24.044\ \%$ New Setup

- The S1 material on carbon veil appears to have greater storage energy than the production material currently used in the graphite bricks. This makes it a viable candidate for testing in bricks.

  Average energy extracted = 21.73 J compared to 14.2 J for the Mk 8A brick material (previous production runs have produced energies of up to 18 J)

- The S1 material has a lower production cost as will be discussed in later bulletins

- The P1 material has lower performance than existing material and is discarded from future study..

- The Ratio of output to input energy is an indication of resistive losses within the material, the S1 material has a slightly lower ratio and hence higher losses than the Mk 8A brick material. Work should be performed on improving conductivity

$$\text{EnergyRatio}_{S1\_032901} := \frac{\text{AvEnergyOut}_{S1\_032901}}{\text{AvEnergyIn}_{S1\_032901}}$$

$$\text{EnergyRatio}_{Mk8ASn6} := \frac{\text{AvEnergyOut}_{Mk8ASn6}}{\text{AvEnergyIn}_{Mk8ASn6}}$$

$$\text{EnergyRatio}_{S1\_032901} = -24.955\,\%$$

$$\text{EnergyRatio}_{Mk8ASn6} = -26.599\,\%$$

Energy Comparison Graph

The graph below compares the third run of the P1, S1 and Mk8A Sn6 samples in terms of accumulated energy

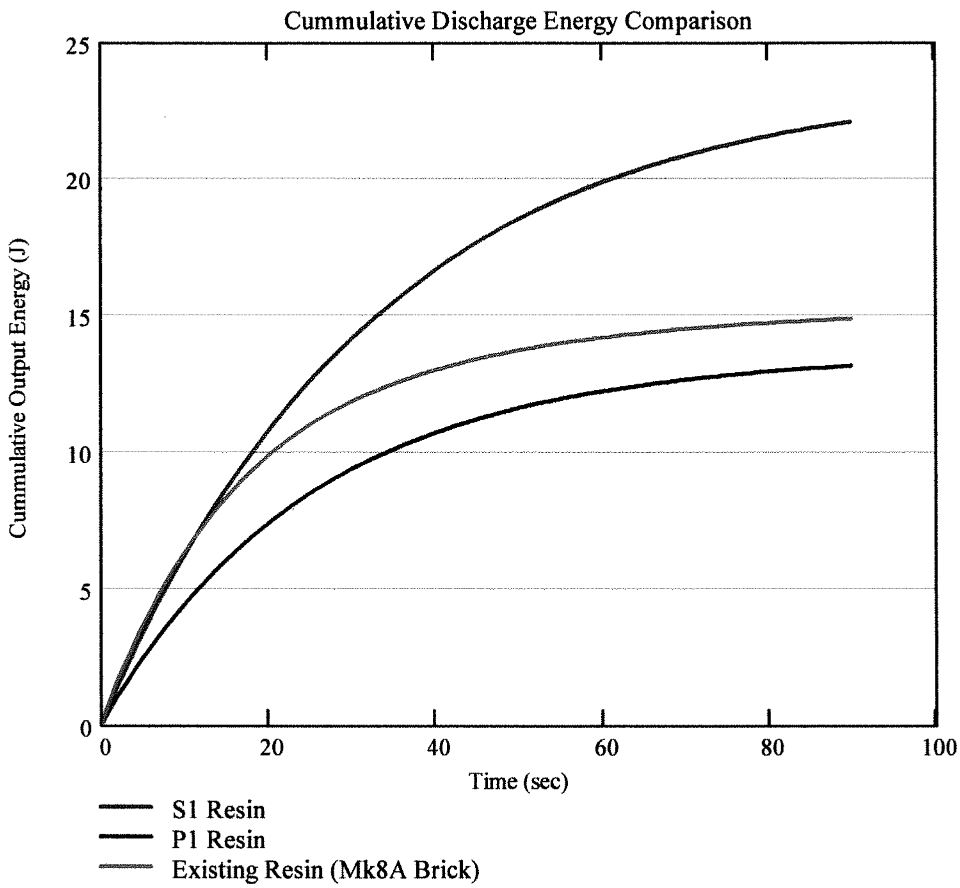

APPENDIX C

LETTER OF ACREDITATION FROM CDT SYSTEMS, INC

TM

CDT SYSTEMS, INC. www.cdtwater.com

13636 Neutron Road, Dallas, Tex~ 75244 * Tel (972) 934-1586 * Fax (972) 934-1592

Prof C.F. Schutte
University of Pretoria
Department of Chemical Engineering Pretoria, 0002
Republic of South Africa

1 September, 2004

Re: Letter of Accreditation to research conducted by T. J. Welgemoed in Capacitive Deionization Technology ™ for partial fulfillment of the requirements for a Master of Engineering Degree.

CDT Systems, Inc. hereby confirms that Mr. Thomas J. Welgemoed was involved in all research mentioned in the attached dissertation, ether directly, or indirectly, in a supervisory/consulting role during the period 1998 to 2004. His practical experience, expertise, dedication and research is, and continue to be, crucial to the development program to commercialize CDT™ from a laboratory scale program to its current industrial scale prototype system.

CDT Systems, Inc hereby also acknowledges that all information published in this dissertation have been reviewed and has been approved for publication as public information by the University of Pretoria.

Yours Sincerely,

Dallas Talley, CEO
CDT Systems, Inc